"IN VITRO VASCULOGENESIS IN 3D"

Katerina Stamati

A dissertation submitted in partial fulfillment of the requirements for the degree of
Doctor of Philosophy in Tissue Engineering

University College London

2014

I, Katerina Stamati confirm that the work presented in this thesis is my own. Where information has been derived from other sources, I confirm that this has been indicated in the thesis

Acknowledgments

I am extremely grateful to my primary supervisor Dr Umber Cheema for her supervision, guidance and support throughout my PhD. I am very grateful to Professor Vivek Mudera, my secondary supervisor for his knowledge and support. I am indebted to both for their time and patience. I am also deeply grateful to Professor John Priestley for his invaluable expertise and involvement in my PhD project.

I would also like to thank my colleagues at the Institute of Orthopaedics for their help and support at different stages of my PhD, both professionally and personally. Professor Robert Brown, Ms Rebecca Porter, Dr Michelle Korda, Dr Jennifer Verhoekx, Dr Tijna Alekseeva, Mr Noah Tan, Dr Jemma Kerns, Mr Prasad Sawadkar, Dr Roberta Ferro De Godoy, Mr Tarig Magdeldin, Ms Claire Walsh, Ms Josephine Wong, Ms Michele Pannaman and Ms Damyanti Bagaria.

I would also like to thank from histopathology at the RNOH: Dr Hongtao Ye, Mr Fitim Berisha and Mr Steve Crane.

I wish to acknowledge Oxford Optronix for their financial support and especially Dr Michael Rau for his help when needed.

Most of all, I would like to thank my family; my parents for all their support and love throughout my education, without them I wouldn't have been able to pursue my ambitions. I would also like to thank my sister Ioanna, her husband Yiannis and my brother Yiannis for all their support. Last but not least, I would like to thank my husband Panicos for his love, support and understanding during my PhD.

Publications and presentations

Stamati Katerina, Priestley V. John, Mudera Vivek and Cheema Umber. "Laminin promotes vascular network formation in 3D *in vitro* collagen scaffolds by regulating VEGF uptake" Journal of Experimental Cell Research, 2014 *in press.*

Review**: Stamati Katerina**, Mudera Vivek and Cheema Umber. "Evolution of oxygen utilisation in multicellular organisms and implications for cell signalling in tissue engineering" 2011, Journal of tissue engineering vol.2, 1

- TCES 2013, Cardiff UK, Oral Presentation: **Stamati Katerina**, Priestley V. John, Mudera Vivek and Cheema Umber "Engineering capillary networks in 3D *in vitro"*
- TERMIS 2013, Istanbul, Turkey, Oral Poster: **Stamati Katerina**, Priestley V. John, Mudera Vivek and Cheema Umber "Engineering Capillary Networks in 3D: It Matters Who You Are With"
- TCES 2012, Liverpool, UK, Oral Presentation: **Stamati Katerina**, Priestley V. John, Mudera Vivek and Cheema Umber "Stem Cell Generated Angiogenic Growth Factor Gradient: Guiding Endothelial Cells"
- Pearce Gould competition, UCL Division of Surgery, Oral Presentation: **Stamati Katerina**, Priestley V. John, Mudera Vivek and Cheema Umber "Basement Membrane Protein Orchestrates Network Formation By Endothelial Cells In 3D" (award)
- TCES 2011, Leeds, UK, Oral Presentation: **Stamati Katerina**, Priestley V. John, Mudera Vivek and Cheema Umber "Basement Membrane Protein

Orchestrates Network Formation By Endothelial Cells In 3d: Laminin The Conductor”

- TERMIS 2011, Granada Spain, Oral Presentation: **Stamati Katerina**, Priestley V. John, Mudera Vivek and Cheema Umber “Starved of oxygen: cells engineer 3d vascular networks *in vitro*”

Abstract

Angiogenesis and vasculogenesis are essential neovascularisation processes. Various cell types and growth factors are involved, with vascular endothelial growth factor (VEGF) and its receptors VEGFR1 and VEGFR2 identified as key components. The PhD project "*In vitro* vasculogenesis in 3D" tested the effect of parameters such as support cells, matrix composition and physiological hypoxia on the morphology and aggregation of ECs in 3D collagen hydrogels.

Different aggregation patterns were identified depending on the culture conditions tested, and these were found to reflect the different developmental pathways that ECs take to form different sized tubular structures. ECs formed contiguous sheets in collagen only hydrogels, analogous to the 'wrapping' pathway in development. In contrast, in co-cultures in 3D collagen-laminin cultures, end-to-end networks formed, mimicking cord hollowing and cell hollowing.

A relationship between matrix composition, growth factors and VEGF receptor levels in 3D collagen hydrogels was shown for the first time in this study. Results showed a key linkage between integrin expression on ECs and their uptake of VEGF, regulated by VEGFR2, resulting in end-to-end network aggregation in HBMSC-HUVEC co-cultures.

The effect of physiological hypoxia on EC aggregation was also tested by lowering the oxygen tension to 5% O_2 using a controlled culture environment. Angiogenic growth factors were quantified using ELISA and their levels were correlated to EC morphological progression within 3D collagen hydrogels.

Overall, the findings here showed how different parameters affected EC morphology and aggregation in 3D *in vitro* collagen hydrogels. The study

provides an understanding of how these individual parameters influence EC morphology and show the mechanisms of how this is achieved in 3D *in vitro*.

List of abbreviations

7AAD- 7-aminoactinomycin-D

Ang- Angiopoietin

ANOVA- analysis of variance

bFGF- basic fibroblast growth factor

BSA- bovine serum albumin

DAPI- 4',6-diamidino-2-phenylindole

DMEM- Dulbecco's modified Eagle's medium

ECM- extracellular matrix

EGM- endothelial growth media

ELISA- enzyme linked immunosorbent assay

FCS- fetal calf serum

FITC- fluorescein isothiocyanate

FSC-A- forward scatter

HBMSC- human bone marrow stem cells

HDF- human dermal fibroblast

HDMEC- human dermal microvascular endothelial cells

HUVEC- human umbilical vein endothelial cells

IGF- Insulin-like growth factor

MEM- minimum essential medium

NaOH- sodium hydroxide

NBF- neutral buffered formalin

ns- not significant

P/S- penicillin streptomycin

PBS- phosphate buffered saline

PDGF- platelet derived growth factor

PGA- polyglycolic acid

PIGF- placental growth factor

PLGA- poly-dl-lactic-co-glycolic acid

PLLA- poly- l-lactic acid

PMA- phorbol myristate acetate

RNOH- Royal National Orthopaedic Hospital

RPM- revolutions per minute

SD- standard deviation

SEM- standard error of the mean

SSC-A- side scatter

TGFβ- transforming growth factor

TMB- tetramethylbenzidine

VEGF- vascular endothelial growth factor

VEGFR1/R2- VEGF receptor 1/2

Contents

List of figures

List of tables

1 Introduction

1.1 Blood vessels

Blood vessels maintain a healthy immune system, supply tissues with oxygen and dispose of waste (Carmeliet and Jain, 2011). Nearly every organ in the human body is vascularised, with cartilage being the main exception. Blood vessels are important for organogenesis and tissue regeneration but are also the means for tumour metastasis and inflammatory disease progression (Carmeliet and Jain, 2011). Blood supply abnormalities can cause stroke, myocardial infarction, pulmonary hypertension and other major diseases (Carmeliet and Jain, 2011). Healthy blood vessels are therefore crucial for maintaining an overall healthy body.

All blood vessels, irrespective of size, from large arteries to small venules have an inner lining of endothelial cells (ECs), the endothelium (Aird, 2007a; Bouïs et al., 2001). The endothelium is important for multiple physiological functions and actively transports small molecules and hormones (Aird, 2007a; Bouïs et al., 2001). It also maintains blood pressure, the continuous movement of blood cells and haemostatic balance (Aird, 2007a; Bouïs et al., 2001). Depending on the location and function of the blood vessel, ECs differ in their exact function, shape and size, known as “EC heterogeneity” (Aird, 2007a).

ECs have strong cell-cell junctions through transmembrane proteins, which link to components within the cell, allowing communication with the actin cytoskeleton (Bazzoni and Dejana, 2004). Cell-cell junctions are important for maintaining homeostasis and controlling permeability to solutes and leukocytes,

while also controlling EC apoptosis and growth through intracellular signalling (Bazzoni and Dejana, 2004). There are two main junctions, adherens junctions and tight junctions, which are also found in the epithelium (Bazzoni and Dejana, 2004). While these are more distinct in the epithelium, there is more overlap between the two junctional systems in the endothelium (Bazzoni and Dejana, 2004; Vestweber et al., 2009).

Of the adherens junctions, the most important is vascular endothelial (VE) cadherin (Bazzoni and Dejana, 2004; Vestweber et al., 2009). Although VE-cadherin is found in similar quantities on ECs as N-cadherin, studies have only shown disruption of the endothelium when VE-cadherin function is blocked (Vestweber et al., 2009). VE-cadherin is almost exclusively found on ECs (cytotrophoblast being an exception) (Bazzoni and Dejana, 2004) and it is mostly concentrated at EC-EC junctions. On the contrary, N-cadherin is distributed throughout the cell membrane and is thought to be associated to EC communication with surrounding cells such as pericytes and smooth muscle cells (Bazzoni and Dejana, 2004).

VE-cadherin is associated intracellularly with β-catenin, plakoglobin, or γ-catenin (Calera et al., 2004; Vestweber et al., 2009; Wallez et al., 2006) and interacts with the actin cytoskeleton through α-catenin (Vestweber et al., 2009). VE-cadherin is involved in cell migration, proliferation and vasculogenesis, especially during development (Calera et al., 2004). It is also closely related to VEGFR2 and affects VEGFR2 action and stability (Calera et al., 2004; Scott and Mellor, 2009).

In addition to adherens and tight junctions, there are other adhesion proteins, such as platelet/endothelial cell adhesion molecule (PECAM-1) (Bazzoni and Dejana, 2004). PECAM-1 is expressed on ECs, lymphocytes and platelets (Aurrand-Lions et al., 2002; Bazzoni and Dejana, 2004). PECAM-1 is found in inter-endothelial junctions and is a transmembrane protein and member of the immunoglobulin family (Aurrand-Lions et al., 2002; Bazzoni and Dejana, 2004). PECAM-1 affects EC migration through its integrin interaction with the matrix (Bazzoni and Dejana, 2004) and can indirectly affect VE-cadherin and EC cell-cell adhesion through intracellular proteins (Wu and Sheibani, 2003). It is also likely responsible for leukocyte migration through the endothelium (Bazzoni and Dejana, 2004; Vestweber et al., 2009). PECAM-1-or CD31 and vascular endothelial (VE) cadherin are the most commonly used markers for the endothelium (Aird, 2007a). Both CD31 and VE-cadherin were chosen as EC markers in this study to test the morphology, aggregation and interaction of the cells.

In larger vessels, ECs are resident on a basement membrane, surrounded by mesenchymal cells and the extracellular matrix (Armulik et al., 2005). This forms the tunica intima of the vessel (Armulik et al., 2005), which is surrounded by a layer of vascular smooth muscle cells, responsible for maintaining the tone and contraction of the vessel (Armulik et al., 2005).

Capillaries are the intermediate exchange vessels and make up the bulk of the vascular system (Aird, 2007b). They are small, on average 10μm or less in diameter and have a thin wall, which consists of pericytes and extracellular matrix, essentially forming a 3D tube of ECs (Aird, 2007b). Pericytes are

vascular mural cells, set within the basement membrane of capillaries and venules (Armulik et al., 2005). Direct communication between pericytes and ECs through tight junctions, gap junctions or adherens junctions occurs where there are gaps in the basement membrane, also known as “peg-socket contacts” (Armulik et al., 2005). Pericytes are important for regulating several EC functions such as remodelling, maturation and stabilization, which are achieved by the direct communication of pericytes with multiple ECs allowing for a coordinated response of ECs (Armulik et al 2005). ECs are maintained in a quiescent state by pericytes and have an average lifespan of a year (Aird, 2007a; Carmeliet and Jain, 2011).

Both ECs and pericytes are resident on a basement membrane consisting of laminins, collagen IV, nidogen/entactin and heparan sulfate (Francis et al., 2008; Grant et al., 1990). Laminin is a large heterodimeric glycoprotein (molecular weight= 800kDa), with α, β and γ chains and at least 15 known isoforms (Francis et al., 2008; Grant et al., 1990). It promotes cell proliferation, differentiation, migration and attachment (Ali et al., 2013; Grant et al., 1990). Collagen IV promotes EC attachment and differentiation, while binding together all basement membrane components (Grant et al., 1990). Laminin and collagen IV have been shown to drive EC migration and angiogenesis in *in vitro* assays and therefore their effect on ECs was tested in the current study (Kubota et al., 1988; Nicosia, 2009; Nicosia et al., 1994)

1.2 Neovascularisation

Neovascularisation is the process by which new blood vessels are formed. Three main processes result in neovascularisation and these are angiogenesis, arteriogenesis and vasculogenesis (Carmeliet, 2000; Phelps and Garcia, 2009). Angiogenesis is the most widely studied and understood process and is found in the presence of tumours, wound healing and ischemia (Phelps and Garcia, 2009). Sprouting angiogenesis starts with pericyte detachment from the vessel (Carmeliet and Jain, 2011). Pericytes are freed from the basement membrane as it is degraded by MMP action. EC junctions become loose in response to VEGF and cells begin to produce a provisional ECM. Integrins then drive EC migration where VEGF and bFGF create a pro-angiogenic environment. ECs migrate by following a lead cell known as the tip cell, guided by several factors and followed by ECs known as the stalk cells as seen in figure 1.1 (Carmeliet and Jain, 2011). Tip cells sense cues from their surrounding environment, while stalk cells provide information on their location to the ECs that follow to elongate the structure (Carmeliet and Jain, 2011).

A blood vessel is fully complete when covered by pericytes and smooth muscle cells. This will occur through signalling from the ECs with factors such as PDGF. EC junctions and basement membrane proteins are also established to allow blood flow (Carmeliet and Jain, 2011).

ECs have oxygen sensors and hypoxia- inducible factors (HIFs), which are used to adapt to changes in blood flow (Carmeliet and Jain, 2011). In normal oxygen conditions, enzymes such as pro-lyl hydroxylase domain 1-3 (PHD) hydroxylate HIF1α and HIF2α, which are then degraded (Carmeliet and Jain,

2011; Stamati et al., 2011). When the environment becomes hypoxic, PHDs are no longer active, which initiates a transcriptional response by HIFs in order to provide adequate oxygen. This response up-regulates angiogenic factors such as VEGF, driving the angiogenic process (Carmeliet and Jain, 2011; Ho et al., 2006).

Vasculogenesis occurs primarily during development but has also been described in adults (Carmeliet, 2000; Drake, 2003). Developmentally, vasculogenesis relies on the differentiation of progenitor cells, or angioblasts, into endothelial cells which then aggregate together into a primitive vascular structure (Carmeliet and Jain, 2011; Carmeliet, 2000; Drake, 2003). Factors such as VEGF, VEGFR2 and bFGF are thought to induce angioblast differentiation (Carmeliet and Jain, 2011; Carmeliet, 2000). The primitive vascular structure becomes mature, organised and adapted to individual organs through remodelling, sprouting and splitting (Carmeliet, 2000; Gerhardt et al., 2003). For some organs, such as the kidneys, lungs and liver, angioblasts drive organ development through their interaction with the endoderm (Drake, 2003; Matsumoto et al., 2007).

In adults, vasculogenesis involves the differentiation of endothelial progenitor cells (EPCs) from the bone marrow or blood circulation (Phelps and Garcia, 2009). The exact source of these progenitor cells and their contribution in vasculogenesis is still somewhat controversial. However, a CD34 positive cell population has been characterised and associated with areas of neovascularisation (Phelps and Garcia, 2009). It is thought that the

differentiation of these cells into endothelial cells is driven by factors including VEGF, bFGF and IGF-1 (Carmeliet, 2000).

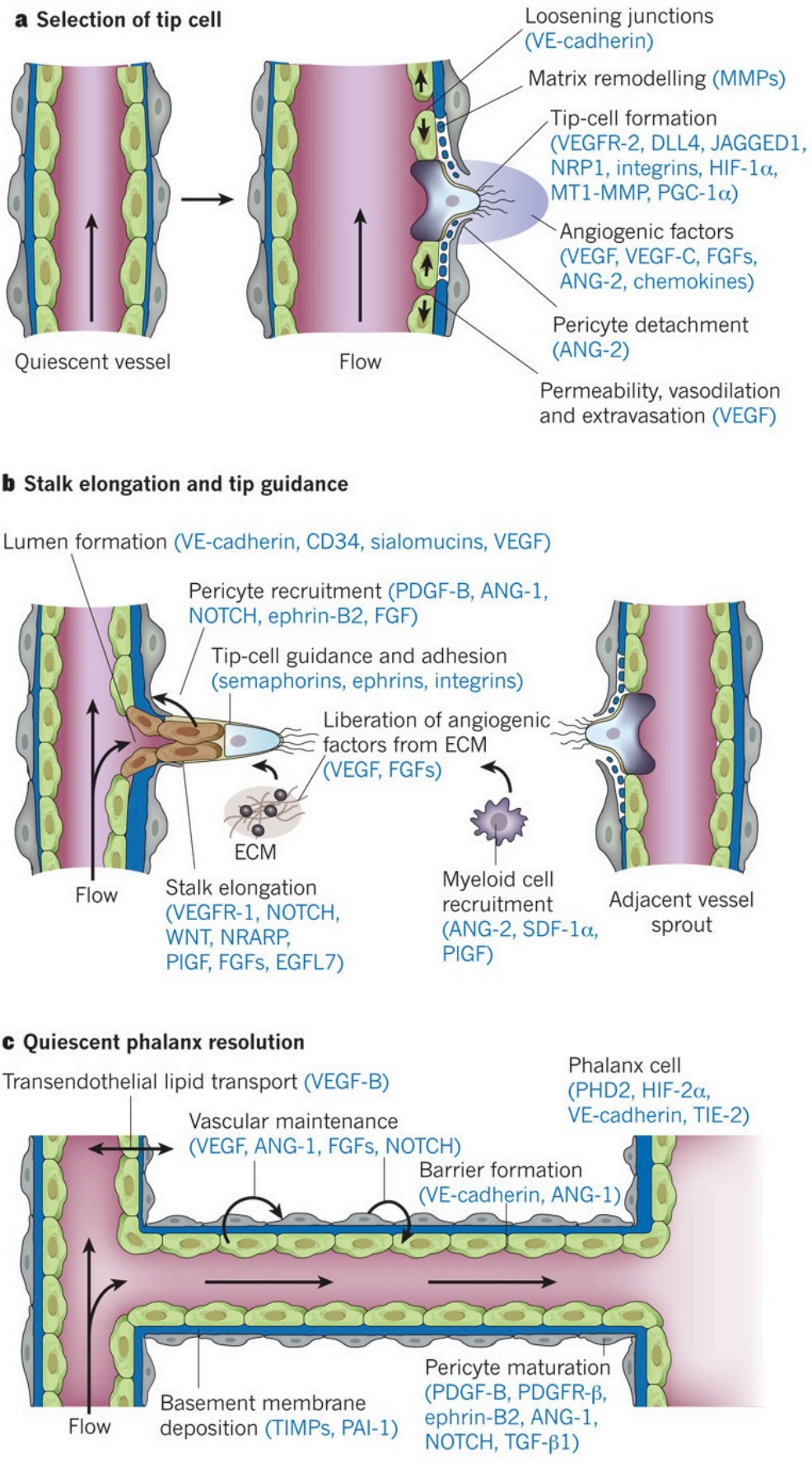

Figure 1.1. A schematic of angiogenesis by Carmeliet and Jain (2011) showing several of the factors and steps involved in the process. a) The process begins after stimulation of ECs with factors such as VEGF and bFGF and the degradation of the surrounding matrix. VE-cadherin junctions become loose, and a provisional matrix is deposited, b) tip cells start migrating using integrins to attach to the matrix and stalk cells follow. Pericytes are recruited to the area by ECs and a basement membrane is deposited, c) neighbouring branches fuse and a lumen forms. VE-cadherin junctions are re-established, the basement membrane fully forms and pericytes surround the new vessel.

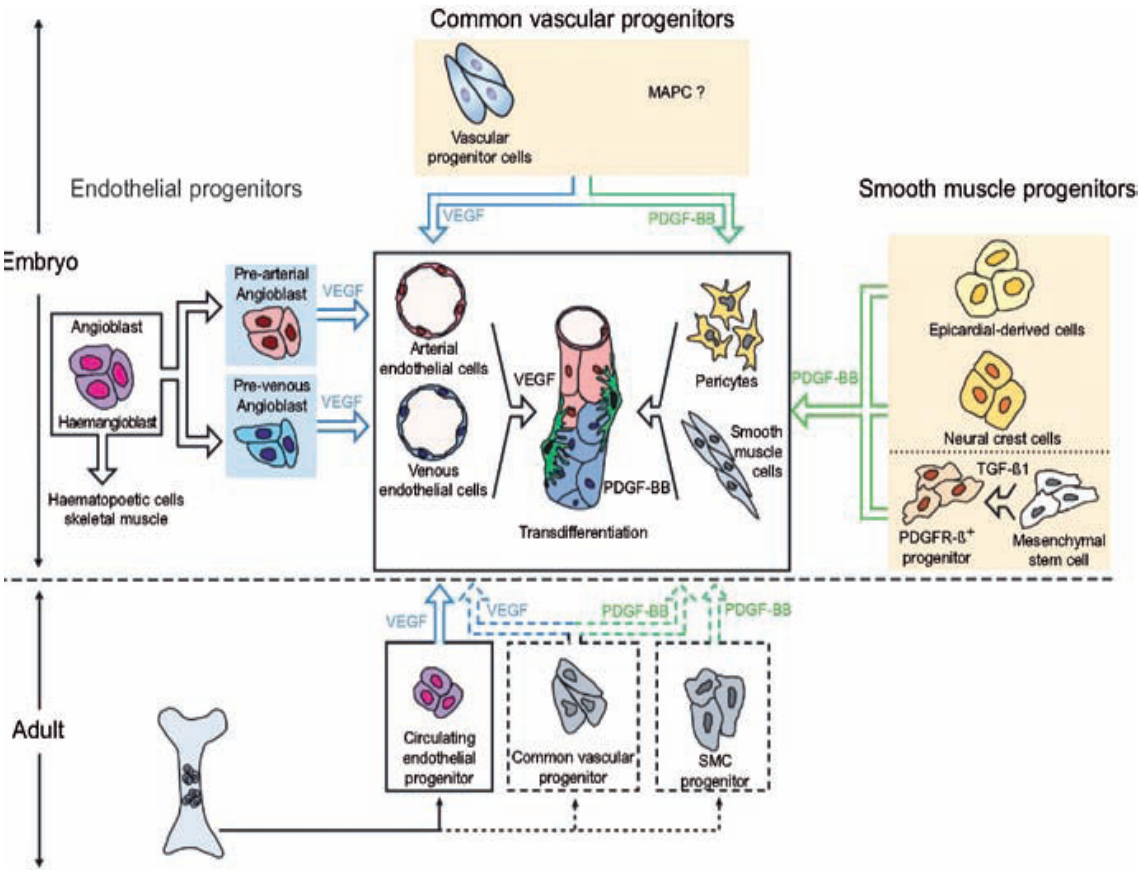

Figure 1.2. The process of cell differentiation for vasculogenesis in the embryo and adult (Fischer et al., 2006).

1.2.1 VEGF and VEGF receptors

Despite the complex interaction of various growth factors, cells and surrounding matrix in blood vessel formation, VEGF is considered a major component in both sprouting angiogenesis and vasculogenesis (Eichmann and Simons, 2012). VEGF is a family of growth factors, which consists of VEGF-A (the most common), VEGF-B, VEGF-C, VEGF-D and placenta growth factor (PIGF) (Eichmann and Simons, 2012).

The effects of VEGF are mediated through binding to its receptors, namely VEGFR1, VEGFR2 and VEGFR3. The receptors are expressed on the surface of different cell types such as endothelial cells, haematopoietic cells, macrophages, some tumour cells and vascular smooth muscle cells (Cébe-Suarez et al., 2006).

The three VEGF receptors have the same structure and contain an extracellular part, where VEGF binding occurs, one transmembrane part, a juxtamembrane domain, a split tyrosine kinase domain and a C-terminal domain (Koch et al., 2011). Receptors can form homodimers with the same receptor type (eg. VEGFR1-VEGFR1), or heterodimers, with a different receptor type (eg. VEGFR1-VEGFR2) (Koch et al., 2011). Receptor dimerization is required for receptor activation and leads to conformational changes of the intracellular part of the receptor. VEGF receptor signalling influences several cell processes after receptor internalisation (Koch et al., 2011).

VEGFR1 has a 10 times greater binding affinity to VEGFA than VEGFR2 but a lower signalling capacity (Chen et al., 2010; Koch et al., 2011). There are suggestions that VEGFR1 is not necessary for EC migration and proliferation. Instead, VEGFR1 can work as a decoy receptor, preventing VEGF action by forming heterodimers with VEGFR2 (Koch et al., 2011).

On the other hand, VEGFR2 is important for EC survival, proliferation, migration and tubulogenesis (Koch et al., 2011). VEGFR2 biology is complex and VEGFR2 can attach to various proteins such as VE-cadherin, Ephrin-B2, integrins and VEGFR3 (Eichmann and Simons, 2012). These interactions affect VEGFR2 signalling and endocytosis (Eichmann and Simons, 2012).

In quiescent ECs approximately 40% of VEGFR2 receptors are found intracellularly. There are constant changes of individual receptor molecules' location, through both fast internalisation of surface receptors and recycling of the intracellular pool (Scott and Mellor, 2009). Approximately 50% of the surface receptors are stable through attachment to VE cadherin, which occurs at EC-EC junctions (Scott and Mellor, 2009). This stabilisation by VE-cadherin inhibits VEGFR2 internalisation (Lampugnani et al., 2006; Scott and Mellor, 2009).

1.2.2 Angiopoietins

Angiopoietins (Ang) are a family of four glycoproteins Ang-1, Ang-2, Ang-3 and Ang-4 that attach and activate receptor Tie-2 or Tie-1 (indirectly though Tie-2 heterodimers) (Fagiani and Christofori, 2013). Ang-1 is involved in blood vessel remodelling and stability in adults and blood vessel maturation during

development. As with other growth factors, maintaining a balanced expression of Ang-1 is important. Mice embryos deficient in Ang-1 die in utero while over expression of Ang-1 leads to enlargement of vessels (Fagiani and Christofori, 2013). It works at different stages to VEGF during angiogenesis, with VEGF having an initial role, while Ang-1 has a later effect (Fagiani and Christofori, 2013).

Ang-1 is not normally released by ECs but by surrounding cells such as pericytes, vascular smooth muscle cells, fibroblasts and tumour cells (Fagiani and Christofori, 2013). Factors such as VEGF and PDGF as well as hypoxia increase Ang-1 expression in these cells. Ang-1 binding to Tie-2 activates several signalling pathways that lead to the survival of ECs, protecting them from apoptosis (Fagiani and Christofori, 2013).

1.2.3 PDGF

Another important factor during neovascularisation, especially for vessel stability is PDGF. PDGF is released by ECs during the angiogenic process in order to attract surrounding pericytes and smooth muscle cells to the neovascularisation area (Carmeliet and Jain, 2011). This is an important part of blood vessel maturation through the recruitment of support cells (Berthod, 2013; Carmeliet and Jain, 2011).

1.2.4 ECM and integrins

In addition to cytokines and growth factors that are known to be important for EC migration during angiogenesis, cell attachment to the extracellular matrix is equally important (Davis and Senger, 2005; Iivanainen et al., 2003).

The ECM surrounding ECs during angiogenesis influences the behaviour of the cells through integrins (Brooks, 1996). Integrins are heterodimeric receptors, which attach cells to the ECM. They consist of α and β subunits, from a group of 18α and 8β subunits (Contois et al., 2009; Iivanainen et al., 2003). Their actions regulate several cell functions (Carmeliet and Jain, 2011; Serini et al., 2006). These include growth factors, growth factor receptors and other cell surface receptors, proteases and ECM components (Contois et al., 2009). Integrins are involved in different stages of the angiogenic process by influencing several EC biological functions. At least 9 integrins have been associated to angiogenesis (Hynes, 2007). These are α1β1, α2β1, α3β1, α4β1, α5β1, α6β1, α6β4, αvβ3 and αvβ5. They are receptors to collagen (α1β1, α2β1), laminin (α1β1, α6β1, α6β4) or fibronectin (α4β1, α5β1) and are expressed on ECs, although some can vary depending on the source of ECs (Hynes, 2007).

1.3 Tissue engineering

Tissue engineering was developed in an attempt to solve immune-compatibility problems with tissue and organ transplants and address the lack of sufficient donor numbers (Kaigler et al., 2003; Kaully et al., 2009; Lee et al., 2011). It is a field that merges biological sciences and engineering by recapitulating developmental and adult biological processes (Lee et al., 2011). Tissue engineering takes advantage of the increasing knowledge of how cells are affected by signal transduction pathways, proteins and growth factors to influence cell differentiation, migration and proliferation (Lee et al., 2011). Three main strategies exist for tissue engineering practices: 1) direct delivery of the cells to the injured area or circulation, 2) cells incorporated into a scaffold to

form a tissue-like structure or 3) delivery of growth factors or drugs within scaffolds.

One of the most important and challenging aspects of tissue engineering is the successful integration of a blood supply within three-dimensional (3D) tissues (Lesman et al., 2011). This is especially important when engineering larger tissues, more than a few millimetres in size, which is more clinically relevant (Kaigler et al., 2003). Once a tissue-engineered tissue is implanted, incorporated cells compete for oxygen and nutrients with each other and with host inflammatory cells (Kaully et al., 2009). Oxygen diffusion is a critical parameter for a metabolically active tissue and if it is slower than cell consumption will lead to cell death (Kaigler et al., 2003; Kaully et al., 2009). Therefore, to ensure cell viability, most cells need to be within close proximity to blood vessels, usually within 200μm, to ensure adequate oxygen is delivered to them (Kaully et al., 2009). In the early stages post implantation, host vasculature is not sufficient to provide cells with oxygen and nutrients, which limits the engraftment and success of implants (Kaully et al., 2009). Incorporating a vascular network within these engineered tissues will therefore increase the short term and long term success of the process. In addition, an integrated vascular supply is also useful during *in vitro* culturing by influencing cell growth and organisation (Kaully et al., 2009; Lesman et al., 2011).

Tissue engineering of capillary networks is mainly based on: i) scaffolds that release growth factors, ii) cultures of ECs in 3D scaffolds or iii) decellularized matrices (Kaully et al., 2009). In the current study I have focused on the use of

co-cultures with ECs in 3D scaffolds as a strategy for engineering capillary like structures.

1.4 In vitro studies

In vitro studies mimic angiogenesis or vasculogenesis. *Ex vivo* and *in vivo* studies are also widely used as models. These include the aortic ring outgrowth assay (Nicosia, 2009; Nicosia et al., 2011), the chick chorioallantoic membrane assay (CAM) (Hudlicka et al., 1989; Primo et al., 2010; Slevin et al., 2007; West et al., 1985), the corneal assay (Staton et al., 2009) zebrafish models and other models using mice and rabbits (Staton et al., 2009). The aortic ring outgrowth assay involves placing freshly isolated vessels from animals into a 3D ECM consisting of collagen and basement membrane proteins or fibrin (Nicosia, 2009; Nicosia et al., 1994). This method tests EC migration into the surrounding matrix over a period of time. This method additionally tests EC interaction with surrounding support cells while in culture. A common *in vivo* assay, the CAM assay is a simple and relatively inexpensive way of testing substances and drugs. This is done in real time while angiogenesis is occurring in the living chick, usually through a small window in the shell of the egg (Staton et al., 2009).

The main difference between angiogenesis and vasculogenesis in *in vitro* approaches relates to the interaction of the ECs with the scaffold as shown in figure 1.3. Angiogenesis studies usually involve seeding cells on top of 3D scaffolds (Bayless et al., 2009; Davis et al., 2000; Joung et al., 2006; Montesano and Orci, 1987; Montesano et al., 1983). Initially designed by Montesano and Orci (Montesano and Orci, 1987), this method involves setting

a confluent layer of ECs on top of a scaffold. ECs migrate within the deeper layers of the scaffold and form tubular structures following the addition of exogenous growth factors such as VEGF and bFGF and/or agents such as Phorbol Myristate Acetate (PMA) (Bayless et al., 2009; Davis et al., 2000; Montesano and Orci, 1987). PMA is a tumorigenic agent that drives EC invasion within scaffolds and promotes EC tubulogenesis (Bayless and Davis, 2003; Bayless et al., 2000; Bell et al., 2001; Montesano and Orci, 1987).

The sandwich assay is another method that tests angiogenesis, where ECs are seeded on top of a collagen or fibrin hydrogel, which is then overlaid by another gel layer (Davis et al., 2000; Montesano et al., 1983). Following the setting of the second gel layer, ECs begin to organise into tubules and migrate through the collagen layers (Gagnon et al., 2002; Staton et al., 2009). The outgrowth of ECs seeded onto polystyrene beads and placed in an extracellular matrix is another method used to test EC migration and capillary structure formation, mimicking angiogenesis (Dietrich and Lelkes, 2006; Ghajar et al., 2006; Nakatsu et al., 2003; Nehls and Detlev, 1995; Vernon and Sage, 1999).

Other angiogenesis assays rely on the organisation of ECs in 2D. This can either be in the form of EC culture and organisation on top of a gel- with no migration within the gel- (collagen, matrigel, fibrin) or on tissue culture plates coated with ECM proteins (Ingber and Folkman, 1989; Kubota et al., 1988; Vailhé et al., 2001, 1997; Vernon et al., 1995).

On the other hand, vasculogenesis research uses single ECs embedded in a scaffold (Davis and Camarillo, 1996; Morin and Tranquillo, 2013). By mixing

ECs in the collagen hydrogels in the current thesis, the experiments were designed to mimic vasculogenesis.

Davis and colleagues in the USA have done extensive work using collagen hydrogels over the last two decades, both for angiogenesis and vasculogenesis. Their vasculogenesis study design involves embedding ECs in a 3D collagen hydrogel, overlaid with Phorbol Myristate Acetate (PMA) and growth factor supplemented media. The presence of these factors results in EC end-to-end network aggregation (Davis and Camarillo 1996, Salazar et al 1999, Bell et al 2001, Bayless et al 2000, Bayless and David 2002). Since the initial publication of this method, (Davis and Camarillo, 1996), subsequent publications by their group (Bayless and Davis, 2003; Bayless et al., 2000; Bell et al., 2001; Salazar et al., 1999) have focused on specific aspects of the network aggregation process.

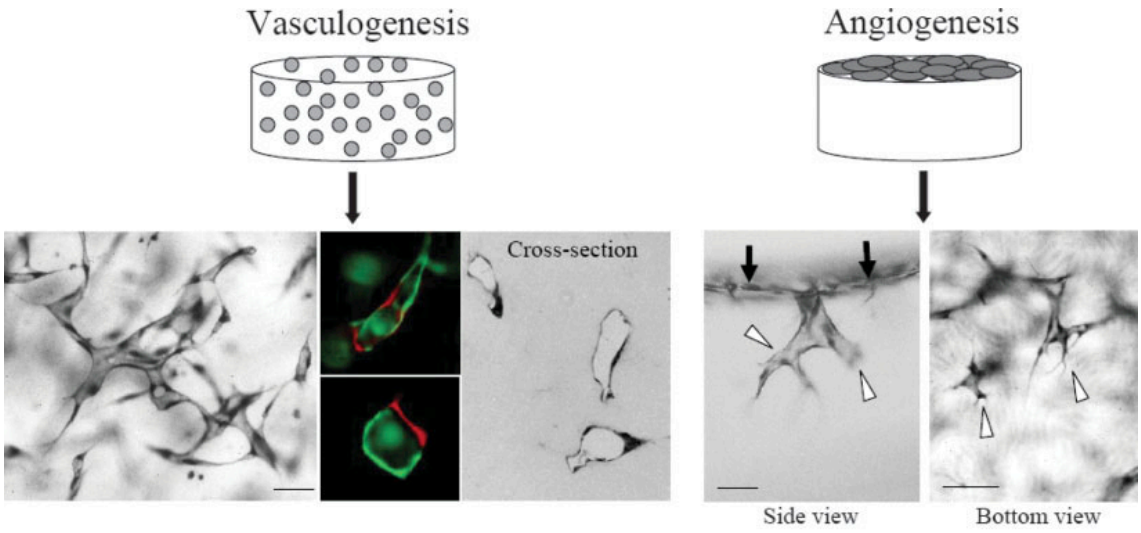

Figure 1.3. The differences in the *in vitro* study designs of vasculogenesis and angiogenesis. Vasculogenesis mimicking studies involve seeding ECs as single cells interspersed throughout the 3D scaffold. Angiogenesis assays seed cells on the surface of a 3D scaffold and rely on the migration of the ECs within the scaffold. The figure was adapted from Davis et al 2007.

Several *in vitro* studies add supplementary cells to EC cultures to support and promote tubulogenesis (Ghajar et al., 2010; Rao et al., 2012; Sorrell et al., 2009). This is mainly through the release of various angiogenic growth factors, including VEGF, bFGF and Angiopoietin-1 (Ghajar et al., 2006; Kolbe et al., 2011). Supplementary cells vary between different studies and include MSCs (Au et al., 2008; Duffy et al., 2011; Kaigler et al., 2003; Kolbe et al., 2011; Rao et al., 2012), HDFs (Kunz-Schughart et al., 2006; Newman et al., 2011), osteoblasts (Hofmann et al., 2008; Unger et al., 2007), smooth muscle cells and pericytes (Sacharidou et al., 2012; Stratman et al., 2011, 2010, 2009). The most common sources are MSCs or HDFs (Duffy et al., 2011; Morin and Tranquillo, 2013; Rao et al., 2012). MSCs and HDFs are the two supplementary cell sources chosen for the current study.

1.5 Scaffolds

The ideal scaffold for tissue engineering purposes should be: 1) biocompatible, 2) biodegradable, 3) have good mechanical properties, 4) appropriate architecture and porosity to allow for blood vessel infiltration and 5) be cost-effective (O'Brien, 2011). There are different scaffolds available, which can be natural polymers, synthetic polymers, or ceramic materials (Glowacki and Mizuno, 2007; O'Brien, 2011), each one with advantages and disadvantages (O'Brien, 2011).

Ceramic materials such as hydroxyapatite and tri-calcium phosphate are suitable for bone tissue engineering due to their good mechanical properties and biocompatibility with osteoblasts (O'Brien, 2011). These materials are therefore selected in some studies, which test the integration of capillaries into

tissue engineered bone (Bulnheim et al., 2014). They are however brittle and have poor remodelling potential once implanted (O'Brien 2011). Synthetic polymers include poly-l-lactic acid (PLLA), poly-dl-lactic-co-glycolic acid (PLGA) and poly-glycolic acid (PGA), which can be moulded into the required architecture giving them a great advantage (Liu et al., 2006; O'Brien, 2011). They can also be manipulated so that cells can attach to their surfaces (O'Brien, 2011). However, there are concerns for their biocompatibility and biodegradability once implanted *in vivo* (Liu et al., 2006; O'Brien, 2011).

A scaffold that is commonly used in studies that test angiogenesis is matrigel (Connolly et al., 2002; Grant et al., 1990; Lawley and Kubota, 1989; Staton et al., 2009). Matrigel has been used both in *in vitro* and *in vivo* studies. It is a mixture of ECM and basement membrane proteins from the Engelbreth Holm sarcoma mouse. Its exact composition is not known and can contain additional growth factors, although a growth factor reduced version is also available (Staton et al., 2009). It is very potent and can induce EC tubule formation within hours of EC plating. The presence of lumens in matrigel cultures has been debated (Bikfalvi et al., 1991), although some studies show some lumen formation (Connolly et al., 2002; Grant et al., 1991). It should be noted that matrigel has also been shown to promote network aggregation in other cells such as fibroblasts and not just ECs (Donovan et al., 2001).

Natural polymeric materials include collagen, hyaluronan, proteoglycans, chitosan and alginate (Glowacki and Mizuno 2007, Huang et al 2013, O'Brien 2011, Liu et al 2007). The main advantages of using natural polymeric materials are biocompatibility, good cell adhesion and growth properties (Brown et al., 2005; Glowacki and Mizuno, 2007; Huang et al., 2013; O'Brien, 2011). In

addition, they are biodegradable, allowing cells to remodel the scaffold and integrate with the surrounding matrix (O'Brien, 2011). The disadvantages of these materials are their poor mechanical strength and in some cases reproducibility of experimental results (O'Brien, 2011).

Collagen is one of the most widely used natural polymers (Glowacki and Mizuno, 2007). It is the most abundant extracellular matrix component found in skin, bone, tendon, blood vessels and cartilage (Liu et al., 2006). While there are more than 20 types of collagen, collagen type I is most commonly used for tissue engineering applications, either on its own or in conjunction with other materials (Liu et al., 2006; O'Brien, 2011). It can be used as a swollen hydrogel or in a lattice like structure (Glowacki and Mizuno, 2007).

The collagen used in the current study is (acetic) acid soluble rat-tail collagen I. The pH of the liquid collagen is increased using sodium hydroxide to a neutral pH to create a "cell friendly" hydrogel in which cells can be incorporated. During this process the collagen molecules aggregate into a random mesh of collagen fibrils (Brown et al., 2005). Hydrogels were selected as the main scaffold used in this study. The method of plastic compression to expel excess water and increase collagen density developed previously in this lab was used in some experiments, taking advantage of the characteristics of these constructs when spiraled into rod-like structures (Brown et al., 2005).

1.6 Developmental tube morphogenesis

Blood vessels, like other organs in the body such as the lungs and kidneys, are composed of tubular structures (Lubarsky and Krasnow, 2003). These can vary in size, shape and specialised functions but five main processes have been described during embryonic development (Lubarsky and Krasnow, 2003). These are: wrapping, budding, cavitation, cord hollowing and cell hollowing (Lubarsky and Krasnow, 2003).

Wrapping is commonly described during neural tube formation (Lubarsky and Krasnow, 2003). It involves the bending of an epithelial sheet; cells that will form the tubular structure move outwards, create an opening and separate from the epithelium until the edges meet. This forms a tubular structure that lays parallel to the initial epithelial sheet, as seen in figure 1.4a. Budding is the process in which cells grow outwards from a pre-existing tube, extending the tube structure as they branch out (Iruela-Arispe and Davis, 2009; Lubarsky and Krasnow, 2003). This is commonly described in branched structures, such as the mammalian lungs and the respiratory system in Drosophila (Lubarsky and Krasnow, 2003). It has also been compared to angiogenic sprouting (Iruela-Arispe and Davis, 2009). Cavitation involves the elimination of cells in the centre of a dense mass creating a hollow lumen, found in salivary gland formation (Lubarsky and Krasnow, 2003). In cord hollowing, which also resembles angiogenic sprouting, lumens are created between cells in a tubular cord. Finally, cell hollowing is the process in which a lumen forms within a single cell, spanning the cytoplasm of the cell. Several hollow cells fuse together to form a tubular structure (Lubarsky and Krasnow, 2003).

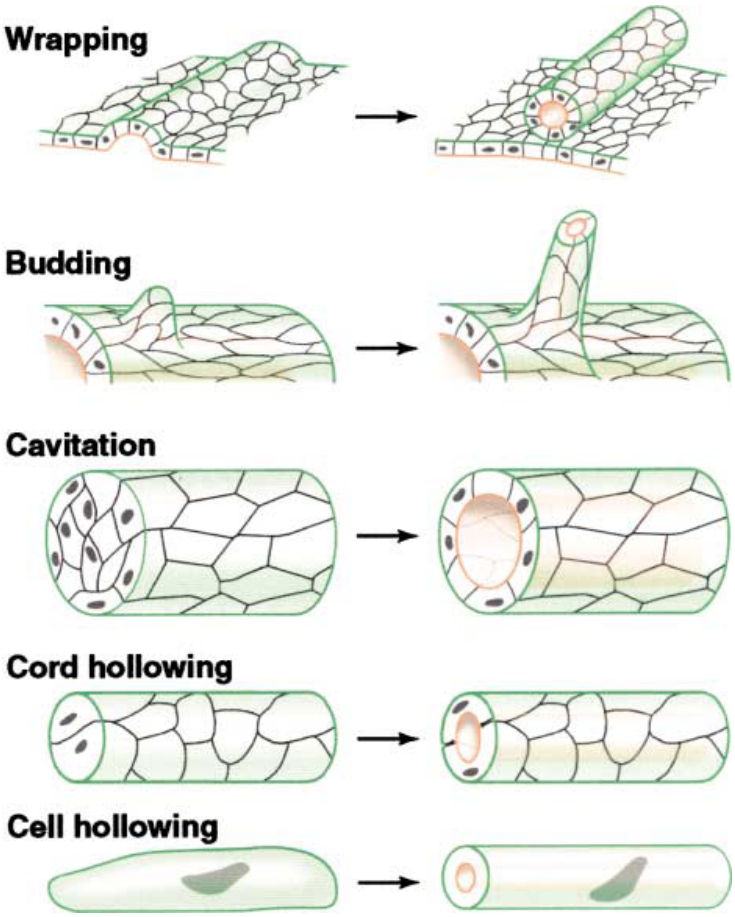

Figure 1.4. The five processes of developmental tubulogenesis. These are wrapping, budding, cavitation, cord hollowing and cell hollowing. A detailed description can be found in the text. The figure was adapted from Lubarsky and Krasnow 2003.

1.7 Thesis overview

The purpose of this study was to test in an *in vitro* 3D controlled environment how parameters involved in neovascularisation affect EC aggregation and morphology. The parameters tested were supplementary cells, as a natural source of pro-angiogenic growth factors, the addition of basement membrane proteins in the ECM and the effect of physiological hypoxia.

Initial experiments focused on the effect of cell-cell interactions, specifically with the use of HBMSCs, on EC morphology and aggregation. Once the HBMSC effect was determined, the effect of cell-matrix interactions was tested using basement membrane proteins laminin and collagen IV. Differences in EC aggregation in these different conditions were correlated to the release of angiogenic growth factors and uptake through receptor up-regulation.

Having identified the effect of HBMSCs and the ECM on EC aggregation, HDFs were used as a different source of supplementary cells. In addition, the effect of oxygen concentration was also tested and physiological hypoxia was compared to normoxia for the effect on EC aggregation.

1.8 Hypotheses under test

1. “ECs form end-to-end network structures when co-cultured with HBMSCs or HDFs in 3D collagen constructs.”

2. “Basement membrane proteins promote EC capillary like structure formation in 3D *in vitro* when added to collagen I hydrogels.”

3. “Physiological hypoxia promotes greater EC end-to-end network aggregation compared to normoxia.”

1.9 Aims and objectives

The aim of this thesis was to determine how angiogenic parameters affect EC morphology and aggregation in 3D collagen hydrogels *in vitro*.

The main objectives were:

1. Test the morphology and aggregation of HUVECs when cultured in 3D collagen hydrogels in the presence of supplementary cells and basement membrane proteins
2. Quantify angiogenic growth factor levels within the cultures in these different conditions and correlate differences to EC aggregation
3. Quantify the number and type of VEGF receptor levels within cultures and relate to VEGF uptake and EC morphology
4. Determine differences in the morphology and aggregation of ECs depending on the source of ECs used
5. Determine the effect of physiological hypoxia on EC morphology and aggregation

2 Materials and Methods

2.1 Endothelial cell culture

Human Umbilical Vein Endothelial Cells (HUVECs) were purchased from PromoCell (Heidelberg, Germany) at passage 0 and grown in complete endothelial cell growth media (EGM) (PromoCell, Heidelberg, Germany) supplemented with 10% Fetal Calf serum (50ml) (FCS) (First Link, Wolverhampton, UK) and 1% Penicillin/ Streptomycin (P/S) (Gibco, Paisley, UK). At initial plating, a seeding density of 7000 cells/cm^2 was used.

For routine cell culture, cells were cultured in T75cm^2 flasks. Flasks were checked daily for confluency, infections and growth using an inverted light microscope. When flasks were 90% confluent, they were passaged using a 1:3 ratio. For passaging, EGM growth media was pipetted out of the flasks and flasks were washed twice with 5ml Phosphate buffered saline (PBS) (Oxoid, Thermo Scientific, Loughborough, UK). Cells were detached from the culture surface by using a 10% Trypsin/EDTA solution (Gibco, Paisley, UK) (0.25%) and incubated for 5 minutes at 37°C. Flasks were checked under the microscope for rounded, floating cells. To neutralise the trypsin solution 10ml of EGM was added to the cells, transferred to a 30ml universal tube and centrifuged at 2000rpm for 5minutes. After centrifugation, the supernatant was discarded without disturbing the cell pellet and the cells were either split into new sterile flasks or used in collagen hydrogels.

For cell counting, cells were re-suspended in 4ml of EGM medium and 30µl of the cell suspension was pipetted into a clean eppendorf tube where it was mixed with an equal amount (30µl) of trypan blue (Sigma, Dorset, UK). Trypan

blue was used to stain dead cells blue, which were excluded from cell counting. Live cells were counted using a haemocytometer as shown below in Figure 2.1. The number of cells in the four 4x4 chambers were counted, averaged and the total number of cells was calculated using the formula $N= M \times V \times D \times 10^4$. M represents the mean number of cells counted, V the media volume the cells were re-suspended in, (usually 4ml) and D the dilution with trypan blue (1:1 dilution of cells and trypan blue, i.e. 2).

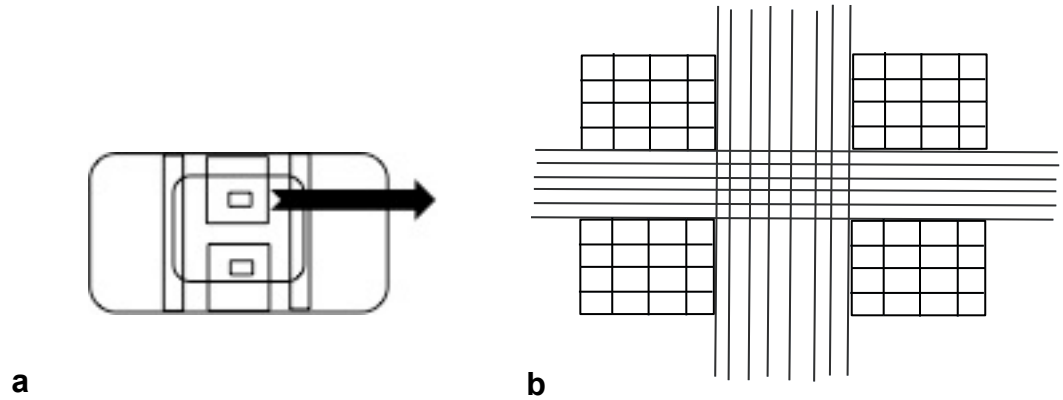

Figure 2.1. A haemocytometer was used for cell counting. a) The haemocytometer was covered with a glass coverslip, adhered on its surface, b) live cells in the four 4x4 chambers were counted and the formula $N= M \times V \times D \times 10^4$ was used to calculate the number of cells.

2.2 Collagen hydrogel preparation

Collagen hydrogels were prepared using the same basic formula for all experiments. The exact amount and dimensions of the collagen hydrogels differed depending on the experimental setup. The standard method involved using acid soluble rat tail collagen type I solution (2.05mg/ml, First Link, Wolverhampton, UK) at an 80% final volume concentration, mixed with 10%

10x Minimum Essential Medium (MEM) (Gibco, Paisley, UK). The collagen solution was neutralised by drop-wise addition of a 5M and 1M sodium hydroxide (NaOH) (AnalaR, UK) solution to reach pH~7.4. Once neutralised, the colour of the collagen solution changed from yellow to light pink (Figure 2.2). The collagen solution was mixed with the cells, in the required cell density, which was prepared in a 10% final collagen volume solution (in cell culture media). The mixed solution was pipetted into the appropriate well- plate or mould and placed in a humidified incubator set at 37°C for 30 minutes. Once gelation was complete, the corresponding media was added to culture the cells.

2.3 HUVEC only hydrogels

HUVECs were trypsinised, counted and used in collagen hydrogels as described in sections 2.1 and 2.2. Collagen hydrogels were cast using 100000 cells in 1ml of collagen, in a 12 well plate. Cells up to passage 5 only were used and experiments were performed in triplicate. Collagen hydrogels were cultured for 7 and 14 days in a humidified incubator set at 37°C, 5% CO_2, with media changes at least once a week. Media samples were kept on days 7 and 14 and stored at -80°C for VEGF and PDGF protein analysis using ELISA. Collagen hydrogels were fixed using 10% neutral buffered formalin (NBF) (Sigma, Dorset, UK) and CD31 immunofluorescence was used for image analysis.

2.4 Phorbol myristate acetate addition to HUVEC only cultures

Collagen hydrogels were prepared as described above in sections 2.2. and 2.3. Phorbol myristate acetate (PMA, Sigma, Dorset, UK) was added in 3 different

concentrations- 10ng/ml, 20ng/ml and 50ng/ml both within the collagen hydrogel (mixed within the cell suspension) and the overlying media.

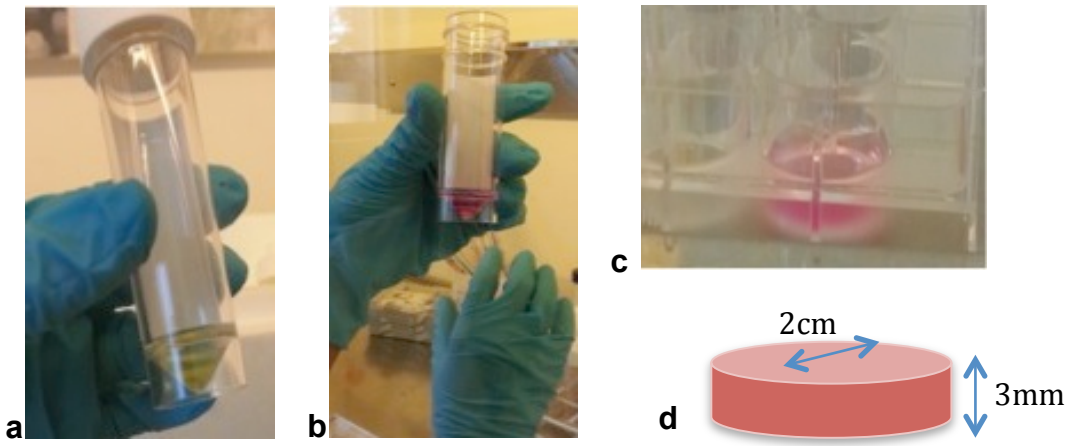

Figure 2.2. The process of collagen neutralisation and gel setting. a) Collagen solution mixed with 10xMEM before neutralisation, b) neutralised collagen solution, c) collagen hydrogel set in a 12 well plate, d) collagen hydrogel dimensions.

2.5 Human bone marrow stem cell culture

Human bone marrow stromal cells (HBMSCs) were isolated and cryopreserved from patients undergoing hip surgeries at the Royal National Orthopaedic Hospital (RNOH), with informed consent and ethical approval. Cells were isolated using the method adapted by Igarashi et al (2007). Bone marrow aspirates (8-10ml) were transferred to a sterile 50ml tube containing 10ml Dulbecco's Modified Eagle's Medium (DMEM, Sigma, Dorset, UK) supplemented with 20% FCS and 1% P/S and 1ml of heparin (1000IU) to prevent blood coagulation. Cells were centrifuged at 1500rpm for 7 minutes. After centrifugation the lipid layer was carefully removed using a sterile Pasteur pipette. An additional 30ml of culture media was added and cells were

centrifuged again at 1500rpm for 7 minutes. The supernatant above the cell pellet was removed and 30ml of media was added and the cells were well mixed. Cells were counted using the protocol described above (section 2.1) and seeded in T75cm^2 flasks initially at a density of 2x10^7. The flasks were not disturbed for the first 72 hours to allow the HBMSCs to attach to the flasks. HBMSCs attached to the flask surface and all floating cells were discarded. Once the cells reached confluency they were passaged into T225 cm^2 flasks. DMEM was removed and replenished twice a week and cells were usually passaged every 10 days.

HBMSCs were passaged at 80% confluency. This involved the removal of the culture medium, followed by two washes with 8ml of PBS and trypsinised with 8ml of Trypsin/EDTA. Flasks were incubated at 37°C for 5 minutes to detach the cells from the tissue culture flask surface. To ensure that the majority of the cells were floating, flasks were gently tapped and checked under an inverted microscope. DMEM (16ml) was added to the flask to neutralise trypsin, transferred to a universal tube and centrifuged at 2000rpm for 5minutes. DMEM was carefully removed from the universal and the cell pellet was split into new flasks in a 1:2 ratio or counted and used in collagen hydrogels.

2.6 HBMSC- HUVEC collagen hydrogels

Collagen hydrogels were cast using HBMSCs and HUVECs. Different ratios of the two cell types were mixed by maintaining a constant number of HBMSCs at 200000 cells/ml but increasing the number of HUVECs between 100000 cells/ml, 200000cells/ml, 300000cells/ml and 400000cells/ml. Cell morphology and endothelial cell aggregation were tested using CD31 immunofluorescence

as described below and media samples were kept at -80°C for VEGF and PDGF protein analysis using ELISA. HBMSC only hydrogels were also set with 200000 cells/ml for control protein analysis.

2.7 Basement membrane incorporation in collagen hydrogels

Collagen IV (mouse, BD Biosciences, Oxford, UK) or laminin (type V, mouse, BD biosciences, Oxford, UK) were added and mixed in collagen hydrogels to test the effect of basement membrane proteins on EC morphology and aggregation. Based on previously published literature (Nicosia et al., 1994) 50µg/ml of collagen IV and/or laminin was added to the cultures. Collagen IV was added to the collagen I solution prior to neutralisation and neutralised with NaOH, before mixing the neutralised solution with the cells. Laminin was added and mixed with the cell suspension prior to mixing with the neutralised collagen solution. Basement membrane proteins were added in both HUVEC only cultures and HBMSC-HUVEC co-cultures.

Constructs were fixed in 10% NBF and were stained with an anti-CD31 antibody and DAPI for cell nuclei (vectashield mounting medium, Vector labs, Peterborough, UK) to test cell morphology and aggregation. Cells that stained positive with both anti-CD31 and DAPI were ECs, while cells that stained with DAPI but were CD31 negative were HBMSCs. The supernatant was kept at -80°C for VEGF and PDGF protein analysis using ELISA.

2.8 Integrin α6 blocking

To test the effect of cell attachment to laminin, anti-integrin α6 antibody (GoH3, Chemicon International, California, US) was added to the cultures. Therefore, while laminin was present in these cultures, α6 integrin blocking prevented

attachment of cells to this protein. Integrins α6β1 and α6β4 are laminin receptors on ECs. Laminin attachment was blocked using 40 µg/ml of the anti-integrin α6 antibody as recommended by the manufacturer. This was done in HUVEC only cultures and HBMSC-HUVEC cultures in collagen-laminin hydrogels. Constructs were cultured for a week and CD31 immunofluorescence was used to test the morphology and aggregation of the HUVECs. In HUVEC only cultures cell morphologies were quantified and compared to HUVEC only cultures with laminin. For HBMSC-HUVEC co-cultures with the anti-integrin antibody, CD31 immunofluorescence was used to test differences in cell morphologies compared to laminin co-cultures.

2.9 CD31 immunofluorescence

For immunofluorescence, collagen whole mounts were used. Collagen hydrogels were fixed in 10% NBF for 1 hour and then washed in PBS 3 times for 10 minutes. Hydrogels were then placed in 1% Bovine serum albumin (BSA) (Sigma, Dorset, UK), 0.2% Triton X (Sigma, Dorset, UK) and PBS solution for 1 hour for permeabilisation and blocking. Hydrogels were then washed again in PBS 3 times for 10 minutes, followed by incubation in anti CD31 mouse primary antibody (JC70/A from Abcam, Cambridge, UK) for 48 hours at 4°C. Following incubation, hydrogels were washed again thoroughly in PBS (3x10 minutes) and incubated with 2^{o} antibody Alexa Fluor 488 goat anti mouse IgG (H+L) (molecular probes, life technologies, Paisley, UK) for 2.5 hours at room temperature. Hydrogels were washed again in PBS for 30 minutes (3x10mins), mounted on glass slides with a drop of DAPI mounting medium (Vector shield, Vector Laboratories, Peterborough, UK) and covered with a coverslip.

Constructs were viewed using an upright fluorescent microscope (Olympus BX61) or a Zeiss LSM confocal microscope.

2.10 Image analysis

Images were captured using the Olympus BX61 microscope or a Zeiss LSM70 confocal microscope. Data were obtained from 8-10 images per sample, from different fields of view and Image J (NIH, USA) software was used for image analysis.

HUVECs were categorised into different cell morphologies, as determined mainly by the 2D characteristics of the cells, stained with CD31. The criteria used to categorise EC morphologies were: cell size, cell shape, cell-cell interactions and proximity, cell processes and cell height.

Cells were initially grouped into spindle-like morphologies and polygonal morphologies. The 2D surface area occupied by the cells was measured in the two polygonal morphologies. The presence or absence of cell processes extending from the cells was also noted as part of the cell shape classification. The intensity of the CD31 staining on the cell surface and the proximity to other HUVECs in culture were also criteria used to categorise cells into different morphologies. Cells were categorised into these groups and the percentage of each type of morphology in each culture condition was calculated at each time-point.

Confocal micrograph images were used to assess the 3D morphology of HUVECs, in HUVEC only cultures. The 3D morphology was quantified by

measuring the height of the HUVECs on day 7 and 14. This was especially useful for determining differences between the polygonal cell morphologies that appeared similar in 2D. Specifically, the height of the cells was measured using confocal micrograph images. This was done by counting the number of views in which individual cell nuclei were visible and correlated to the depth within the construct, in micrometres.

In co-cultures with HBMSCs with and without laminin, the criteria described above were used to classify HUVECs within the cultures. In co-cultures with added laminin, HUVECs also aggregated into end-to-end networks by fusing and attaching to neighbouring ECs. A structure was characterised as a network if it contained more than 2 ECs and contained visible nuclei. These networks were measured in length in micrometres using Image J software.

2.11 VE Cadherin immunofluorescence

Whole mount collagen hydrogels seeded with HBMSCs and HUVECs with or without laminin were fixed in 10% NBF for 1 hour and then washed in PBS 3 times for 10 minutes. They were permeabilised in 1% Bovine serum albumin (BSA) (Sigma, Dorset, UK), 0.2% Triton X (Sigma, Dorset, UK) in PBS for 1 hour at room temperature. Hydrogels were then washed again in PBS 3 times for 10 minutes, followed by incubation in anti VE cadherin mouse primary antibody (F-8: sc-9989, Santa Cruz Biotechnology, Texas, USA) overnight at 4°C. Following incubation, hydrogels were washed again thoroughly in PBS (3x10 minutes) and incubated with 2^{o} antibody goat anti mouse Alexa Fluor 488 (Abcam, Cambridge, UK) for 2.5 hours at room temperature. Hydrogels were

washed again in PBS for 30 minutes (3x10 minutes), mounted on glass slides with a drop of DAPI mounting medium (Vector labs, Peterborough, UK) and coversliped. Constructs were viewed using an upright fluorescent microscope Olympus BX61. The distribution of the staining was noted for differences between the two culture conditions.

2.12 Protein analysis –ELISA

Enzyme Linked Immunosorbent assay (ELISA) kits were purchased from R&D systems (Abingdon, UK). The protocol was provided with each individual kit and was followed precisely, as recommended by the manufacturer. ELISA is a quick and reproducible method for quantifying proteins present in media, serum and tissue samples. ELISA kits contained one 96 well plate, protein standards, an antibody conjugate, a substrate solution, a wash buffer and a stop solution. Microplates were purchased pre-coated with the appropriate capture antibody for the protein tested (Figure 2.3).

Each sample and control was assayed in duplicate and averaged to ensure the accuracy of the readings. Standards were diluted as directed in the protocol (slightly different between proteins tested) to obtain a standard curve of different protein dilutions. The standard curve was always run in parallel to the experimental samples and an equation in the form of y=ax+b (example shown in Figure 2.4) was obtained.

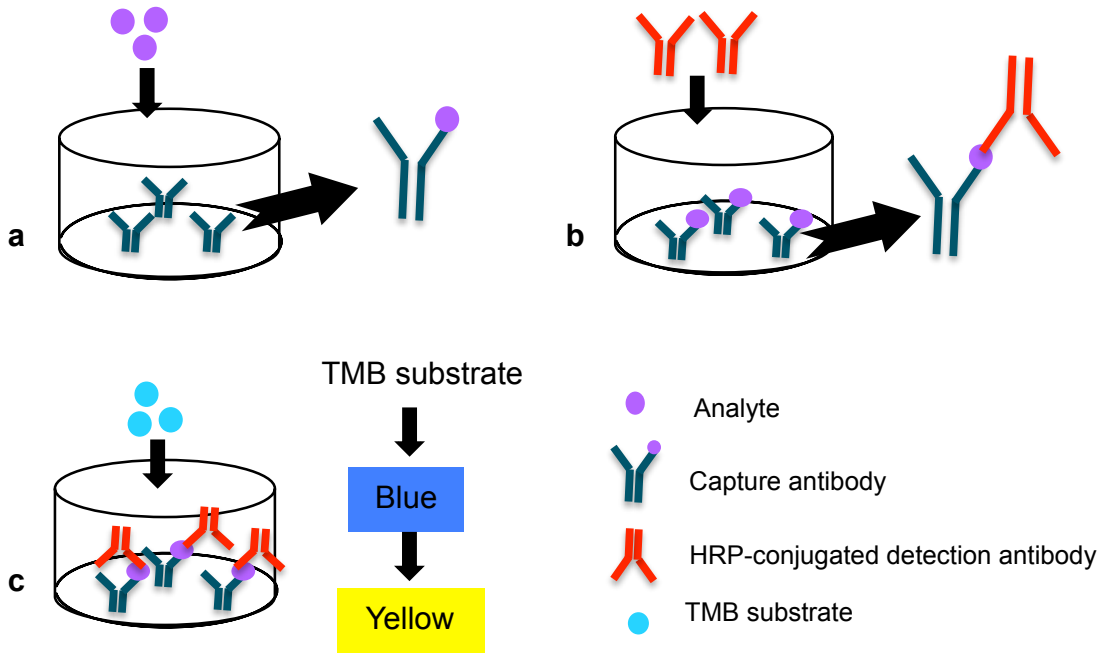

Figure 2.3. ELISA principles. a) Culture media containing the protein/analyte is added to the well, which binds to the capture antibody. Any excess analyte is washed away, allowing for the conjugated detection antibody to bind to the analyte, b) the analyte at this stage is already bound to the capture antibody on the plate, c) the substrate solution is added and changes the colour of the solution to blue. The stop solution turns the colour yellow, which is then read on a microplate reader.

The exact quantity of each solution used and the incubation timings differed depending on the protein assayed. A detailed description of them can be found in table 2, which includes all proteins assayed in this study. The first step of the process involved pipetting the appropriate amount of assay diluent (table 2.1) into each well. Media samples and standards were then pipetted into the 96 well plates carefully noting where each sample was placed. The plate was sealed with a plate sealer provided in the kit and incubated for 2 hours at room temperature. At this stage the antibody that was coated onto the microplate bound any analyte present in the culture media. The excess liquid was removed

and washed away thoroughly with the wash buffer. The washing stage was critical for the accuracy of the readings. The wells were washed three times and the plate was gently tapped onto paper towels to remove all excess liquid. HRP conjugated detection antibody was then added to each well, covered with a plate sealer and incubated at room temperature. Following the incubation, the plate was washed again thoroughly three times. The tetramethylbenzidine (TMB) substrate solution was added to the wells, leading to a change in colour from colourless to blue. The intensity of the colour was proportional to the amount of analyte (i.e. protein) present. The plate was incubated in the dark for 30 minutes (20 minutes for VEGF) and the colour development was stopped with the addition of 50µl of stop solution to each well. The stop solution turned the colour from blue to yellow. The colour absorbance was measured using a plate reader at 450nm with wavelength correction set at 570nm.

	Assay diluent	Sample/ standard	Conjugate	Substrate solution	Stop solution
VEGF	50µl	200µl-2hrs	200µl-2hrs	200µl- 20mins	50µl
PDGF	100µl	100µl-2hrs	200µl-1.5hrs	200µl- 30mins	50µl
bFGF	100µl	100µl-2hrs	200µl- 2hrs	200µl-30mins	50µl
Ang-1	100µl	50µl-2hrs	200µl-2hrs	200µl - 30mins	50µl
TGFβ_1	50µl	50µl-2hrs	100µl-2hrs	100µl- 30mins	100µl

Table 2.1. Protein levels were quantified using ELISA. ELISA kits were purchased for VEGF (generic), PDGF, bFGF, TGFβ_1 and Angiopoietin-1. The table shows the solution volumes and incubation timings used for each solution for the different proteins.

The readings for the standards were used to plot a standard curve and the equation was used to convert all sample readings into pg/ml. An example of a protein standard can be seen in Figure 2.4.

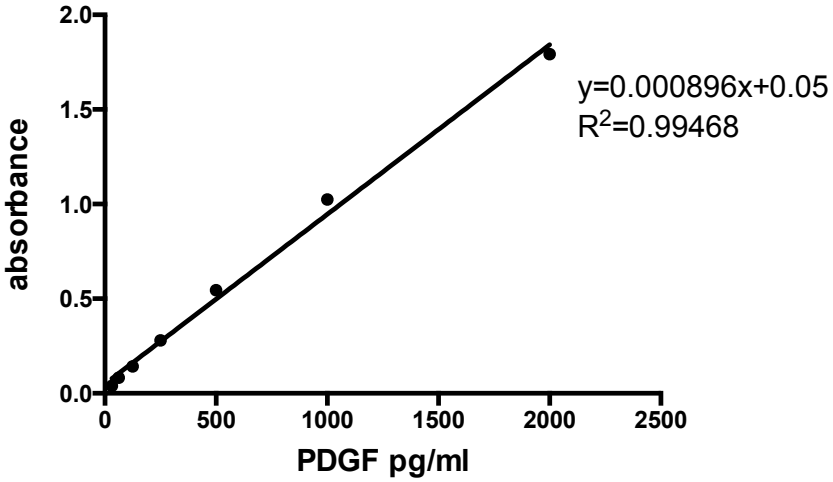

Figure 2.4. Example of a PDGF standard curve. The equation was used to convert the readings into pg/ml for each experimental sample.

2.13 Flow cytometry for VEGFR1 and VEGFR2

Flow cytometry is a laser-based technique that allows the analysis of various biological, chemical and physical characteristics of cells. It can be used to obtain qualitative and quantitative characteristics of cells. These characteristics can relate to the size of the cells, their complexity, DNA and RNA content and the presence of various membrane bound or intracellular proteins. Antibodies conjugated with fluorescent dyes can bind these proteins and can be used to quantify the percentage of cells that specifically express these proteins (Brown and Wittwer, 2000). The principles of flow cytometry can be seen in the schematic below, in Figure 2.5. The forward light scatter on the flow cytometer

provides information on the size of the cells while the side scatter gives information on the granularity of the cells.

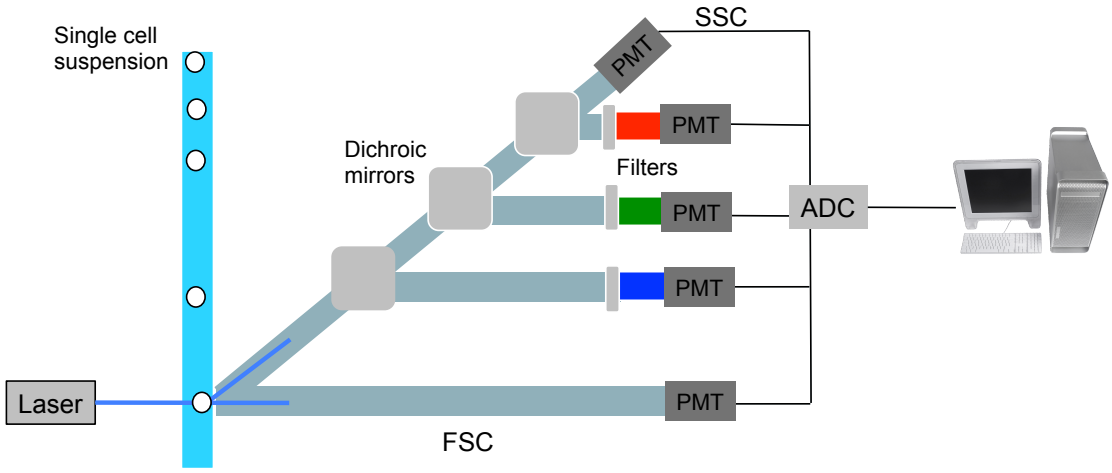

Figure 2.5. Schematic of the principles of flow cytometry. The well-mixed cell suspension passes through the cytometer where it intersects the argon-ion laser. Forward light scatter (FSC) detectors and side scatter light detectors (SSC) collect the signals and provide information on cell size and granularity respectively. Fluorescence emission detectors can be used to distinguish different cell populations. The signals are digitally converted for analysis on a computer screen (ADC- analogue digital converter) (Brown and Wittwer, 2000).

Collagen hydrogels were set and cultured as described above. Flow cytometry analysis was used to quantify VEGF receptor levels in collagen vs collagen-laminin constructs. Specifically, HUVEC only constructs with and without laminin and HBMSC-HUVEC co-culture constructs with and without laminin were analysed on day 2 and day 7.

Collagen constructs were digested using collagenase type IV (Sigma Aldrich, Dorset, UK) on a shaker, at 37°C for 30 minutes. Cells were centrifuged, placed in media and incubated at 37°C on a shaker for 4 hours to enable the regeneration of the receptors, as suggested by the manufacturer. $1x10^5$ cells (in 25µl) were function blocked using mouse IgG (R&D systems, Abingdon, UK) for 15 minutes at room temperature. Cells were washed and stained separately with 10µl phycoerythrin (PE) conjugated anti-VEGFR1 or anti-VEGFR2 (R&D systems, Abingdon, UK), as recommended by the manufacturer and published in (Imoukhuede and Popel, 2012, 2011). Tubes were incubated on ice for 30 minutes and then washed with stain buffer (PBS 0.5% BSA, EDTA) twice. Cells were re-suspended in 200µl stain buffer for flow cytometry analysis. In co-cultures, 5µl FITC conjugated anti CD31 antibody (BD biosciences, Oxford, UK) was also used to distinguish endothelial cells from HBMSCs. Cells stained with an isotype were also used as controls to calculate the number of PE positive cells.

Flow cytometry was performed using BD LSRII. Tubes were mixed well before they were placed in the flow cytometer and 5µl 7aminoactinomycin D (7AAD)(BD pharmigen, Oxford, UK) was added to exclude dead cells. At least 10000 events were collected for each sample.

For data analysis, the FlowJo software (version 10.0, TreeStar, USA) was used. To obtain the percentage of HUVECs positive for VEGFR1 and VEGFR2 several steps were followed. Cells stained with an isotype control without 7AAD were first used to gate for live cells. This was done by plotting a graph of 7AAD (laser PE-Cy5-A) against the linear forward scatter (FSC-A) as shown in Figure

2.6a. The cells stained with the isotype and 7AAD were then used to quantify the percentage of live cells in the culture (Figure 2.6b). This was applied to all the data. For each different experimental parameter this was repeated with the appropriate cells.

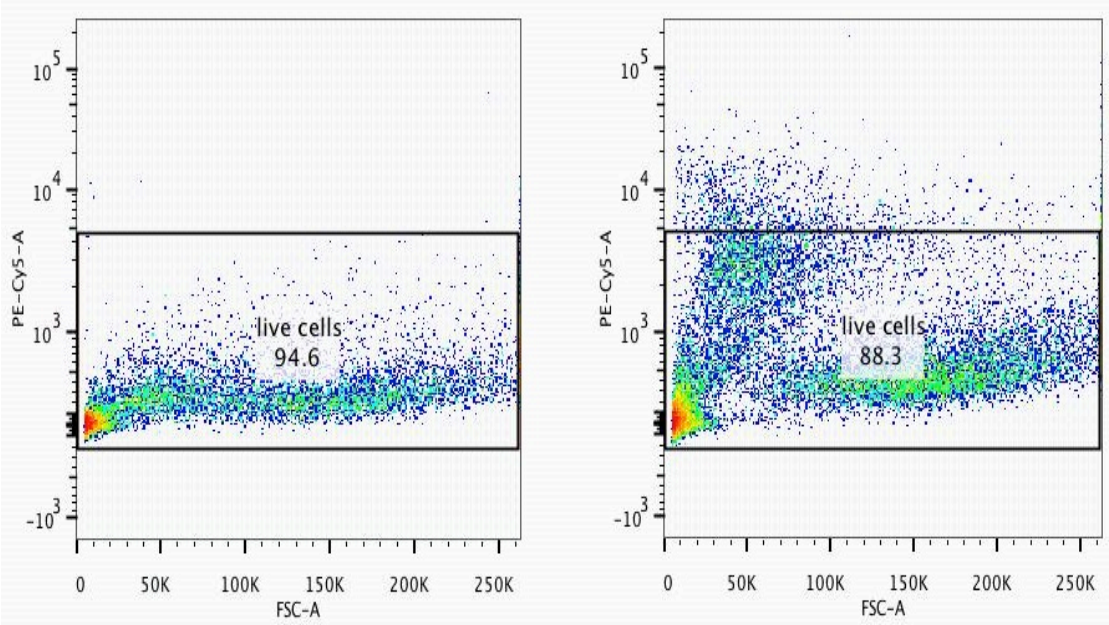

a **b**

Figure 2.6. Gating for live cells. a) HUVECs stained with isotype only were placed in the cytometer and run. PE-Cy5-A without 7AAD was plotted against FSC, b) HUVECs stained with isotype and with 7AAD were placed in the machine and using the information from a) the percentage of live cells was obtained.

Once the percentage of live cells in the cultures was calculated, the percentage of PE positive cells (VEGFR1 or VEGFR2) was quantified. A Side Scatter (SSC-A) graph against PE-A (VEGFR1 or VEGFR2) was plotted using the isotype control cells. The PE positive area on the right of the graph, as shown in figure 2.7a was gated and applied to the live cell populations of all samples.

For HUVEC only cultures this quantified the percentage of HUVECs that were both alive at the time of running the experiment and positive for either VEGFR1 or VEGFR2. In co-cultures, the addition of an anti-CD31 antibody was necessary to distinguish the HUVECs from either the HBMSCs or HDFs. Cells this time were gated for FITC (Alexa Fluor 488) on the control isotype live cells, similar to the PE positive cells and applied to all the live cells that were also PE positive. Thus, as can be seen in the example in Figure 2.7b a high percentage of cells (93.6%) were CD31 positive. This suggested that the majority of PE positive cells were indeed HUVECs.

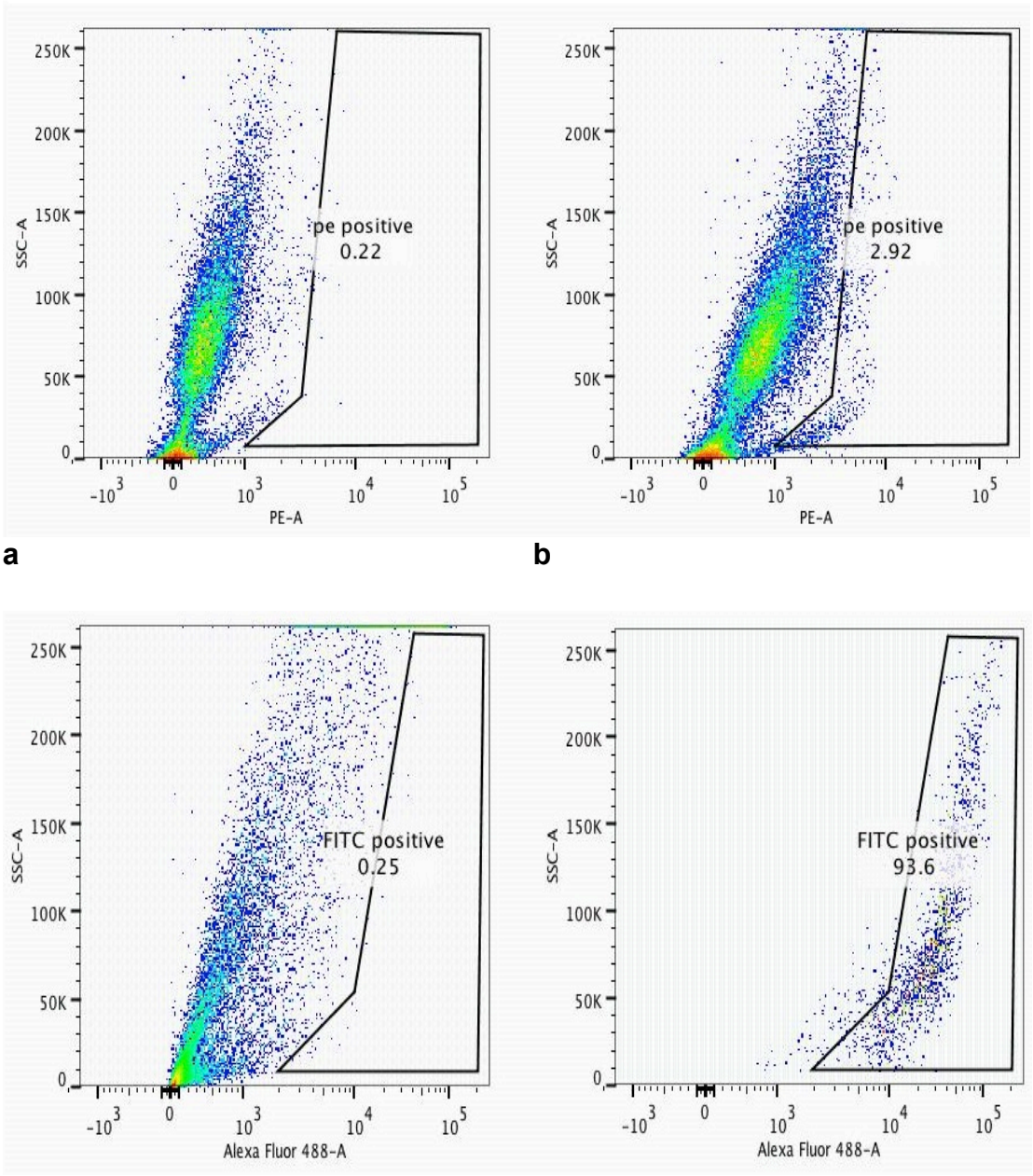

Figure 2.7. Gating for PE and CD31 positive cells. Examples of a) isotype control HUVEC only, gating PE positive cells, b) PE positive HUVECs in HUVEC only culture, c) isotype control in co-cultures used to gate for FITC (CD31) positive cells, d) FITC positive cells that were also PE positive. SSC-side scatter

2.14 Number of VEGFR1 and VEGFR2 per cell

Quantibrite PE beads were purchased from BD biosciences (Oxford, UK). Each tube contained pellets of beads, conjugated with four quantities of PE. They were used to convert the amount of fluorescence per cell to the number of receptors per cell (Figure 2.8). The beads were run on the flow cytometer separately from the experimental tubes, but using the same settings as those for cell data acquisition.

A linear side to forward scatter plot was used for gating PE bead singlets (Figure 2.8a). A histogram of the bead singlets against PE was plotted, with the four peaks representing the four different PE quantities, as seen in Figure 2.8b. The four peaks were selected on the histogram and the fluorescence geometric means were calculated using FlowJo (version 10.0.6 CA, USA) (Figure 2.8c). By using the number of PE molecules/bead provided by the manufacturer, a calibration curve was plotted. The lot specific values for the Quantibrite beads purchased were: high=62336 molecules/bead, medium-high=23843 molecules/bead, medium-low= 5359 and low=474 molecules/ bead. A curve was plotted for log molecules/bead vs log geometric means. The curve was fitted by linear regression y=ax+b and by solving for x= $\log_{10}$ (PEmolecules/cell) (eg. x= $\log_{10}$ (geometric mean+1.0381) /1.0033) the number of receptors bound per cell was calculated.

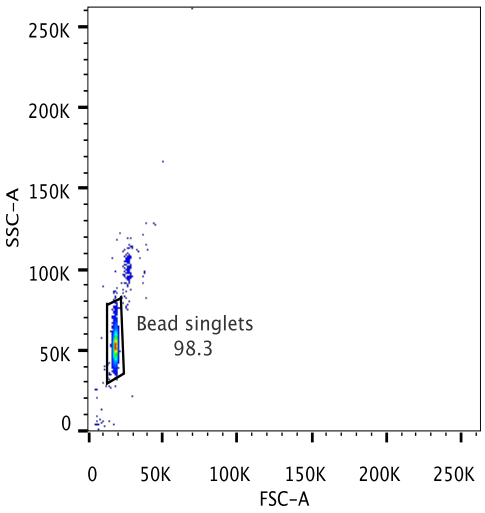

a

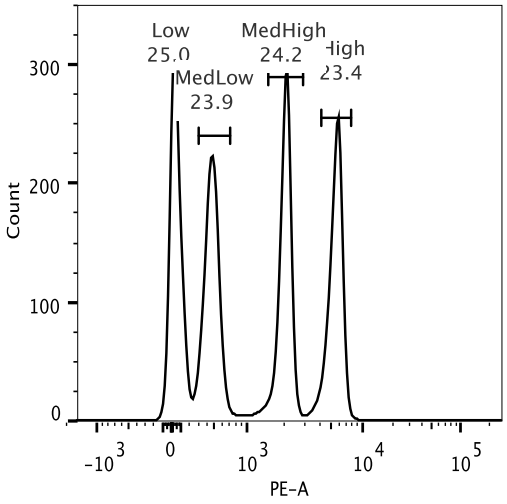

b

	Geometric means	Log geometric means	PE molecules/bead	Log molecules
Low	44.3	1.646	474	2.675
Med Low	509	2.706	5359	3.729
Med high	2223	3.346	23843	4.377
High	5980	3.776	62336	4.794

c

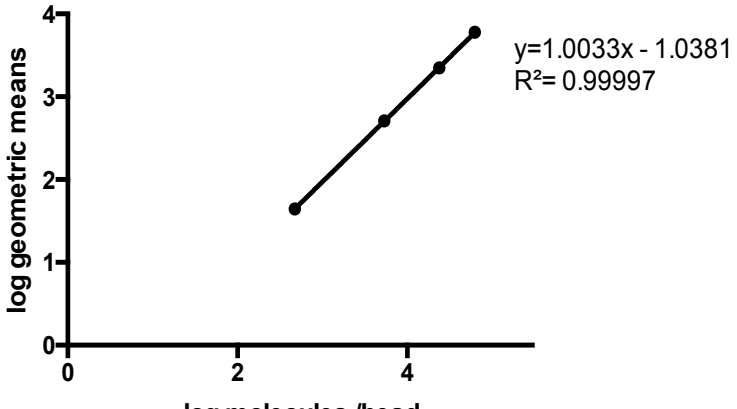

d

Figure 2.8. Flow cytometry of quantibrite beads used for calibration of fluorescence intensity. a) The quantibrite beads were analysed using a side vs forward scatter plot. Cells were selected and a histogram (b) was plotted to select the four peaks representing the 4 fluorescence quantities, c) the table shows an example of the geometric means calculated for the beads and d) shows an example of the standard curve obtained for the beads.

For the experimental samples, cells were gated as described above for live and PE positive cells. In co-cultures, CD31 positive cells that were also PE positive were selected. A side scatter vs forward scatter plot was graphed and cells were selected on the basis of their size and granularity. Cells between 50K and 100K on the forward scatter and 50K-125K on the side scatter were selected. This limited the number of clusters of cells, but also limited the amount of debris or disintegrated cells analysed.

The geometric means of the single cell population was then calculated using FlowJo. The standard curve equation was then used to convert the geometric means into the number of PE molecules per cell, i.e the number of receptors per cell.

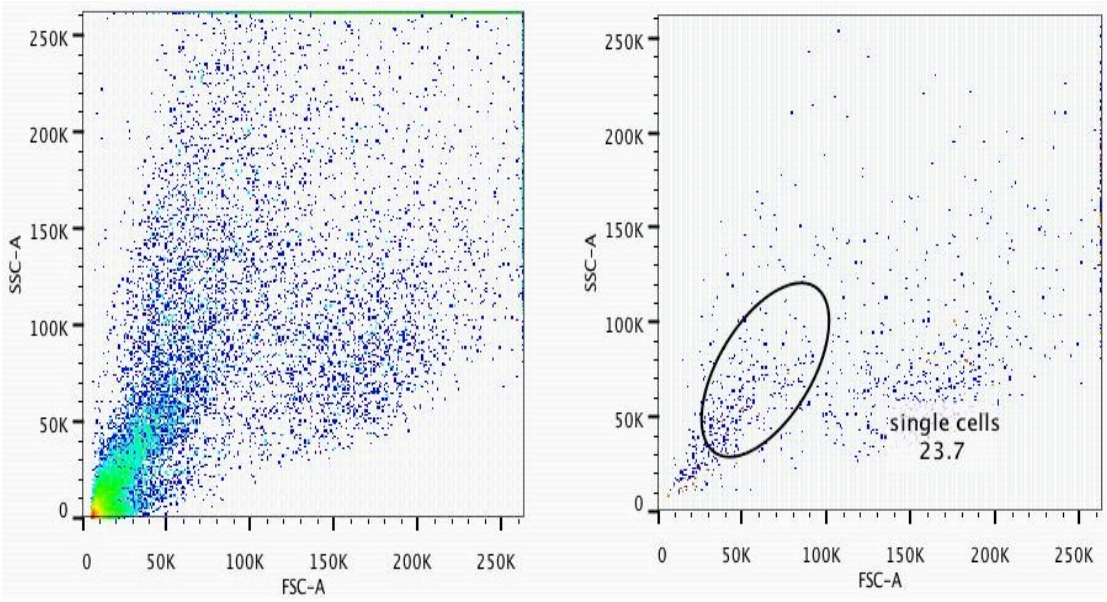

a **b**

Figure 2.9. Single cell selection. a) SSC vs FSC plot of the whole cell population, b) single cells were selected from the PE positive cell population (in co-cultures CD31/PE double positive cells). The single cell population was used to quantify the number of receptors per cell.

2.15 Human Dermal Microvascular Endothelial Cells culture

Adult human dermal microvascular endothelial cells (HDMECs) were purchased from Invitrogen (Paisley, UK) at passage 1 and plated in four T25cm^2 flasks at a density of 5x10^3 cells as recommended by the manufacturer. Flasks were pre-treated with 3ml of attachment factor (Invitrogen, Paisley, UK) for 30 minutes at 37°C, which was removed prior to plating the cells. The vial of cryopreserved cells was warmed for a few seconds in the palms of the hands, before the addition of 1ml of pre warmed Medium 131 (Invitrogen, UK) supplemented with microvascular growth supplement (Invitrogen, Paisley, UK) and 1% P/S. Cells were centrifuged, the supernatant removed and the cells were plated in the pre-treated flasks with 5 ml of medium 131. For routine culture, cells were grown in T75cm^2 pre-treated flasks and passaged in a 1:2 ratio. Cell passaging and counting was followed as for the HUVECs. Cells were used up to passage 6 for all experiments.

2.16 HDMECs collagen hydrogels and collagen-laminin hydrogels

Collagen hydrogels were set using 100000 HDMECs as described for HUVECs. Laminin was also added in the collagen hydrogels and the morphology and aggregation of the cells was compared. Co-cultures with HBMSCs with and without laminin were also set using 200000 HBMSCs and 400000 HDMECs, which was established from HUVEC cultures as the best ratio for EC morphology. The morphology and aggregation of the cells was tested using CD31 immunofluorescence.

2.17 HDMEC culture image analysis

HDMEC image analysis was done using the same criteria used for HUVEC only cultures and co-cultures (section 2.10).

2.18 Collagen hydrogel compression

Collagen hydrogels were prepared using the same basic method as described in 2.2. Three million HBMSCs were seeded in a 5ml final volume collagen hydrogel and cast in one of the two compartments of a rectangular mould, placed on a glass slide. Each chamber of the mould measured 33x22x10 mm^3. Following the 30-minute gelation stage, (at room temperature) constructs were compressed to expel 90% of the water, resulting in a compacted, ~11% collagen density construct (Brown et al 2005). The process of compression involved placing the collagen hydrogel onto three layers of Whatman's filter paper (grade 1, 150mm diameter) and a nylon mesh. Another nylon mesh was placed on top of the gel to protect it from the mould and glass slide (120grams) which were placed on top of the collagen construct in order to speed up the process of compression.

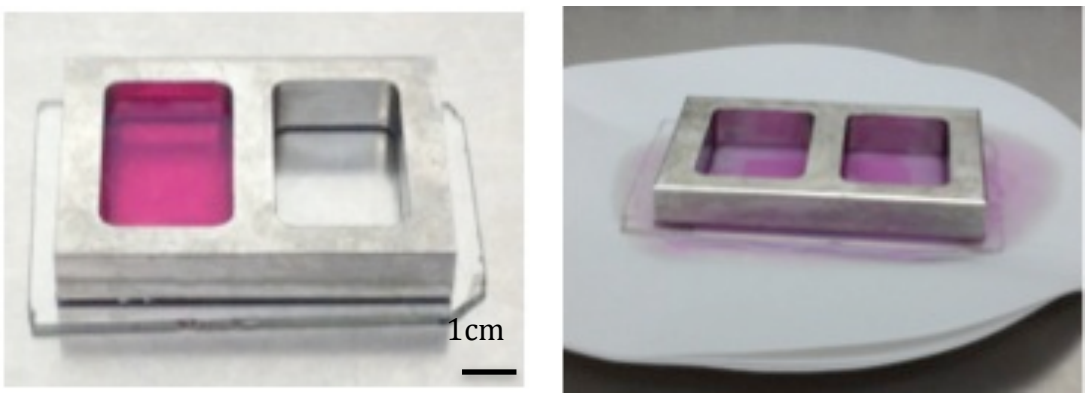

a **b**

Figure 2.10. Collagen hydrogels were set in a) stainless steel moulds and b) compressed into flat sheets using the weight of the glass slide and stainless steel mould.

Following a 5-minute compression, the glass slide and mould were removed. The compressed sheet of collagen measuring ~100μm was spiralled on its short axis using a sterile scalpel blade, to form a tightly spiralled cylindrical rod (Figure 2.11).

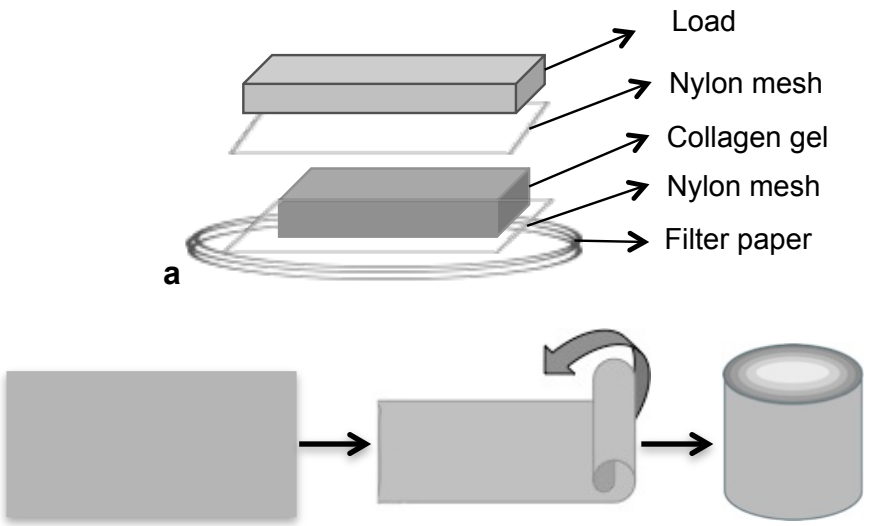

Figure 2.11. A schematic of the process of collagen hydrogel compression and spiralling. a) Following the 30-minute gelation, the constructs were placed on filter paper, sandwiched between two nylon meshes and compressed using the weight of the glass slide and stainless steel mould, b) the resulting flat sheet was then spiralled on its short axis. Spiralled constructs measured ~2.3mm in diameter and 21mm length.

2.19 Segregated co-cultures of HBMSCs and HUVECs

Triplicate samples of compressed, spiralled HBMSC constructs were set. Constructs were cut into 4 equal pieces and placed in a mould where freshly neutralised collagen hydrogel covered the spiral and the mould. The mould used was 38x30x4 mm in size, (internal dimensions 30x14x4 mm), with dividers

allowing for compartmentalisation of different cell seeded collagen hydrogels (figure 2.12a).

HBMSC constructs were split into four groups: i) the spiral was placed in a hydrogel with or without HUVECs on the same day it was compressed and spiralled (day 0) ii) the construct was snap-frozen in liquid nitrogen on day 0 and then placed in the hydrogel, iii) the HBMSC spiral was cultured for a week and then placed in a hydrogel or iv) pre-cultured for a week, snap frozen in liquid nitrogen and then placed in the hydrogel with or without HUVECs.

HBMSC spirals were placed in acellular hydrogels to test the presence of angiogenic growth factors in the area of the spiral versus the acellular area. In other constructs, HUVECs were seeded in the hydrogels and were only present in the area of the hydrogel away from the spiral (Figure 2.12). Hydrogels were cultured at 37°C 5% CO_2, 21%O_2 for 1 week.

Acellular hydrogels were used for protein analysis. At the end of 1-week culture the constructs were cut in two parts: region 1 was where the HBMSC construct was present, while region 2 was the acellular part (Figure 2.12). The gels were snap frozen and stored at -80°C. Constructs were then powdered using a pestle and mortar to release the protein trapped within the matrix. The medium used to culture the constructs was also kept for ELISA analysis of VEGF, PDGF and bFGF. Hydrogels with HUVECs were fixed in 10% NBF for CD31 immunofluorescence staining and the medium was kept at -80°C for ELISA analysis.

2.20 Image analysis

Whole mounts of collagen constructs were stained for CD31 and viewed using the upright fluorescent microscope. Images were captured and analysed for HUVEC morphology using the criteria used for the HUVEC only constructs and co-culture constructs (section 2.10).

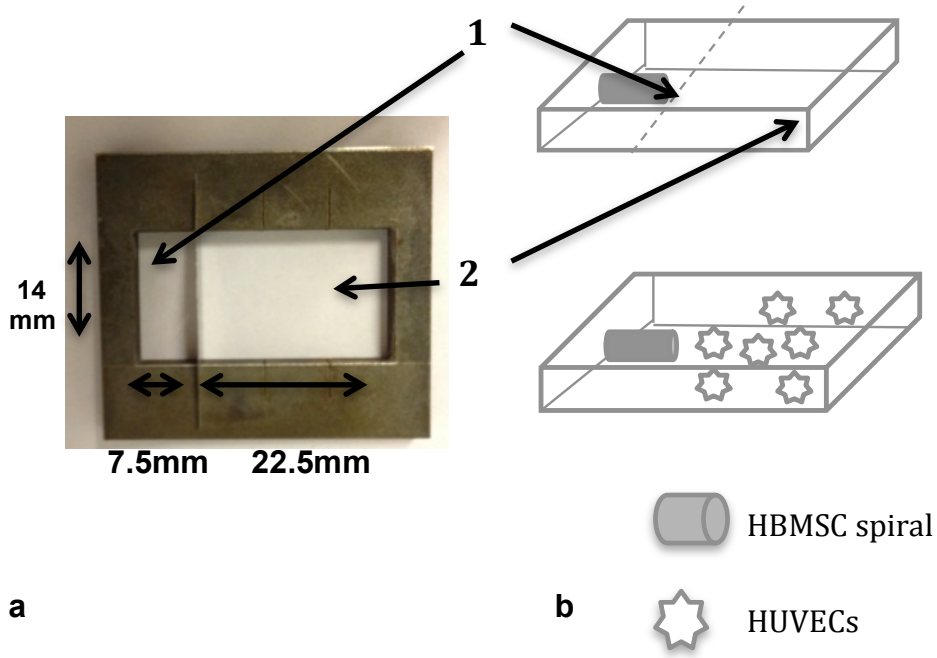

Figure 2.12. Schematic of the experimental setup. Moulds with dividers (a) were used to segregate the two cell types. The divider was removed within a minute of the fresh collagen setting to ensure the integration of the two hydrogels but to avoid mixing the HUVECs and the HBMSC spiral. For protein analysis regions 1 and 2 as shown above were analysed in addition to the media of HBMSC only constructs and HBMSC-HUVEC constructs. HUVECs were seeded in the hydrogel separate from the HBMSC spiral, as shown above, in region 2.

2.21 Effect of oxygen concentration on HUVEC morphology

HBMSC-HUVEC (2:4 ratio) collagen-laminin hydrogels were prepared as described in 2.6 and 2.7. The constructs were placed in either normal atmospheric conditions in a humidified incubator set at 37°C, 5% CO_2, 21% O_2 or in an incubator (SANYO) set at 37°C, 5% CO_2, 5% O_2 (the oxygen was lowered by pumping nitrogen into the incubator to displace oxygen). Cells were cultured for 7 days, fixed and stained for CD31. CD31 images were used for analysis of HUVEC morphology and aggregation, as described in section 2.10. The supernatant was stored at -80°C for ELISA analysis of VEGF, PDGF, Angiopoietin-1 and TGFβ_1. HBMSC only cultures served as controls for protein analysis, as did HUVEC only cultures.

2.22 Human dermal fibroblast culture

Adult human dermal fibroblasts (HDFs) were isolated from healthy adult skin discarded following reconstructive surgery. The skin was washed, de-fatted and dissected into small pieces. The tissue was digested in DMEM composed of 1% P/S, 5% FCS and type I collagenase (Worthington Biochemical Corporation, New Jersey, USA) for 3 hours at 37°C on a shaker. The supernatant was pipetted in a sterile universal tube and centrifuged for 5 minutes at 2000rpm. The cell pellet was obtained and re-suspended in fresh DMEM with 10% FCS, 1%P/S and plated in a T225 flask. Cells were monitored for attachment and confluence until they reached 80% confluence. Media changes occurred every 3-4 days. Cells up to passage 7 were used in all experiments and cell passaging was done using the same method described for HBMSCs.

2.23 HDF: HUVEC co-cultures

HDF: HUVEC collagen hydrogels with added laminin were set in 12 well plates as described above. 200000 HDFs and 400000 HUVECs /1 ml hydrogel were used in all experiments. HDF only hydrogels were also set for control protein analysis. Constructs were cultured in a normal humidified incubator set at 37°C, 5% CO_2 and 21%O_2 or an incubator set at 37°C, 5% CO_2 and 5% O_2.

HUVEC morphology and aggregation was tested with CD31 immunofluorescence and media samples were used for protein analysis using ELISA kits for VEGF, PDGF, Angiopoietin-1 and TGFβ_1.

2.24 Flow cytometry for VEGFR1 and VEGFR2

VEGF receptors were quantified using flow cytometry in collagen hydrogels (with laminin) cultured in normoxia and physiological hypoxia on day 2. HUVEC only cultures and HBMSC-HUVEC and HDF-HUVEC co-cultures, cultured at 20% vs 5% O_2 were quantified. The methods described above (section 2.13) were used to digest hydrogels and stain the cells. The number of receptors per cell was also calculated by obtaining a new standard curve for the quantibrite beads, as described above.

2.25 Statistical analysis

Statistical analysis was done using Prism software version 6 (Graph Pad). Statistical significance was set at 0.05. When two data groups only were analysed a t-test was used to test for differences (eg. HUVEC cell height and 2D surface area of cell morphologies). Differences between cell morphologies, protein levels, and flow cytometry analysis where there were multiple groups, a one-way analysis of variance (ANOVA) or a Kruskal-Wallis test was used. Post-

hoc tests were used to identify which group comparisons had significant differences, using either a post-hoc Bonferroni test or a Tukey's test.

3 Results

3.1 Endothelial cell morphology in 3D collagen hydrogels

These initial experiments were designed to test HUVEC response when cultured in collagen hydrogels in the absence of any supplementary cells or growth factors. This is an area that lacks in research as most researchers focus on driving EC tubulogenesis with the addition of various factors.

The hypothesis under test was that HUVECs attach and spread throughout the collagen hydrogels, without forming any end-to-end networks. Cell seeded collagen hydrogels were cultured for 1 and 2 weeks as described in the methods (2.2, 2.3). Constructs were stained using CD31 immunofluorescence as described in section 2.9 and HUVEC morphology and aggregation were tested using fluorescence microscopy as described in (2.10). Results showed a change in cell morphology with increasing culture time. Three different HUVEC morphologies were identified in these cultures: 1) multipolar, 2) flattened, and 3) cobblestone (Figure 3.1, cells shown with arrows).

Multipolar cells were spindle-like cells with multiple cell processes extending from them. Flattened cells were usually polygonal in shape, with faint CD31 staining in their cytoplasm. Cobblestone cells were smaller cells than the flattened, with more intense cell membrane CD31 staining and usually aggregated in groups. A major component, which defined these different morphologies, was the 2D size of the cells as described in the methods 2.10, which was significantly different ($p<0.01$) between the flattened (1600μm^2) and cobblestone cells (345μm^2) (as seen in Figure 3.1 d, e, f). The height or

thickness of the flattened (7.16 μm) and cobblestone (7.57μm) cells was quantified using confocal microscopy as described in 2.10 but showed no statistical difference in the z plane between the two cell morphologies (Figure 3.3c).

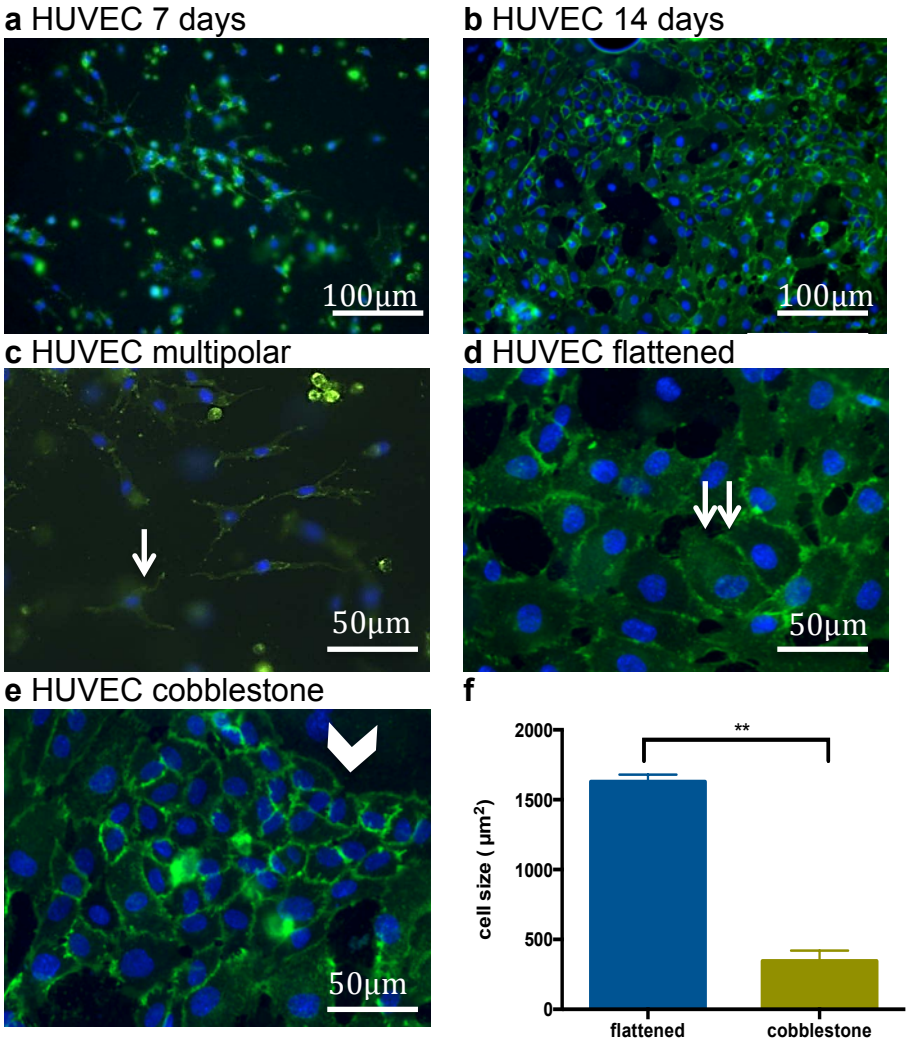

Figure 3.1. HUVEC morphologies in collagen constructs. a,b) HUVEC morphologies on day 7(a) and day 14 (b), c,d,e higher magnification of HUVEC morphologies: c- multipolar (arrow), d-flattened (two arrows) and e- cobblestone (arrowhead). CD31- green, DAPI-blue, f) Graph shows the 2D size of the flattened and cobblestone cell morphologies on day 14, error bars- SD, *p<0.05.

The cobblestone morphology of ECs was similar to the morphology commonly described when culturing and expanding endothelial cells on conventional 2D surfaces (Grant et al., 1990). The flattened morphology was an intermediate morphology between the multipolar and cobblestone morphologies as evidenced by the increasing number of flattened cells with culture time. The progression from multipolar to flattened to cobblestone morphology was mainly time dependent (Figure 3.2). Increasing the culture time of the HUVEC only collagen hydrogels from 1 to 2 weeks resulted in a significant increase ($p<0.05$) in the number of flattened cells (from ~50% to ~68%) within the cultures, with the striking absence of the multipolar cells and presence of cobblestone cells (Figure 3.2).

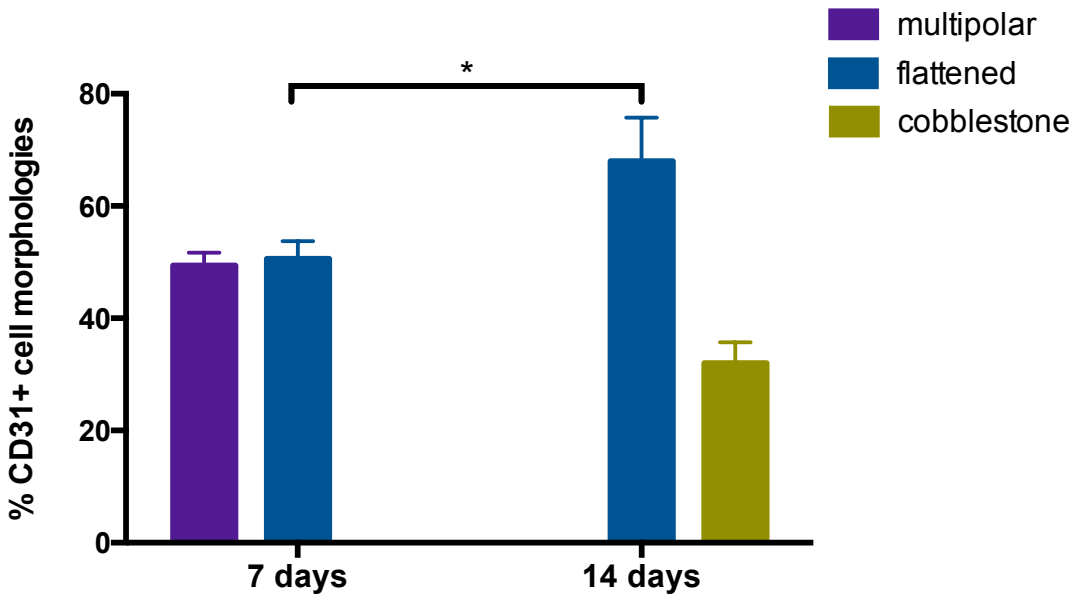

Figure 3.2. HUVEC morphologies on day 7 and 14 in collagen hydrogels. Cells were stained for CD31 and the percentage of multipolar, flattened and cobblestone morphologies were quantified. *$p<0.05$ Note: disappearance of multipolar cell morphology. Error bars represent SD.

As culture time increased, HUVEC migration within the collagen hydrogels was evident, with the majority of the cells at the end of the two-week culture period found on the ventral surface of the scaffold. Cell migration was initially seen using a normal upright microscope and confirmed using confocal microscopy (Figure 3.3). As cells migrated to the top of the ~3mm deep scaffold a cobblestone-flattened cell sheet in 3D formed (Figure 3.1,Figure 3.3). This cell sheet was mainly found on the 33μm ventral aspect of the constructs (Figure 3.3). Z stack images of HUVEC only collagen constructs on day 7 showed cell nuclei interspersed throughout the hydrogel (Figure 3.3a). In contrast, on day 14 cell nuclei were primarily present on the ventral surface of the scaffold (Figure 3.3b).

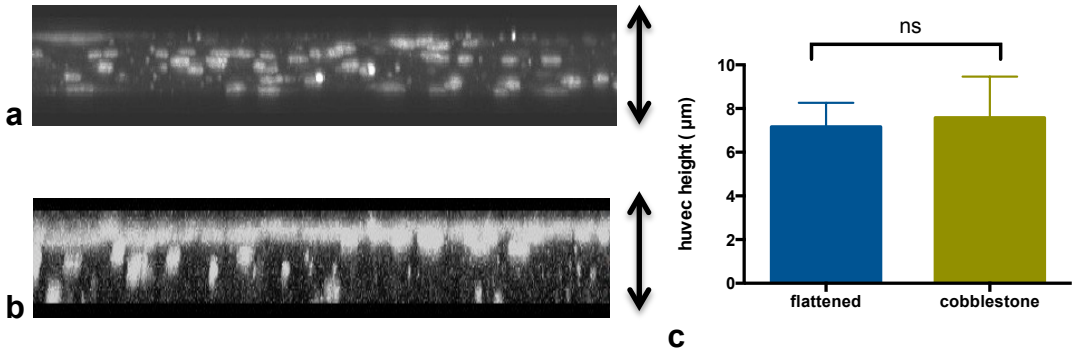

Figure 3.3. Confocal micrographs of HUVEC only cultures in collagen hydrogels. a) 7 days, cells are interspersed within the matrix, b) after 14 days, cells aggregate on the ventral surface of the construct. Images depth 33μm (of a ~3mm gel), c) HUVEC height measured using confocal microscopy- ns=not significant, error bars are SD.

HUVEC migration to the surface of the collagen constructs suggests a cell response mimicking the "wrapping" process found in development (Lubarsky

and Krasnow, 2003). *During "cell wrapping" ECs migrate outwards from a cell sheet to form a tubular structure. This will be further discussed in the discussion and is an area that will require future investigation.*

Results confirmed the initial hypothesis that HUVECs attach and spread within the collagen hydrogels. In addition, as hypothesised, cells did not aggregate into end-to-end networks but formed cobblestone aggregates on the ventral aspect of the collagen hydrogels. This HUVEC response within 3D collagen hydrogels was used as a baseline to test the effect of cell-cell and cell matrix interactions.

3.2 The effect of PMA on HUVEC morphology

Phorbol Myristate Acetate (PMA) is widely used in studies testing angiogenesis and vasculogenesis as it promotes EC tube/network formation and EC invasion within 3D scaffolds (Bayless and Davis, 2003; Davis and Camarillo, 1996; Montesano and Orci, 1987). PMA was added in HUVEC only cultures to test the hypothesis that PMA promotes end-to-end network formation. PMA was added in the collagen and overlying media of HUVEC only cultures as described in the methods (2.4). Due to the varying amounts of PMA used in literature, three different concentrations (10ng/ml, 20ng/ml and 50ng/ml) were tested. Constructs were cultured for up to 14 days and at 48 hours, 7 days and 14 days CD31 immunofluorescence was used to test cell morphology and aggregation.

HUVECs aggregated into end-to-end networks by 48hours in culture, proving the hypothesis (Figure 3.4). An early time point was chosen as most studies testing PMA have shown that the effect of PMA on EC tubulogenesis is very

rapid (Bayless and Davis, 2003; Davis et al., 2000; Montesano and Orci, 1987). There were no flattened or cobblestone cells in any of the cultures.

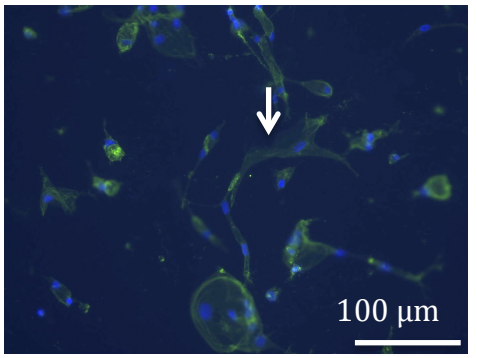

a

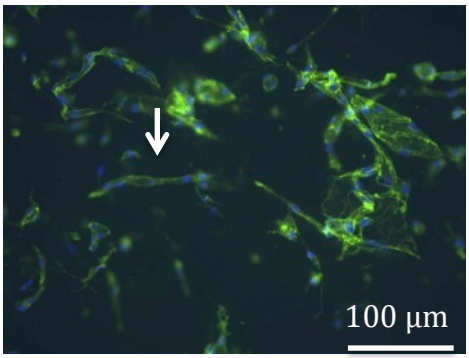

b

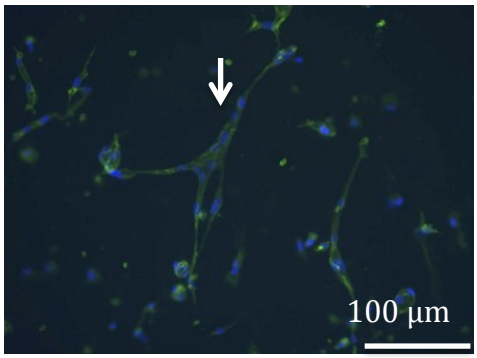

c

Figure 3.4. HUVEC only cultures with PMA. Images show CD31 stained HUVECs on day 7 with a) 10ng/ml, b) 20ng/ml and c) 50ng/ml. The arrows show the end-to-end network aggregation.

There were significant differences ($p<0.05$) in network lengths depending on the PMA concentration as shown in Figure 3.5. In the first 48 hours the shortest networks (86µm length) formed in the 10ng/ml PMA concentration, which were significantly shorter ($p<0.05$) than both the 20ng/ml (134µm length) and 50ng/ml (150µm length) networks. There was no difference in network lengths between the 20ng/ml and 50ng/ml concentrations. On day 7 there was also a significant difference ($p<0.05$) in the mean length of end-to-end networks that formed between the lowest concentration- 10ng/ml (138µm) and both 20ng/ml (190µm) and 50ng/ml (188µm). There was no difference between 20ng/ml networks and 50ng/ml networks. On day 14 network lengths did not significantly increase in any of the three concentrations. On the contrary, in the 20ng/ml constructs

network lengths decreased from 190μm to 161μm. In the 10ng/ml and the 50ng/ml constructs there were small non-significant increases ($p>0.05$) in network lengths from 138μm to 147μm and from 188μm to 202μm respectively.

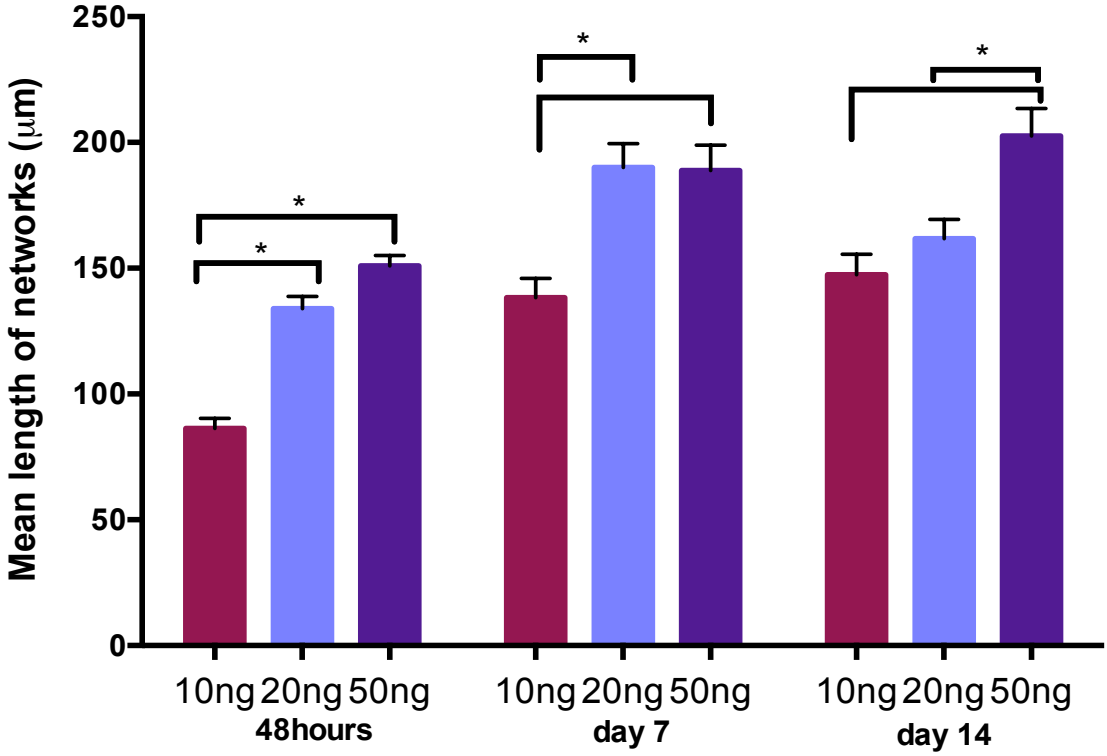

Figure 3.5. Mean length of networks with the three concentrations of PMA tested at 48hours, 7 days and 14 days in culture. *$p<0.05$

These results proved the hypothesis that PMA promotes end-to-end network formation when added to HUVEC cultures. Results showed that networks completely formed by day 7 and peaked at their maximum lengths for all three PMA concentrations at this time point. The results also showed that there was no difference between the 20ng/ml and 50ng/ml constructs, while both promoted significantly greater network aggregation compared to the lowest concentration of 10ng/ml. Results on day 14 suggest that culturing constructs beyond day 7 does not promote further network aggregation. In fact as shown

by the 20ng/ml results further culture can cause disintegration of the networks and results in smaller networks than earlier time points.

The average number of nuclei visible within networks was also quantified as seen in Figure 3.6. Results were in agreement with the network lengths. Results at 48 hours showed that there were significantly fewer nuclei ($p<0.05$) in the 10ng/ml constructs (~4) compared to the 50ng/ml (~7). There was no difference between the 20ng/ml constructs (~5) and 10ng/ml or 50ng/ml. On day 7 there were significantly ($p<0.05$) fewer nuclei per network in the 10ng/ml constructs (7) and the 20ng/ml (11) and 50ng/ml (10). On day 14 there was no difference in the number of visible nuclei per network between any of the PMA concentrations (around 8 nuclei per network). Results supported findings with network lengths and showed that the optimum network aggregation occurred by day 7.

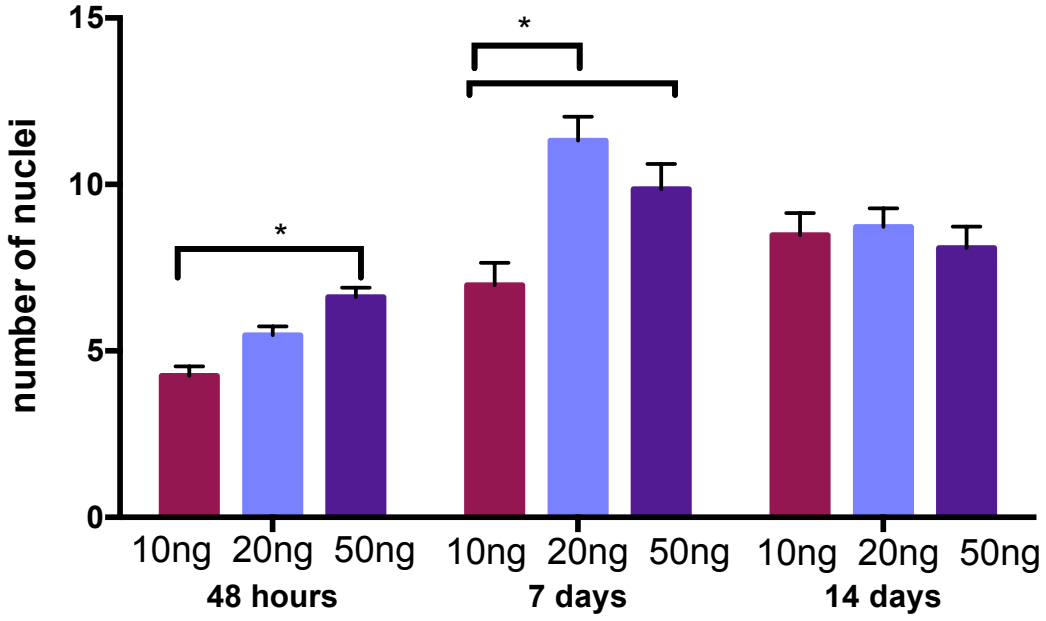

Figure 3.6. The number of nuclei per network was quantified. Nuclei were counted in constructs with 10ng/ml, 20ng/ml and 50ng/ml of added PMA at 48hours, 7 days and 14 days. *$p<0.05$

Experiments with PMA proved its ability to drive HUVEC end-to-end network formation. These findings were used as a comparator to the following experiments, which tested the effect of cell-matrix interactions and cell-cell interactions on HUVEC morphology and aggregation in the absence of PMA.

3.3 HUVEC morphology in co-cultures

HUVEC morphology and aggregation was tested in collagen hydrogels with and without PMA as described in the previous sections and the results were used as a standard for HUVEC behaviour in collagen hydrogels. The hypothesis under test was that co-cultures with HBMSCs would promote HUVEC end-to-end network aggregation due to HBMSC released angiogenic growth factors. This hypothesis was based on previous findings by this group and others showing that HBMSCs release various angiogenic growth factors (Cheema et al., 2010; Kachgal and Putnam, 2011).

Collagen hydrogels were seeded with varying HBMSC and HUVEC numbers to test how co-cultures affect HUVEC morphology and aggregation. Specifically, 200000 HBMSCs/ml were used in all co-cultures, while the number of HUVECs was varied to test the effect on EC morphology. HUVECs were used in co-cultures at 100000/ml (2:1 HMBSCs:HUVECs), 200000/ml (2:2), 300000/ml (2:3) and 400000 cells/ml (2:4). Cells in co-cultures were cultured for 7 days. HUVEC morphology and aggregation were tested using CD31 immunofluorescence as described in the methods (2.9). CD31 positive cells were HUVECs, while HBMSCs were only stained with DAPI for cell nuclei. This was confirmed by staining HBMSC only cultures, using the same CD31 protocol with no positive cells observed. The percentages of multipolar, flattened and

cobblestone HUVECs were quantified, similar to that described for HUVEC only cultures in 3.1. The overlying medium and collagen hydrogels were also kept for protein analysis using ELISA.

Addition of HBMSCs to the HUVEC cultures resulted in a reduction in the number of single multipolar cells and a progression towards the increased aggregation of the ECs towards the cobblestone morphology. The presence of HBMSCs within the cultures resulted in the formation of the cobblestone morphology within 7 days. This was faster than HUVEC only cultures where limited cobblestone formation was found on day 7 (Figure 3.2). This however, could be due to the higher cell density in co-cultures where both HUVECs and HBMSCs were present. The combined presence of both cell types would result in increased cell- cell contact due to the proximity of the cells. To test the hypothesis that the presence of a greater number of cells was sufficient to induce a change in HUVEC morphology and aggregation, a higher number of HUVECs was cultured in single cultures. 400000 HUVECs were cultured in single cultures (equal to the highest number of HUVECs used in the co-cultures) in collagen hydrogels. While the percentages of the 3 different cell morphologies (multipolar, flattened and cobblestone) were not quantified, there were no multipolar cells visible and cells were mainly flattened as seen in Figure 3.7. On the contrary, in the initial 100000 HUVECs/ml cultures ~50% of the cells were multipolar on day 7 and ~50% were flattened. The absence of multipolar cells in these cultures with a higher number of HUVECs suggests that the number of cells present had a substantial effect on the speed of change in cell morphology, from multipolar to flattened, to cobblestone morphologies.

Despite the fact that a higher number of HUVECs can promote a quicker change towards the flattened morphology, cobblestone aggregates were found throughout the collagen hydrogels. ECs did not specifically aggregate on the ventral surface of the collagen constructs as found in HUVEC only cultures. Evidence of this, can be seen in figure 3.8. with cells seen in different focal planes. HUVECs migrated to the ventral surface of the collagen constructs in HUVEC only cultures as cell morphology changed from flattened to cobblestone. The absence of evident migration of HUVECs to the ventral side of the collagen constructs in co-cultures indicates that the presence of HBMSCs and potentially the growth factors released by them (as shown by the VEGF data shown in the next section) limit this migratory phenomenon. This could be as HUVECs try to maintain close proximity to growth factors produced by the HBMSCs or obtain cell contact with them as well as other HUVECs.

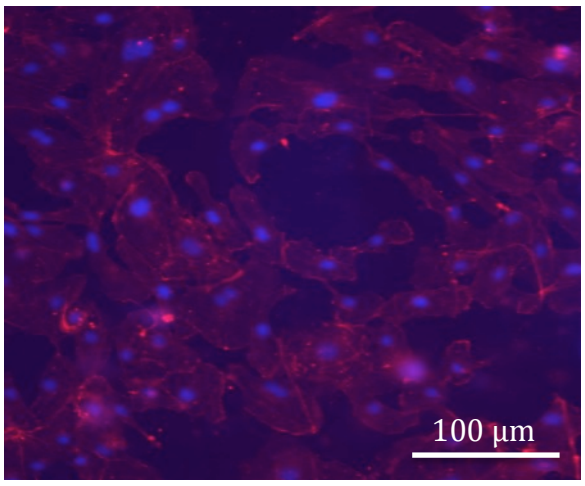

Figure 3.7. Phalloidin staining in HUVEC only cultures on day 7. 400 000 cells/ml were seeded in collagen only cultures to test the effect of cell number on cell migration and morphology. Cells started migrating to the top by day 7.

The percentages of the multipolar, flattened and cobblestone morphologies were quantified in the different co-culture ratios to test the effect of HBMSCs on HUVEC aggregation and morphology. No significant differences between the 4 ratios tested were found, mainly due to the high variance observed in the

cultures. Multipolar cells were only present in the 2:1 and 2:2 ratios, ~25% and ~5% respectively. The highest percentage of flattened cells was found in the 2:1 ratio, ~58%, while the other ratios had similar values close to 25%. The 2:1 ratio had the lowest cobblestone morphology (~30%), while high percentages of ~ 70-80% were found in the 2:2, 2:3, 2:4 ratios (Figure 3.8). Therefore, the greatest HUVEC aggregation was found in these higher HUVEC number cultures.

HUVECs did not aggregate into end-to-end networks in any of the co-culture conditions in collagen hydrogels, disproving the hypothesis. In contrast, HUVECs aggregated into cobblestone aggregates. The hypothesis that HBMSCs released angiogenic growth factors was tested in the following experiments, using VEGF as an exemplar factor.

Figure 3.8. HUVEC morphology in HBMSC-HUVEC co-cultures. a-d: CD31 immunofluorescence (green) of different cell ratios tested. HBMSCs were 200000/ml and HUVECs increased from 100000/ml (a) to 400000/ml (d). Double arrows show flattened cells and arrowheads point to cobblestone aggregates. HBMSCs were $CD31^-$ and therefore all CD31+ cells were assumed HUVECs. Nuclei were stained blue with DAPI. e) Percentage of EC (CD31+) morphologies in mixed co-cultures with HBMSCs. Cell morphologies were categorized into three morphologies and the percentages were calculated for different cell ratios tested. Error bars- SEM, **p<0.01

a 2_1 HBMSC HUVEC

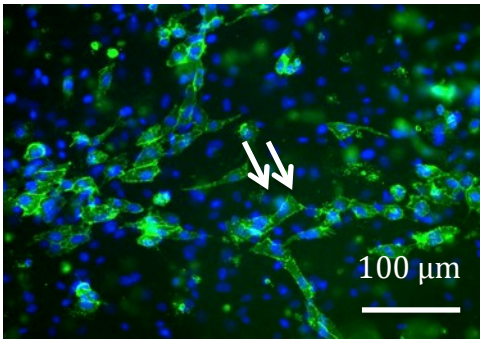

b 2_2 HBMSC HUVEC

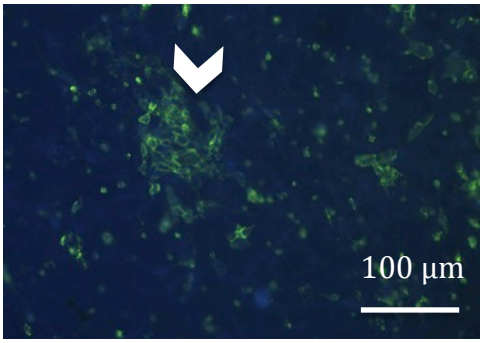

c 2_3 HBMSC HUVEC

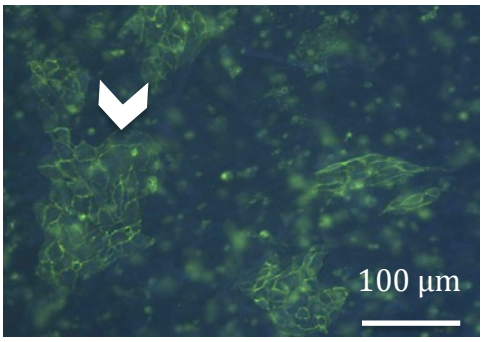

d 2_4 HBMSC HUVEC

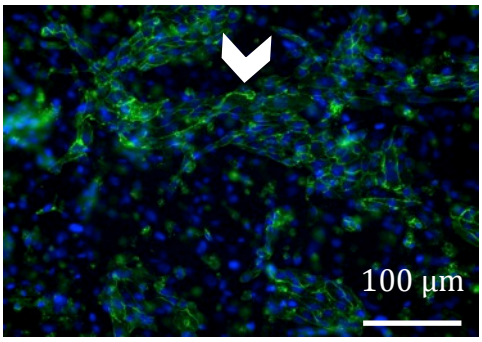

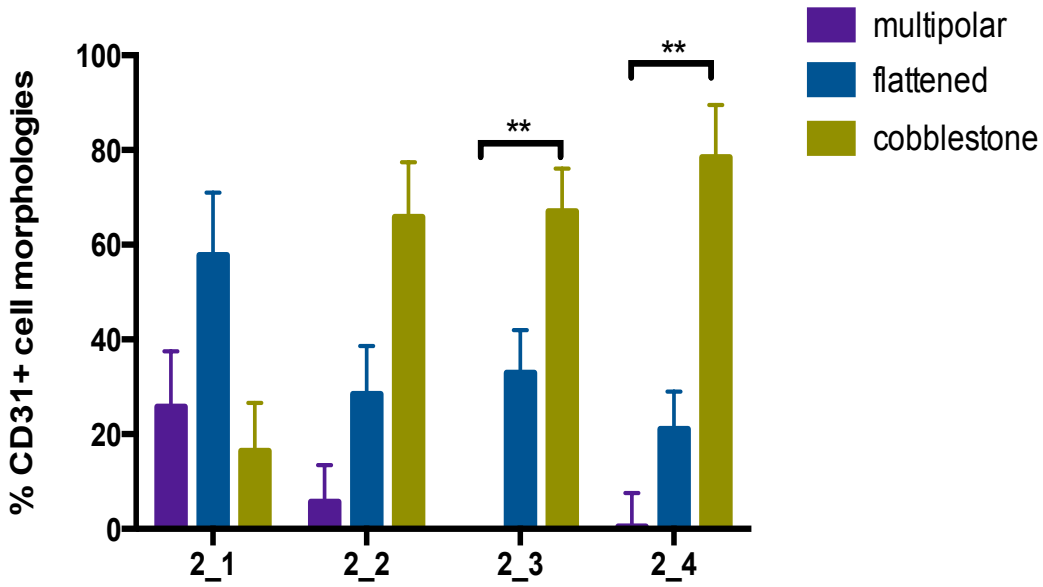

e

3.4 VEGF protein levels

During angiogenesis and vasculogenesis *in vivo* multiple growth factors guide ECs and promote new vessel formation. Despite the multitude of growth factors involved, VEGF is still considered to have a significant role, especially during the early stages (Eichmann and Simons, 2012). Based on previous findings from this group and others (Cheema et al., 2010; Kolbe et al., 2011) the hypothesis under test was that HBMSCs would be releasing angiogenic proteins, with VEGF tested as an exemplar factor.

VEGF was quantified using ELISA both within the collagen co-culture constructs and in the surrounding media (as described in 2.12). VEGF levels were also quantified in HUVEC only cultures and HBMSC only cultures, once the optimum culture conditions for HUVEC aggregation were established and are described in section 3.9.

Results showed that approximately 4 times more VEGF diffused into the surrounding media (1360-2000pg/ml) than retained within the matrix (202-517pg/ml). As collagen hydrogels have high water content, diffusion of such factors is quick and efficient. VEGF levels within the collagen hydrogels were not different between different cell ratios. In the media, there was significantly more ($p<0.05$) VEGF in the 2:3 and 2:4 ratio compared to the 2:2 ratio. Taking into account both the high cobblestone aggregation of the HUVECs and the presence of higher VEGF levels in the 2:4 ratio, this ratio was selected for all future studies. It allowed for both optimum cell-cell contact and high VEGF protein levels released by HBMSCs (Figure 3.9).

VEGF results proved the hypothesis that HBMSCs would be releasing angiogenic growth factors. Despite the presence of VEGF, HUVECs aggregated into cobblestone, similar to HUVEC only cultures. This suggested that HBMSC presence was not sufficient to induce a significant change in cell aggregation. The next experiments focused on the effect of cell-matrix interactions on HUVEC morphology and aggregation, both in the presence and absence of HBMSCs.

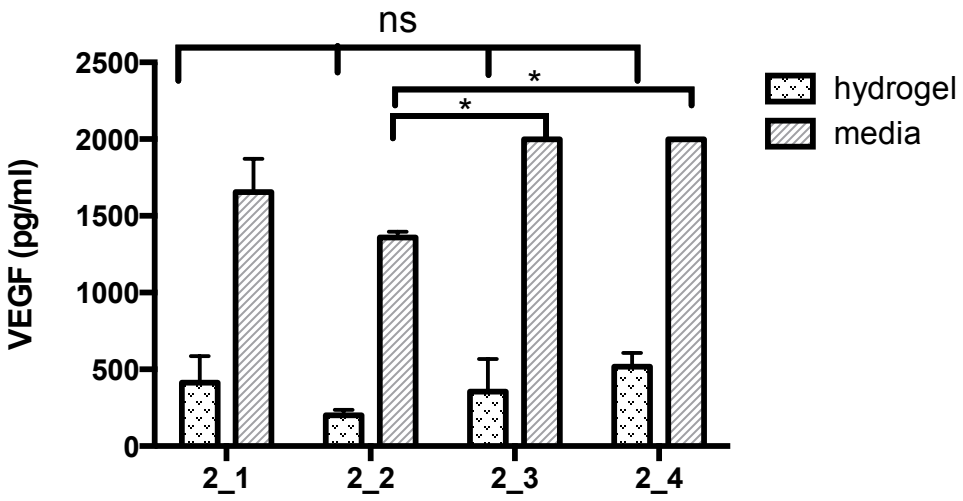

Figure 3.9. VEGF levels in mixed co-cultures in collagen only constructs. VEGF was quantified in the constructs and media samples of mixed co-cultures at day 7 of culture. Approximately 4 times more of the factors diffused in the surrounding media than retained within the constructs. Error bars-SD

3.5 Effect of basement membrane proteins on EC aggregation

Endothelial cells are usually in contact with basement membrane proteins *in vivo*, which include laminin and collagen type IV (Francis et al., 2008; Grant et al., 1990). These proteins have also been found to affect EC morphology in different experimental models *in vitro,* by promoting EC migration and capillary

like structure formation (Kubota et al., 1988; Nicosia et al., 1994). Collagen IV or laminin (50µg/ml) were added in collagen I hydrogels to test HUVEC aggregation and morphology in their presence as described in the methods 2.7.

Firstly, the hypothesis tested was that there would be no cobblestone aggregation in HUVEC only cultures, in contrast to the cobblestone sheet that formed in collagen only cultures. In addition, experiments tested the hypothesis that the presence of basement membrane proteins and VEGF releasing HBMSCs would promote HUVEC end-to-end network aggregation.

In HUVEC only cultures, HUVEC morphological progression and cell fusion changed in the presence of laminin (Figure 3.10). At 7 days, ~90% of cells showed the multipolar morphology and ~10% showed the flattened morphology, in contrast to collagen only hydrogels where 55% were multipolar and 45% were flattened cells. Increasing culture time to 2 weeks resulted in an increase in the number of flattened cells to ~45% of cells and a decrease in multipolar cells to ~55% (Figure 3.10). There were no cobblestone cells present at either 7 or 14 days in laminin cultures, in contrast to collagen only hydrogels in which ~20% cells were cobblestone at 2 weeks. These findings proved the first hypothesis and showed that the presence of laminin alters EC morphology and aggregation compared to culture within a collagen I only scaffold.

In co-cultures, the 2:4 ratio (HBMSC:HUVEC) ratio was chosen based on the results of co-cultures with collagen only (Figure 3.8,Figure 3.9). These experiments tested the effect of both laminin and HBMSCs on HUVEC morphology. Results showed that HUVECs aggregated into end-to-end networks as opposed to the cobblestone aggregation (Figure 3.10,Figure

3.11,Figure 3.12) and there were no cobblestone aggregates in collagen-laminin co-cultures (Figure 3.10). This confirmed the hypothesis that in the presence of both laminin and HBMSCs, HUVECs aggregate into end-to-end networks.

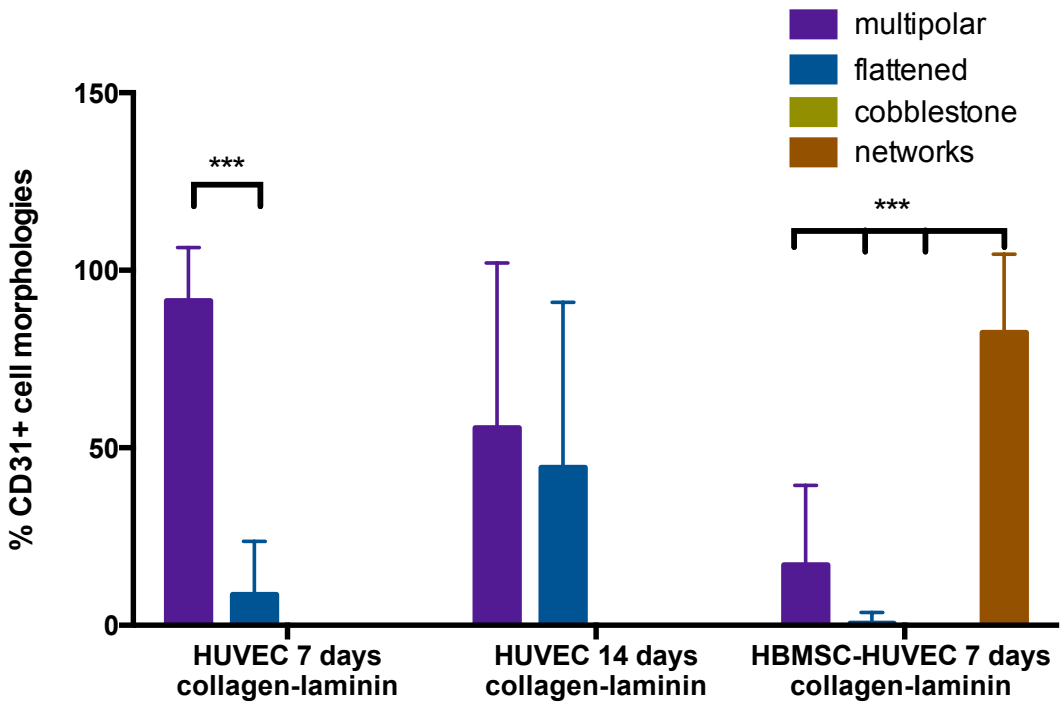

Figure 3.10. HUVEC morphologies in collagen-laminin constructs. The percentage of CD31+ cell morphologies in HUVEC only cultures on days 7 and 14 and HBMSC-HUVEC cultures on day 7. The percentage of multipolar, flattened, cobblestone and networks was quantified. *p<0.05, error bars- SD

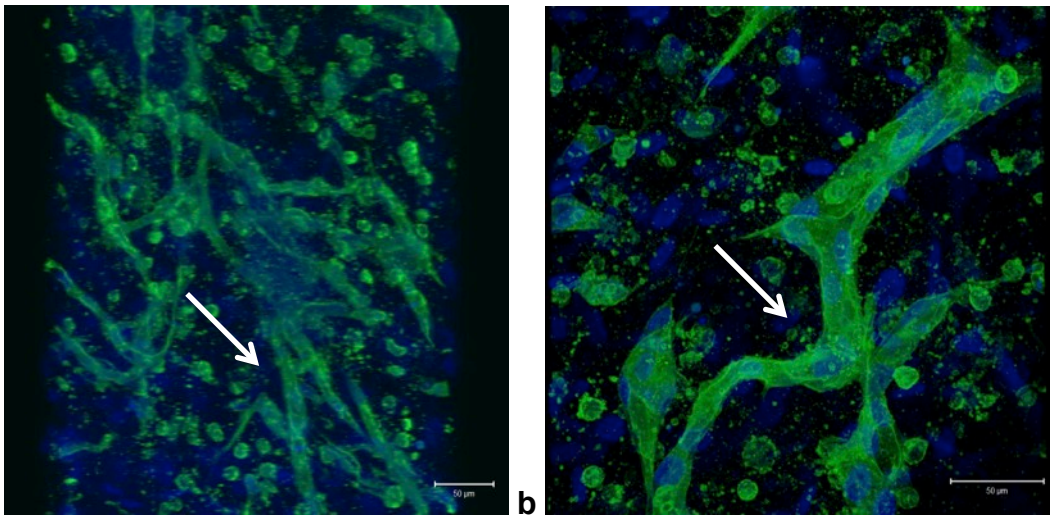

Figure 3.11. Confocal micrograph images of HBMSC HUVEC co-cultures in collagen laminin constructs (Maximum projections of z stack images). HUVEC aggregated into end-to-end networks (arrows), CD31-green, DAPI blue. a) x20, b) x40 magnification of different areas of the constructs. Scale bar= 50μm

The effect of collagen type IV, as a different basement membrane protein, on HUVEC morphology was also tested (Figure 3.12a). Addition of collagen type IV to collagen I showed that laminin is a more potent stimulus for network formation (Figure 3.12a,b,table). On average, networks with collagen IV were around 74μm in length, (40-120μm) whereas with laminin approximately 95μm (50-250μm length) ($p<0.05$) (Figure 3.12-table). There were also fewer networks per hydrogel (experimental observation) in the collagen I and IV hydrogels. The data suggested that laminin induced a faster and greater change in EC aggregation compared to collagen IV.

In summary, HUVECs aggregated into end-to-end networks in cultures containing laminin, only when HBMSCs were present. These findings showed that both ***HBMSCs and laminin were necessary to promote end-to-end network aggregation.*** *As shown by the co-culture results with collagen only,*

HBMSCs released VEGF. It was therefore hypothesised that VEGF released by HBMSCs promoted HUVEC aggregation into end-to-end networks only in the presence of laminin. VEGF protein levels were tested in laminin co-cultures and compared to both collagen only co-cultures and to baseline levels produced by HBMSCs when cultured alone (as shown in the following sections). Before testing VEGF levels, the importance of cell attachment to laminin for HUVEC end-to-end network aggregation was tested using α6 integrin antibodies.

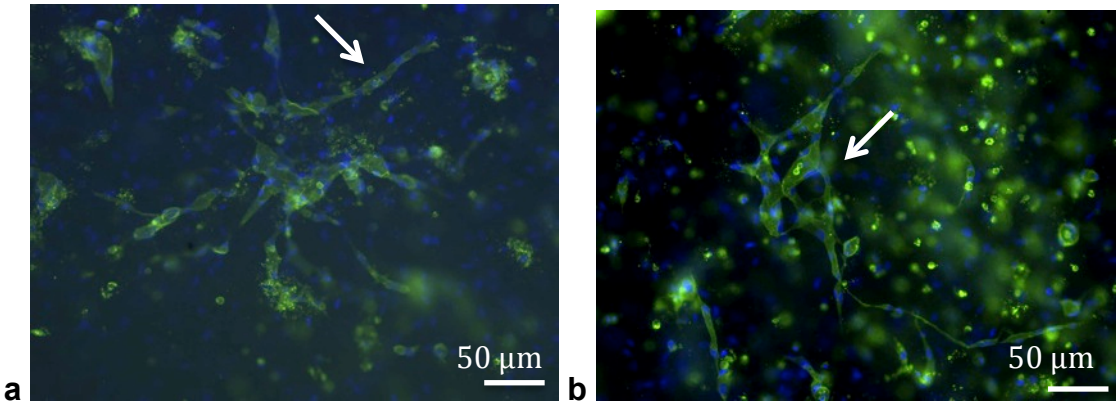

Endothelial cell networks			
	Average length (µm)	Average number of nuclei	Average area occupied (µm^2)
Collagen I + Collagen IV	74.84 ± 21.14	3.23 ± 1.09	245.29 ± 63.62
Collagen I + laminin	95.85 ± 48.78	5.18 ± 2.93	822.16 ± 562.5

Figure 3.12. Endothelial cell networks in HBMSC-HUVEC co-cultures with basement membrane proteins. Collagen IV (a) or laminin (b) were added to the cultures and the length of the networks (arrows), the number of nuclei per network and the average area occupied by the networks were quantified (table). Scale bar= 50 µm

3.6 The effect of a6 integrin blocking

Integrins are receptors that attach cells to the ECM. Their actions are thought to regulate various cell processes and are critical during angiogenesis and vasculogenesis (Carmeliet and Jain 2011). Each integrin heterodimer is found on different cell types and it conveys information between different matrix components.

Laminin experiments showed that the presence of laminin had a significant effect on EC morphology and aggregation. Integrins α6β1 and α6β4 are specifically involved in the attachment of ECs to laminin (Primo et al 2010). The hypothesis under test was that blocking α6 integrin would block cell attachment to laminin and revert HUVEC morphology and aggregation back to the morphology found in collagen only cultures. An integrin α6 antibody was chosen and added to collagen- laminin hydrogels to inhibit EC attachment to laminin, both in HUVEC only cultures and co-cultures, as described in section 2.8. After a week in culture, CD31 immunofluorescence was used to test EC morphology.

Blocking α6 integrin resulted in 46% of the ECs in the HUVEC only cultures showing the “flattened” morphology (Figure 3.13a), similar to the percentages (55.6%) seen in collagen only cultures. Therefore, the morphology of the cells reverted back to the morphology observed in collagen only hydrogel cultures (Figure 3.1,Figure 3.13). Cells in co-cultures aggregated in the cobblestone morphology as seen in figure 3.13c, similar to results with collagen only co-cultures. Although the percentage of the different morphologies was not quantified, there was no evidence of end-to-end network aggregation as found in collagen-laminin co-cultures (Figure 3.13).

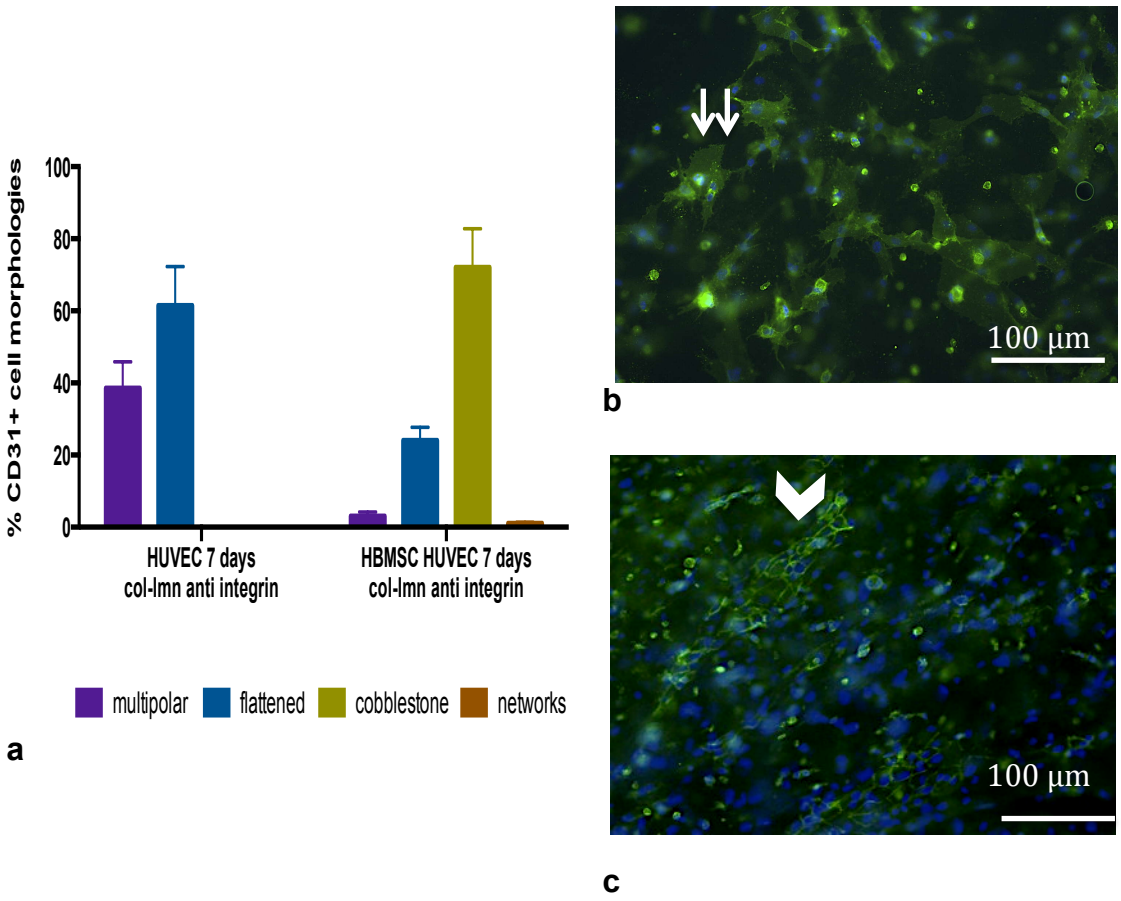

Figure 3.13. HUVEC morphologies in collagen-laminin cultures with added anti-integrin antibody. a) HUVEC morphologies in HUVEC only cultures and co-cultures with anti-integrin antibody, (error bars- SD) b) image showing HUVEC morphology in HUVEC only cultures, the arrows show a flattened cell c) cobblestone aggregates shown with an arrowhead in co-cultures with HBMSCs with anti-integrin antibody.

Results here showed that blocking HUVEC attachment to laminin through a6 integrin essentially reverted HUVEC morphology back to collagen only morphology and aggregation. This proved the hypothesis that cell attachment to laminin was critical for promoting HUVEC end-to-end network formation in co-cultures. The effects of laminin on HUVEC morphology and behaviour were

further investigated by testing VE-cadherin distribution, VEGF and PDGF release by the cells.

3.7 VE-cadherin expression

VE-cadherin is one of the adherens junctions found on ECs. It interacts with the cytoskeleton of the cells and controls cell migration, proliferation and vasculogenesis, especially during development (Calera et al., 2004). The hypothesis under test was that VE-cadherin expression on HUVECs in end-to-end networks would be more prominent than on HUVECs in cobblestone aggregates.

VE-cadherin staining was used in co-cultures with HUVECs and HBMSCs in collagen hydrogels cultured with or without laminin after a week in culture. Immunofluorescence staining showed differences in the distribution of the staining on HUVECs in constructs with or without laminin. When laminin was present, staining was mainly present on the HUVEC membrane. Where laminin was absent staining was distributed throughout the cytoplasm of the cells (Figure 3.14).

These differences in VE-cadherin distribution suggest differences in HUVEC-HUVEC communication in these cultures. This shows that where HUVECs aggregated into cobblestone in collagen only co-cultures, cells did not form strong HUVEC-to-HUVEC junctions, at least by 7 days in culture. On the contrary, HUVECs in co-cultures with added laminin show clear membrane localisation, and stronger HUVEC-to-HUVEC junctions. These findings proved

the hypothesis that VE-cadherin expression would be more prominent in co-cultures with laminin, where HUVECs showed end-to-end cell attachment.

Higher VE-cadherin membrane localisation is critical for initiating cell-signaling cascades and can have a significant effect on cell behaviour. VE-cadherin is also closely linked to growth factor receptors such as VEGFR2 (Calera et al 2004, Scott and Mellor 2009). Therefore VEGF release and VEGF receptor expression were quantified to test a link between these factors and VE-cadherin distribution.

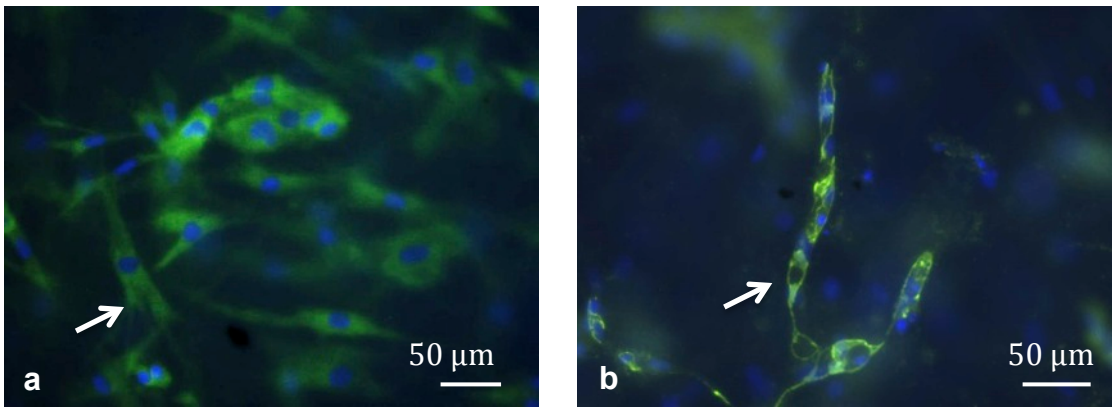

Figure 3.14. VE-cadherin immunofluorescence images. Immunofluorescence of a) HBMSC-HUVEC co-cultures in collagen only hydrogels, b) HMBSC-HUVEC co-cultures in collagen-laminin hydrogels. VE-cadherin- green, DAPI-blue, scale bar= 50µm

3.8 PDGF levels

PDGF is a growth factor involved in the neovascularisation process. It is mainly released by ECs to attract cells such as pericytes and smooth muscle cells for additional support to the new vessel (Carmeliet and Jain, 2011). It was

therefore hypothesised that the main PDGF releasing cells would be the HUVECs. In addition, based on the significant differences in HUVEC morphology in the presence of laminin, HUVEC attachment to laminin was also hypothesised to increase PDGF release by the cells.

PDGF levels were quantified using ELISA. The surrounding medium only was analyzed based on previous findings with VEGF. VEGF findings had shown that approximately 4 times (3.8 times) more protein was released into the medium (2000pg/ml) than retained within the hydrogels (517pg/ml). Medium from HUVEC only constructs, HBMSC only constructs and co-cultures were all analyzed, in collagen hydrogels with and without laminin.

HUVECs were found to be the only PDGF producing cells. PDGF was only present in HUVEC only cultures and was absent in HBMSC only cultures and co-cultures (Figure 3.15,Table 3.1). For protein analysis purposes, 400000 HUVECs were seeded in monocultures, in order to ensure that PDGF levels reflected the number of cells present in co-cultures as well. The absence of any protein in co-cultures suggests either uptake of the protein by HBMSCs or a feedback mechanism that prevents PDGF release by HUVECs in co-cultures. However the exact mechanisms involved in this were not studied in this thesis.
PDGF levels were quantified in HUVEC only cultures in collagen hydrogels with and without laminin. It was found that HUVECs released significantly ($p<0.05$) more PDGF in collagen-laminin cultures than in collagen only cultures. This suggests that cell attachment to laminin has an effect on the release of angiogenic growth factors by HUVECs. The difference in protein levels was also accompanied by the increasing number of multipolar cells found in collagen-

laminin cultures. Cell-attachment to laminin therefore affected both protein release by HUVECs and cell morphology and aggregation.

In summary, these findings proved the hypothesis that HUVECs would be the main PDGF releasing cells. The absence of any PDGF in co-cultures suggests either uptake by HBMSCs or a feedback inhibition mechanism. Results also proved an increase in PDGF levels in the presence of laminin, which showed that HUVEC attachment to laminin affected the release of angiogenic growth factors. This was accompanied by an increase in multipolar cells. The next hypothesis under test was that cell attachment to laminin also affected VEGF release and uptake.

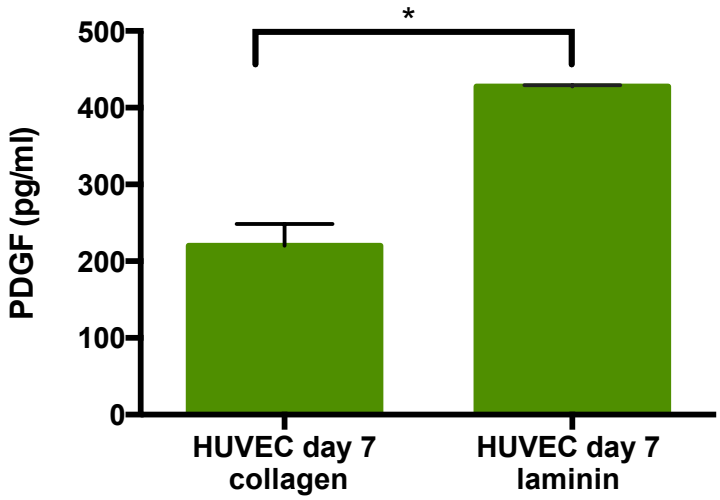

Figure 3.15. PDGF ELISA levels in collagen only cultures and collagen-laminin cultures. PDGF was only present in HUVEC only cultures, absent in co-cultures. *p<0.05, error bars-SD.

3.9 The effect of cell attachment to laminin on VEGF protein levels

Initial co-culture experiments in collagen only hydrogels showed that VEGF was present in the medium of the cultures. The hypothesis under test was that HUVEC aggregation into end-to-end networks in co-cultures with laminin (in contrast to the cobblestone aggregation with collagen only) was correlated to an increase in VEGF protein levels. VEGF protein levels were quantified in collagen-laminin cultures and compared to VEGF levels in collagen only cultures.

ELISA was used to quantify VEGF in the medium of HUVEC only cultures, HBMSC only cultures and in co-cultures, with and without laminin. HUVECs did not produce any VEGF in either collagen only or collagen-laminin cultures (Table 3.1). There were no significant differences in VEGF levels in HBMSC only cultures with or without laminin. This strongly suggests that laminin did not directly affect the release of angiogenic growth factors by HBMSCs or trapped any of the VEGF. This was in contrast to the effect of laminin on HUVEC release of PDGF, with an increase in PDGF release by HUVECs in collagen-laminin cultures. In contrast, there was a significant ($p<0.05$) decrease in the amount of VEGF in the medium of laminin co-cultures (880pg/ml) compared to collagen only hydrogels (2000pg/ml) (Figure 3.16). The decrease in VEGF in cultures where laminin is present suggested an increase in the uptake of VEGF by ECs. This highlighted a connection between VEGF uptake and cell attachment to basement membrane proteins.

In summary, there was a decrease in the amount of VEGF detected in collagen-laminin co-cultures disproving the hypothesis that cell-attachment to laminin increased VEGF release. However, the combination of VEGF levels in HBMSC

only cultures and co-cultures suggested greater protein uptake by ECs, which was hypothesised to promote HUVEC end-to-end network aggregation. In order to test the hypothesis that VEGF uptake was increased when laminin was present, the number and type of VEGF receptors expressed on HUVECs were quantified.

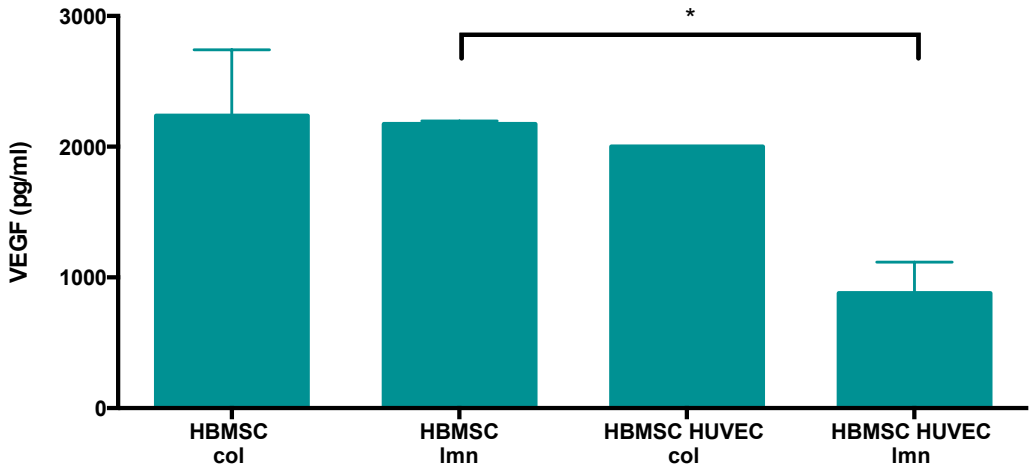

Figure 3.16. VEGF protein levels in constructs with and without laminin. HUVECs did not produce any VEGF, while HBMSCs produced the same amount in both the presence and absence of laminin. There was a significant decrease in VEGF in co-cultures with laminin, while there was no difference in collagen only co-cultures. * P<0.05, error bars- SD, no error bars on collagen co-cultures as the maximum value was exceeded. (N=3 samples)

	VEGF		PDGF	
	Collagen	**Laminin**	**Collagen**	**Laminin**
HUVEC only	**0pg/ml**	**0pg/ml**	**Yes (fig.3.15)**	
HBMSC HUVEC	**Yes (fig. 3.16)**		**0pg/ml**	**0pg/ml**

Table 3.1. VEGF and PDGF presence in HUVEC only cultures and HBMSC-HUVEC cultures in collagen only hydrogels and collagen-laminin hydrogels.

3.10 Number and type of VEGF receptors expressed on HUVECs

VEGF receptors are important regulators of VEGF activity and depending on the type of receptor that VEGF binds to, it can have a positive or negative effect on angiogenesis (Carmeliet and Jain, 2011; Eichmann and Simons, 2012). VEGFR2 is thought to be the main pro-angiogenic receptor, while VEGFR1 can bind VEGF as a decoy receptor (Eichmann and Simons, 2012). The main hypothesis under test was that there would be significantly higher VEGFR2 levels in collagen- laminin cultures where HUVECs aggregated into end-to-end networks, compared to collagen only cultures.

VEGFR1 and VEGFR2 receptors were quantified using flow cytometry as described in the methods 2.13, 2.14. The number of cells positive for each type of receptor and the average number of receptors per cell were quantified. These receptor differences were then correlated to HUVEC morphological differences as well as the differences in VEGF protein levels.

3.10.1 HUVEC only cultures

As shown in Figure 3.17, in HUVEC only cultures, there were significantly ($p < 0.001$) more VEGFR2 positive cells (~15%) in collagen-laminin cultures than collagen only cultures (~4%). There were also significantly ($p<0.001$) more VEGFR2 positive cells (~15%) than VEGFR1 (~2%) positive cells in collagen-laminin cultures. These findings proved the hypothesis that cell attachment to laminin increased the percentage of VEGFR2 positive cells, promoting a pro-angiogenic response.

The number of receptors per HUVEC was then analyzed using quantibrite beads as described in the methods. Using the equation for the bead calibration the number of receptors per cell was calculated in the cultures. It was found that HUVECs in collagen only cultures had significantly ($p<0.05$) more VEGFR1 receptors per cell (40000 receptors/cell) than collagen-laminin (20000 receptors/cell) cultures. There was no difference between VEGFR2 levels per HUVEC in the presence or absence of laminin.

These findings showed that when HUVEC attach to laminin a pro-angiogenic response was more likely as there were overall more VEGFR2 (%) positive cells. However, in the absence of VEGF in HUVEC only cultures, end-to-end networks did not form (Figure 3.10). The next step was to test VEGF receptor levels in co-cultures, where VEGF releasing HBMSCs were also present.

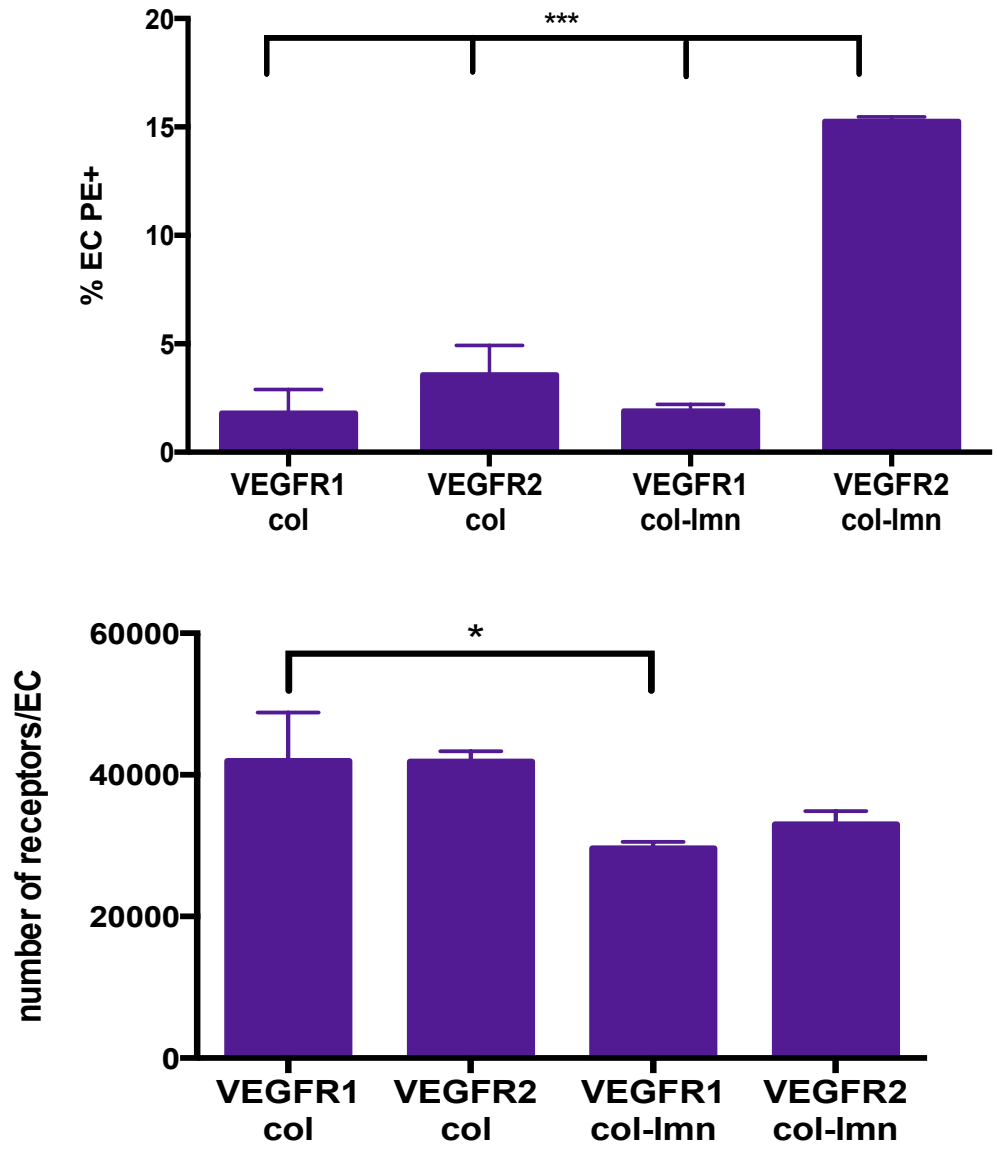

Figure 3.17. The percentage of positive HUVECs for each VEGF receptor was quantified using flow cytometry. PE conjugated VEGF receptor antibodies were used. Separate tubes were stained for each receptor type. The number of receptors per cell was calculated using quantibrite beads. For each receptor triplicate cell samples were analyzed. *p<0.05 ,***p<0.001. error bars- SD (col-collagen, lmn-laminin)

3.10.2 HBMSC-HUVEC co-cultures

VEGF protein levels in collagen-laminin co-cultures were significantly lower than collagen only cultures. Thus, it was hypothesised that there would be overall higher VEGF receptor levels in collagen-laminin co-cultures to reflect greater protein uptake by the cells. It was hypothesised that specifically VEGFR2 levels would be higher than VEGFR1 to reflect the end-to-end network aggregation of the cells in collagen-laminin co-cultures.

VEGF receptor analysis was done as described in the methods (2.13, 2.14) and an anti-CD31 antibody was used in addition to VEGF receptor antibodies to select HUVECs only for analysis. Therefore, the number of cells positive for both the receptors and CD31 were calculated and the percentages below all relate to double positive cells. On day 2, there were significantly ($p<0.001$) more VEGFR2 positive cells compared to VEGFR1 positive cells in both collagen only cultures (~7% to ~4%) and collagen-laminin cultures (~11% to ~6%) (Figure 3.18a). However, VEGFR2 positive cells were significantly higher ($p<0.001$) in collagen-laminin (~11%) cultures compared to collagen only (~7%). This suggests that although there were more VEGFR2 positive HUVECs in both matrix conditions, cell attachment to laminin further increased VEGFR2 positive cells. Higher receptors levels at this early stage would have allowed for greater VEGF uptake by HUVECs, reflected in the drop in VEGF protein levels measured by ELISA in collagen-laminin co-cultures. The higher number of VEGFR2 positive cells in collagen-laminin cultures also correlates to the end-to-end network aggregation of the cells, a pro-angiogenic response by the cells.

On day 7, the number of cells positive for both VEGFR1 and VEGFR2 was significantly lower ($p<0.05$) in laminin cultures (~ 5% each) compared to

collagen only cultures (~10% each). This decrease in receptor percentages on day 7 compared to day 2 suggests VEGF binding and receptor internalisation. The lower VEGF protein levels found in collagen-laminin co-cultures compared to collagen only cultures strongly support higher VEGF binding.

The number of receptors per cell was also analyzed and no differences were found between the two culture conditions and the receptor types on day 2. On day 7 however there was a significant increase ($p<0.01$) in the number of receptors per cell (~40 000 receptors/cell) for both VEGFR1 and VEGFR2 in collagen-laminin cultures compared to day 2 (30 000 receptors/cell) (Figure 3.18b). There were also significantly ($p<0.001$) more receptors, both VEGFR1 and VEGFR2, in collagen-laminin cultures (~40 000 receptors/cell) compared to collagen only (~30000 receptors/cell) cultures.

In summary, on day 7 the percentage of HUVECs positive for each receptor type decreased compared to day 2, while at the same time the number of receptors per cell increased. Stronger HUVEC-HUVEC junctions compared to collagen only cultures accompanied the higher number of receptors per cell. Stronger cell junctions were suggested by the increased membrane localisation of VE-cadherin, as shown by immunofluorescence (Figure 3.14), in collagen-laminin co-cultures. Previous studies had shown that VE-cadherin stabilises receptor expression on the surface of cells (Lampugnani et al., 2006). While the percentage of cells positive for each receptor type was not affected by VE-cadherin, surface expression of receptors increased as receptors are hypothesised to have stabilised by this mechanism. This is an area that should be tested further in the future.

*The data showed that cell attachment to laminin increased the presence of VEGFR2 receptors at early stages (*Figure 3.18*). Results on day 2 proved the hypothesis that higher VEGFR2 levels would be present in collagen-laminin co-cultures to reflect the end-to-end network response by HUVECs. In addition, it proved the hypothesis that an overall higher percentage of VEGF receptors would be present to allow for greater VEGF uptake by HUVECs.*

By day 7, the continuous release of VEGF by the HBMSCs resulted in increasing uptake of the protein by HUVECs, which resulted in internalisation of the receptors as time in culture progressed. This was shown with a decrease in VEGF receptor percentages in collagen-laminin co-cultures, but not in collagen only cultures. Overall, these findings suggest an important link between VEGF receptors, especially VEGFR2 and laminin.

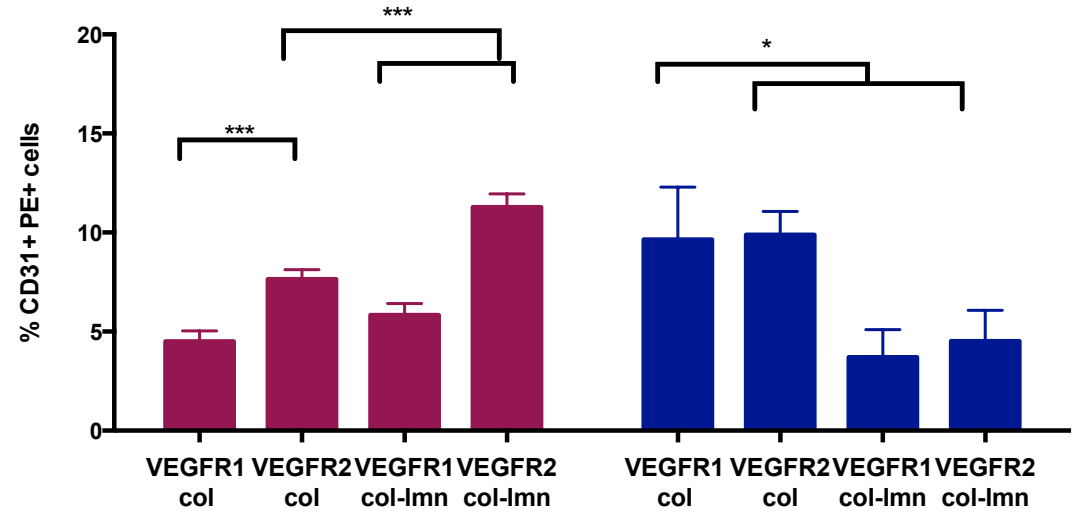

a

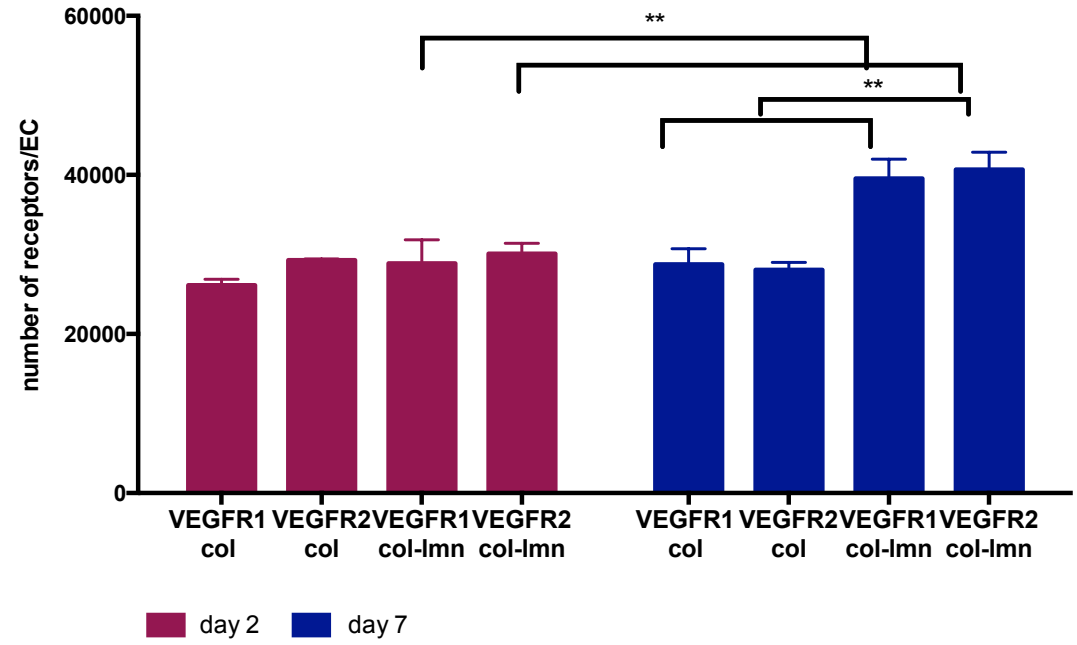

b

Figure 3.18. VEGFR1 and VEGFR2 levels in co-cultures with HBMSCs in collagen hydrogels with or without laminin. a) Cells were stained with both anti-CD31 (FITC) and anti-VEGFR1/2 (PE) to calculate the percentage of HUVECs (double positive cells) positive for each receptor type. b) The number of receptors per cell was calculated using quantibrite beads. Single cells positive for both FITC and PE only were used. Error bars represent SD and *p<0.05, **p<0.01,***p<0.001.

3.11 HDMEC morphology in collagen constructs

In vivo ECs differ in their exact function, shape and size depending on the vessel they are found in (Aird, 2012, 2007b). The hypothesis under test was that there would be significant differences in cell behaviour, migration and morphology between large vessel ECs such as HUVECs and microvascular ECs, HDMECs. Based on differences observed in 2D culture by us and others (Kumar et al., 1987) between large vessel and micro-vessel ECs the hypothesis under test was that there would be an increase in multipolar cells and no cobblestone cells in HDMEC cultures.

HDMECs were seeded in collagen hydrogels, as described for HUVECs. HDMECs were initially cultured alone in collagen only hydrogels and cell morphology and aggregation were tested. As shown in Figure 3.19 ~60% of the cells were multipolar on day 7 and ~40% were flattened. On day 14 the number of multipolar cells significantly ($p<0.01$) decreased to approximately 40% while the number of flattened cells increased to ~60%. This finding suggested a time-dependent change in cell morphology, similar to the HUVEC cultures, from the multipolar morphology to the flattened morphology. In agreement with the hypothesis, in contrast to the HUVEC cultures, there were no cobblestone aggregates in any of the HDMEC cultures. The absence of cobblestone aggregates was also accompanied by the absence of HDMEC migration to the top of the collagen scaffold. In contrast, HUVECs had formed a cobblestone cell sheet by day 14 on the top surface of the collagen scaffold (Figure 3.2,Figure 3.3).

These experiments proved the hypothesis that there would be cell-source dependent differences and that there would be no cobblestone aggregates in HDMEC cultures. This highlights the differences between large vessel and small vessel ECs in in vitro 3D cultures. These differences will be discussed further in the discussion.

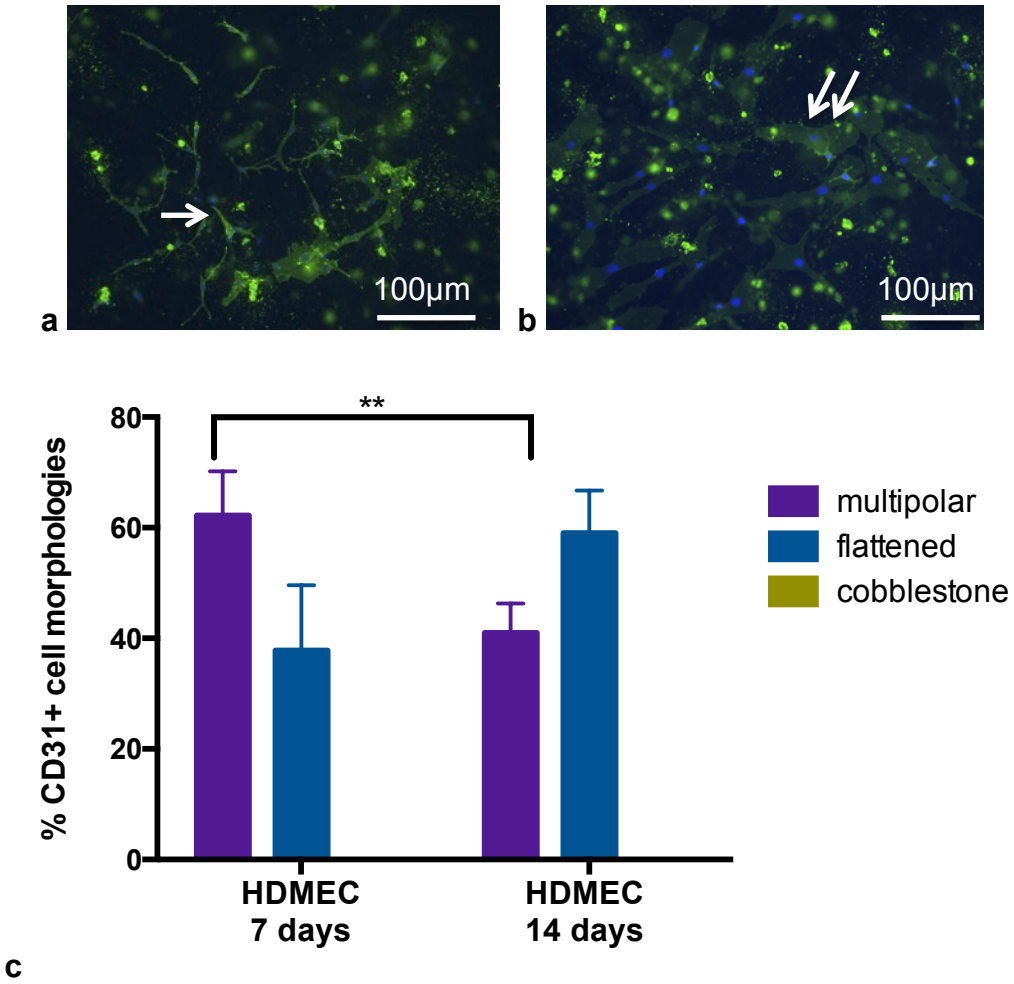

Figure 3.19. HDMEC morphology on day 7 and 14 in collagen only hydrogels. a,b) HDMEC only morphology in 3D collagen hydrogels, day 7 (a) and day 14 (b). Single arrow shows multipolar cells and double arrows show flattened cells. Scale bar is 100 µm, CD31 is green, DAPI is blue. c) The graph shows the percentage of cells positive for the multipolar and flattened morphologies at 7 and 14 days (Kruskall Wallis) **p<0.01, error bars- SD.

3.12 HBMSC-HDMEC co-cultures

Culturing different EC types in monocultures in collagen hydrogels showed significant differences in cell morphology and migration. Next, the effects of the presence of HBMSCs and/or laminin in these cultures were tested. The first hypothesis under test was that there would be no cobblestone aggregates in co-cultures in collagen only, similar to the absence of any cobblestone in HDMEC only cultures. In collagen-laminin co-cultures it was hypothesised that HDMEC attachment to laminin would promote end-to-end network aggregation, similar to HUVEC co-cultures.

HDMECs were co-cultured with HBMSCs using the 2:4 ratio, shown in the HUVEC co-cultures as the optimum ratio for cell aggregation and protein release. Cells were cultured for a week and stained for CD31 for cell morphology analysis as seen in Figure 3.20a,b. In collagen only co-cultures, HDMECs were mainly multipolar, with ~97% of the cells multipolar and only ~3% of the cells flattened ($p<0.001$) (Figure 3.20c). Cobblestone cells were absent in HDMEC co-cultures, proving the hypothesis that there would be no cobblestone cells. These morphologies were very different to HUVEC co-cultures in collagen, where there were no multipolar cells and ~80% of HUVECs were cobblestone and 20% were flattened.

When laminin was added to collagen constructs, the number of multipolar cells decreased to ~20% of HDMECs, while the flattened cells increased significantly ($p<0.01$) to ~80%. While in co-cultures with HBMSCs and HUVECs there were abundant end-to-end HUVEC networks, in HDMEC co-cultures there was a striking absence of any networks. This disproved the hypothesis that HDMEC

attachment to laminin in the presence of HBMSCs would also promote end-to-end networks.

Results showed that HBMSC and laminin addition did not successfully promote HDMEC end-to-end network aggregation. This suggests that cell-cell and cell-matrix interactions with HDMECs were significantly different than HUVECs. Other supplementary cells, such as HDFs, which are also derived from skin, could have a different effect on HDMEC aggregation. This could be tested in the future.

Thus, there were significant differences between HDMEC cultures and HUVEC cultures in terms of EC morphology, migration and aggregation. This was evident in both EC only cultures and co-cultures. Both the cobblestone sheet and the end-to-end networks that were found in HUVEC cultures could be useful for tissue engineering purposes. The absence of HDMEC aggregation in any of the cultures, proved less attractive for tissue engineering applications. Therefore HUVECs were used for all subsequent experiments and different parameters were tested that could further stimulate specific HUVEC aggregation patterns.

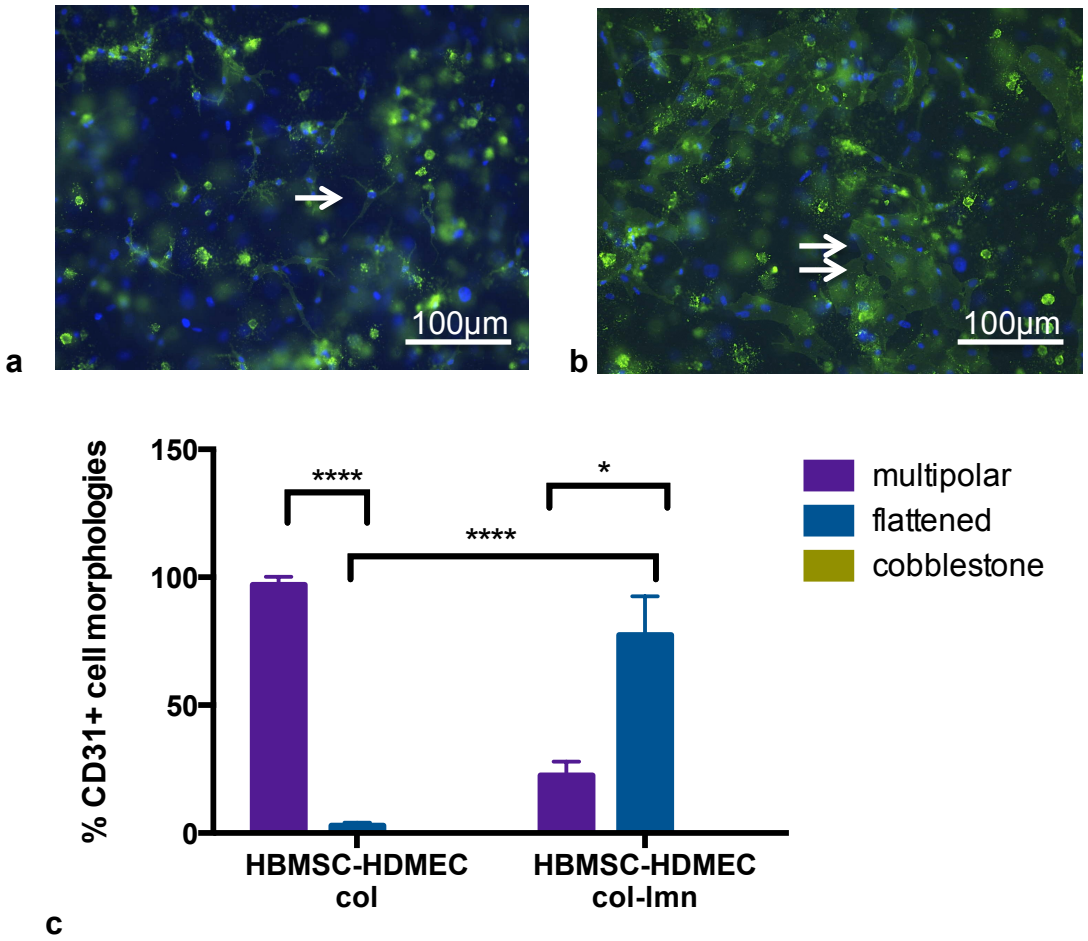

Figure 3.20. HDMEC morphologies in co-cultures with HBMSCs in collagen only constructs and collagen-laminin constructs. a,b) CD31 immunofluorescence images showing HDMEC morphologies in co cultures (a) collagen, (b) collagen-laminin, CD31-green, DAPI-blue, scale bar 100µm. Single arrow showing multipolar cells and double arrows showing flattened cells. c) The graph shows the percentages of HDMEC morphologies in collagen only and collagen-laminin constructs on day 7. Error bars represent SD and *p<0.05, ****p<0.0001

3.13 Segregated co- cultures

During angiogenesis *in vivo* there is a gradient of angiogenic growth factors that drives EC migration and new vessel formation to the ischemic area (Carmeliet and Jain, 2011; Phelps and Garcia, 2009). The hypothesis under test was that the experimental setup as described in 2.19 would mimic the gradient of angiogenic factors found in angiogenesis, with a gradual decrease in angiogenic growth factor levels from the HBMSC spiral, distally to the HUVEC populated hydrogel area. The hydrogel, in which the HBMSC spiral was embedded, was initially cut into three sections: the spiral or depot region (1 on schematic in Figure 2.12), the mid section and distal section as shown in figure 2.12. Protein analysis showed no difference between mid and distal regions of the hydrogels, disproving this hypothesis. Therefore the results for the mid and distal sections were merged into one, the acellular hydrogel. As a result, the experimental setup was used to test the effect of the presence of growth factors, released by HBMSCs, in the absence of direct HBMSC-HUVEC contact. The hypothesis was that the release of angiogenic growth factors by the HBMSCs would promote HUVEC end-to-end network aggregation.

Four different culture conditions for the HBMSC spirals were then tested as described in the methods 2.19 to find the optimum culture conditions that would result in the maximum release of angiogenic growth factors by HBMSCs. These conditions were: 1) pre-culturing the HBMSC spirals for a week, 2) pre-culturing and “fixing” (snap freezing) the HBMSC spirals, 3) placing the HBMSC spirals within the hydrogel without pre-culturing (day 0 live) and 4) “fixing” (snap freezing) the HBMSC spiral on day 0.

For the first condition HBMSC spirals were pre-cultured for a week before placing within the hydrogel. The hypothesis here was that pre-culturing would result in up-regulation of various angiogenic proteins before placing the spiral within the collagen hydrogel. Additionally, HBMSCs would continue to release angiogenic factors once placed within the collagen hydrogel. The release of a greater amount of these angiogenic factors was hypothesised to increase HUVEC end-to-end network aggregation and migration, to a greater extent compared to the other conditions tested.

The second culture condition tested the hypothesis that “snap freezing” the HBMSC construct (i.e. fixing HBMSCs) would result in slow release of factors retained within a compressed collagen matrix. Only protein trapped within the compressed collagen matrix would be released with no additional protein release by the HBMSCs. The growth factors released were hypothesised to promote HUVEC end-to-end network aggregation, but more limited than the pre-cultured “live” constructs.

The final two conditions were used as comparisons to the pre-cultured spirals and were hypothesised to result in the least amount of angiogenic growth factors and HUVEC aggregation. HBMSC spirals were placed in a hydrogel (with or without HUVECs as shown in Figure 2.12) on the same day that compressed collagen spirals were set (day 0).

Protein levels were quantified in the collagen depot, acellular hydrogel and medium of HBMSC cultures and in the medium of cultures with both the HBMSC spiral and HUVECs.

3.14 VEGF protein levels

VEGF protein release and uptake was found to be important in the aggregation of HUVECs in mixed co-cultures. Therefore, VEGF protein levels were quantified in segregated co-cultures. The hypothesis under test was that HBMSCs would be producing VEGF, which would diffuse into the hydrogel and surrounding media. In addition, it was hypothesised that there would be no VEGF in day 0 “snap frozen” cultures (in any of the regions tested) and that the highest VEGF levels would be present in the 1-week pre-cultured (live) cultures. VEGF levels were quantified using ELISA in the depot region of the collagen hydrogels (1 on schematic figure 2.12), the remaining acellular region of the construct (2 on schematic figure 2.12) and the surrounding medium after a week in culture.

VEGF levels were significantly higher within the depot (~1200pg/ml) ($p<0.01$) and acellular (~1000pg/ml) ($p<0.001$) regions of hydrogels in day 0 constructs compared to pre-culture constructs (~500pg/ml and 110 pg/ml) (Figure 3.21). This disproved the hypothesis that higher protein levels would be detected in pre-cultured live constructs. In contrast, there was no difference in VEGF levels within the medium of HBMSC constructs, with ~1500pg/ml in day 0 constructs and 1300pg/ml in pre-culture constructs. These results show that the majority of VEGF is released within the first week of HBMSC spiral culture. This suggests that VEGF produced in the pre-culture constructs was “lost” in the pre-culture medium resulting in lower protein levels within the hydrogels.

VEGF was almost absent in the “snap frozen” HBMSC cultures, except in the medium of pre-culture constructs where there were ~150pg/ml of VEGF. The

absence of any significant amount of VEGF in pre-cultured constructs suggests that VEGF was not efficiently trapped within the collagen spiral. It is also possible that VEGF diffused out of the spirals immediately after it was placed in the hydrogels and was lost in the media change on day 3 of the hydrogel cultures.

In conclusion, the high levels of VEGF found in day 0 (live) cultures compared to the pre-culture constructs suggest that the majority of VEGF is produced within the first week of HBMSC culture. This disproved the hypothesis that pre-culturing the HBMSC spirals would result in the highest VEGF levels. In addition the data showed that "snap-freezing" HBMSC constructs did not "trap" sufficient angiogenic proteins.

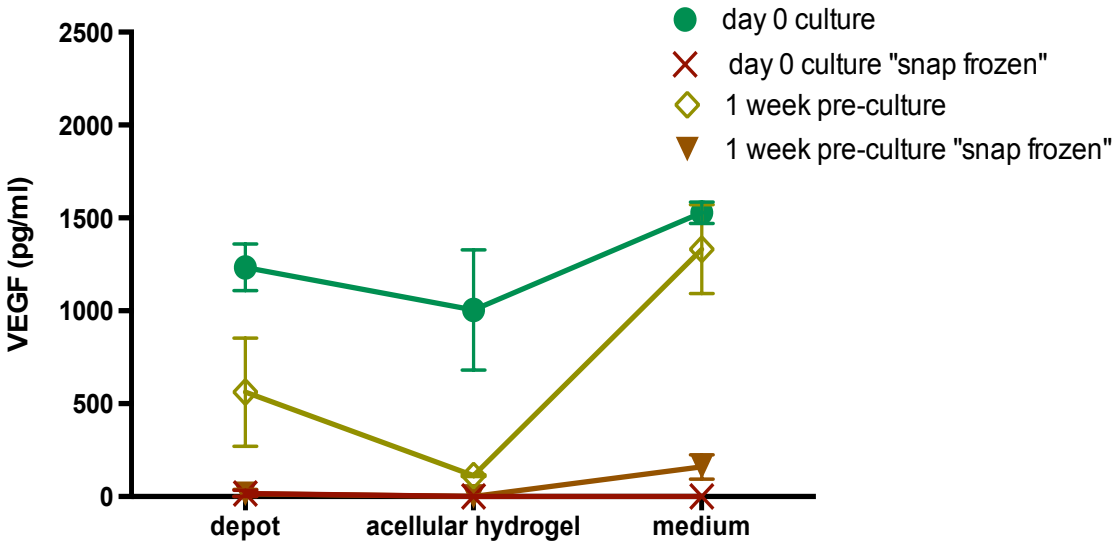

Figure 3.21. VEGF protein levels measured by ELISA. VEGF levels were measured in the proximal (spiral area), acellular hydrogel region and surrounding medium of HBMSC only constructs. Error bars- SD, n=3, significance described in the text

3.15 bFGF protein levels

bFGF was tested as another exemplar angiogenic factor in these cultures. Protein levels were analysed using ELISA, as described above for VEGF. The hypotheses under test were that bFGF levels would be highest in the pre-cultured (live) group and absent in day 0 “snap frozen”.

bFGF levels in the pre-culture constructs were significantly lower than day 0 constructs. This was found both within the proximal region (~500pg/ml vs ~1300pg/ml) ($p<0.001$), where the HBMSC spiral was located and in the surrounding medium ($p<0.01$). This shows that the majority of the protein was produced within the first week of culture. Therefore, similar to VEGF, some of the bFGF would have been released and “lost” in the media of the pre-culture constructs.

In addition, bFGF levels in day 0 constructs within the depot region (~1300pg/ml) were significantly ($p< 0.0001$) higher compared to the remaining hydrogel (~60pg/ml) and surrounding media (230pg/ml) ($p<0.0001$) (Figure 3.22). This suggests that at this time-point the majority of the protein was trapped within the compressed collagen matrix and did not diffuse into the surrounding media, or indeed into the hydrogel.

In contrast, both day o and pre-culture constructs in which the HBMSC spirals had been snap-frozen had very low (80pg/ml) to undetectable (0pg/ml) protein levels. Thus, bFGF was not effectively trapped in pre-culture constructs, similar to VEGF.

The results for bFGF support VEGF data and show that for protein release purposes pre-culturing the HBMSCs does not maximise protein levels. In fact, instead this results in protein "loss" into the pre-culture medium. In addition, "snap freezing" HBMSC constructs after pre-culturing does not effectively trap enough proteins within the collagen matrix. Co-culture medium was then also tested for VEGF and bFGF levels.

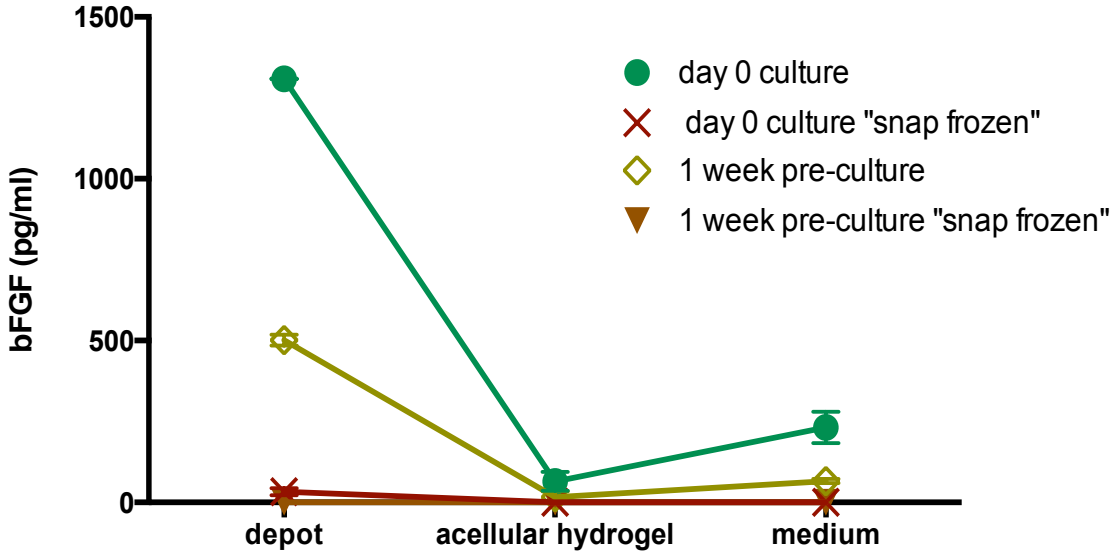

Figure 3.22. bFGF protein levels using ELISA. bFGF was quantified in the constructs and medium of HBMSC only constructs. Day 0 live and "snap frozen" and 1 week pre cultured live and "snap frozen" HBMSC constructs were used. Error bars- SD. Analysis after 1 week in culture, significance described in text.

3.16 Co-culture protein levels

3.16.1 VEGF and bFGF protein levels

VEGF and bFGF levels were tested in the medium of co-cultures, when HUVECs were present in the hydrogel. The hypothesis under test was that

VEGF and bFGF levels would not increase, based on initial experiments with HUVECs only (table 3.1) where there were no detectable levels of VEGF.

Results showed that HBMSCs were the only VEGF producing cells in co-cultures. This was proven by the absence of VEGF in the medium of day 0 “snap frozen” co-cultures, where HUVECs were the only live cells. There was also no VEGF in the pre-cultured “snap frozen” co-cultures (Figure 3.23). In day 0 “live” cultures there was no difference between VEGF detected in the medium of the HBMSC only cultures (1500pg/ml) and the co-cultures (1300pg/ml). However, in pre-culture constructs, VEGF was significantly lower in the co-culture medium (300pg/ml) compared to the HBMSC only medium (1300 pg/ml). This shows either uptake of the protein by HUVECs or a feedback mechanism that reduces VEGF release by HBMSCs when HUVECs are present.

bFGF levels in co-culture medium were very low to absent in all HBMSC culture conditions. For day 0 “snap frozen”, 1 week pre-culture and 1 week pre-culture “snap frozen” these low bFGF levels were not different to the levels measured in the HBMSC only medium. For day 0 (“live”) constructs however, there was a sevenfold drop in protein levels compared to the HBMSC only levels (232 pg/ml to 32 pg/ml). This suggests either uptake of bFGF by the HUVECs or down-regulation of bFGF release by HBMSCs due to the presence of the HUVECs and factors released by them.

Results for VEGF and bFGF proved the hypothesis that HBMSCs were primarily responsible for both proteins released. Therefore, the levels of both VEGF and bFGF did not increase in any co-culture conditions compared to

HBMSC only cultures. In contrast, VEGF levels decreased in 1-week pre-cultured co-cultures, while bFGF levels decreased in day 0 co-cultures. This suggested that the presence of HUVECs affected VEGF and bFGF levels, however in different ways. PDGF levels were finally quantified, with the hypothesis under test that PDGF would only be produced by HUVECs.

3.16.2 PDGF protein levels

PDGF was quantified in initial collagen hydrogel experiments, where it was released by HUVECs when in culture alone. In HBMSC only cultures and in HBMSC-HUVEC mixed co-cultures there was no PDGF.

ELISA was also used in these segregated cultures to quantify PDGF (Figure 3.23). PDGF was absent in all HBMSC only cultures and was only detected when HUVECs were present. In HBMSC-HUVEC segregated cultures there was approximately two times more PDGF in the medium of day 0 cultures (327-458pg/ml) compared to the pre-culture constructs (122-200pg/ml). PDGF levels were significantly higher in day 0 “snap-frozen” cultures compared to the pre-culture constructs, both live and “snap-frozen” ($p<0.01$). Differences between “live” and “snap frozen” within the same time-point were not significant.

In summary, these results proved that PDGF was only produced by HUVECs. bFGF levels were low in all culture conditions but showed a drop compared to HBMSC only cultures in day 0 cultures. VEGF levels decreased the most in 1-week cultures compared to HBMSC only cultures. This could have been due to greater uptake of VEGF by HUVECs, however, this was not tested. Overall,

from these results there was no obvious relationship between the levels of the three different proteins in co-cultures.

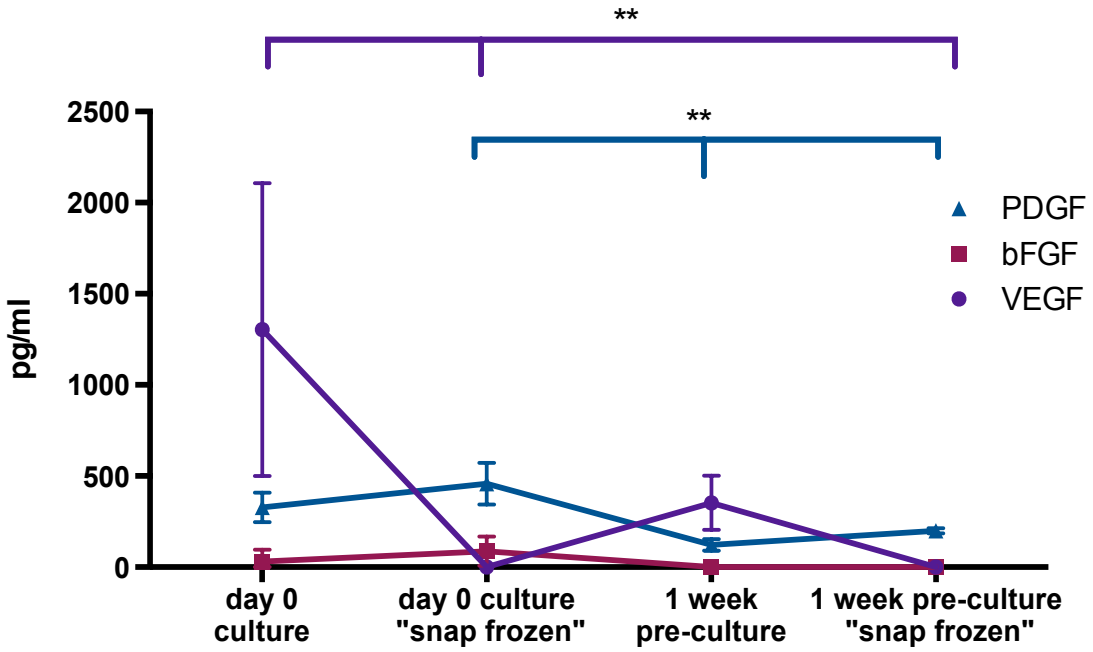

Figure 3.23. Protein levels assessed using ELISA. PDGF was absent in HBMSC only constructs, in both within the hydrogel and surrounding medium. This included the area of the spiral and the surrounding medium. Error bars represent SD, **p<0.01, triplicate samples

3.17 HUVEC morphology in segregated cultures

The initial hypothesis of these experiments was that there would be a gradient of angiogenic factors from the HBMSC depot to the distal part of the HUVEC hydrogel, which was disproven early on. Despite the absence of a gradient of factors, segregated co-cultures tested the effect of the presence of a source of angiogenic growth factors in the absence of HBSMC-HUVEC contact on HUVEC morphology.

CD31 immunofluorescence was used as an indicator of HUVEC morphology in the different culture conditions. As the images in Figure 3.24 show HUVECs had mainly a flattened morphology. However, due to the complexity of these experiments it was concluded that this experimental setup was not successful. Therefore, detailed analysis of cell morphology and aggregation was not undertaken.

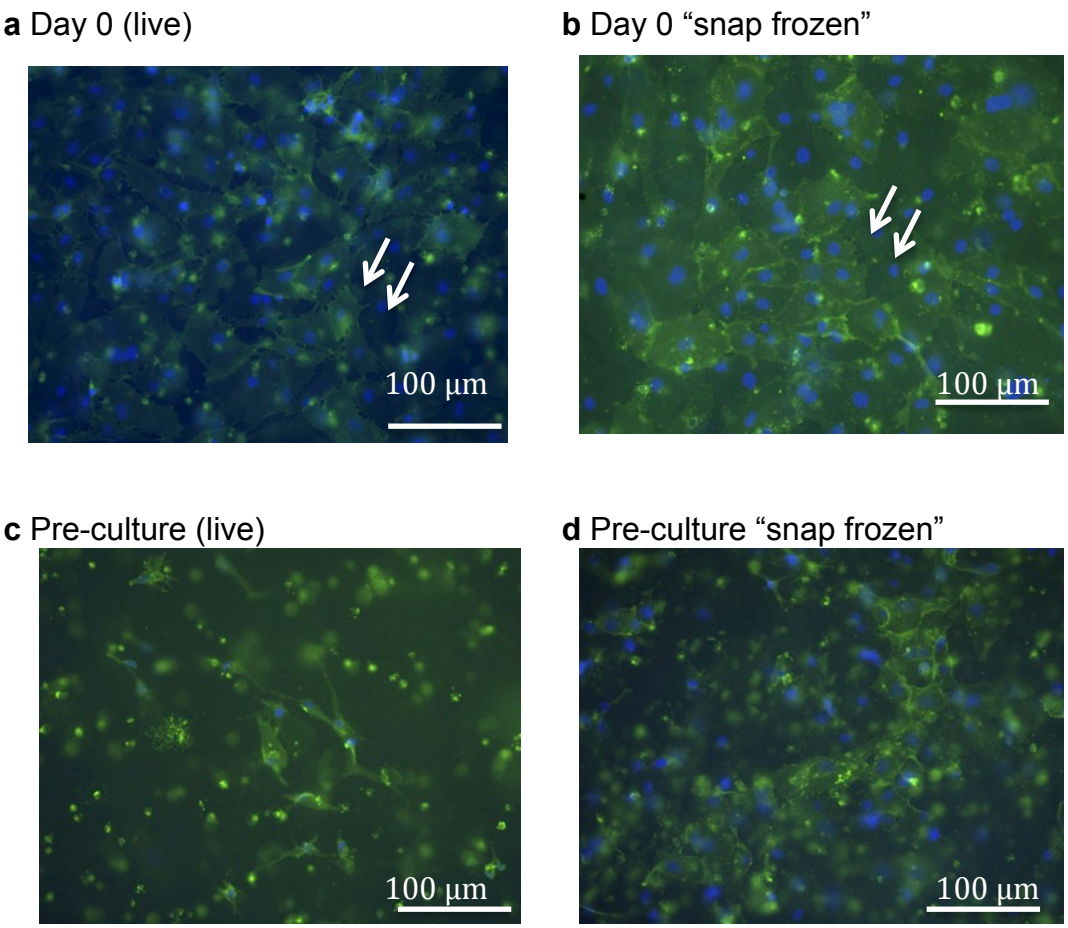

Figure 3.24. HUVEC morphologies in the four different culture conditions of the HBMSC spirals. HUVECs did not aggregate into networks in any of the conditions tested and were predominantly flattened cells (shown with double arrows).

3.18 HUVEC network formation in normoxia and physiological hypoxia

Cells are commonly cultured at atmospheric oxygen conditions set at 21% O_2, 5% CO_2. However, much lower oxygen levels surround most cells in the body. A 5% O_2 culture environment was chosen as it falls within the "physiological hypoxia" conditions found *in vivo* in various tissues, including the bone marrow (Stamati et al., 2011). The hypothesis under test was that HUVECs would optimally aggregate into networks when cultured in physiological hypoxia (5% O_2) compared to normoxia (21% O_2). Greater network aggregation was hypothesised to be due to the presence of higher levels of angiogenic growth factors, released by the support cells.

HUVECs were co-cultured with HBMSCs or HDFs in collagen-laminin cultures and CD31 immunofluorescence was used to test HUVEC morphology. HDFs were chosen as a different source of support cells to test their effect on HUVEC aggregation in both oxygen conditions.

Results showed longer and more (experimental observation) network aggregates in HBMSC co-cultures cultured in normoxia (98-150 μm) compared to hypoxia (73-104 μm). In HDF co-cultures, network aggregates were only present in physiological hypoxia (93-105 μm), with no visible networks in normoxia (Figure 3.25). There were no cobblestone aggregates in any of the culture conditions. The absence of any network aggregation or any cell-cell (HUVEC) interaction in HDF co-cultures in normoxia suggested that there were significant differences in HUVEC response depending on the support cells present.

These results showed that in fact in HBMSC co-cultures HUVECs aggregated into networks more when cultured in normoxia, contrary to the intial hypothesis. On the contrary, in HDF co-cultures, the hypothesis that HUVECs would form more networks in hypoxia was supported.

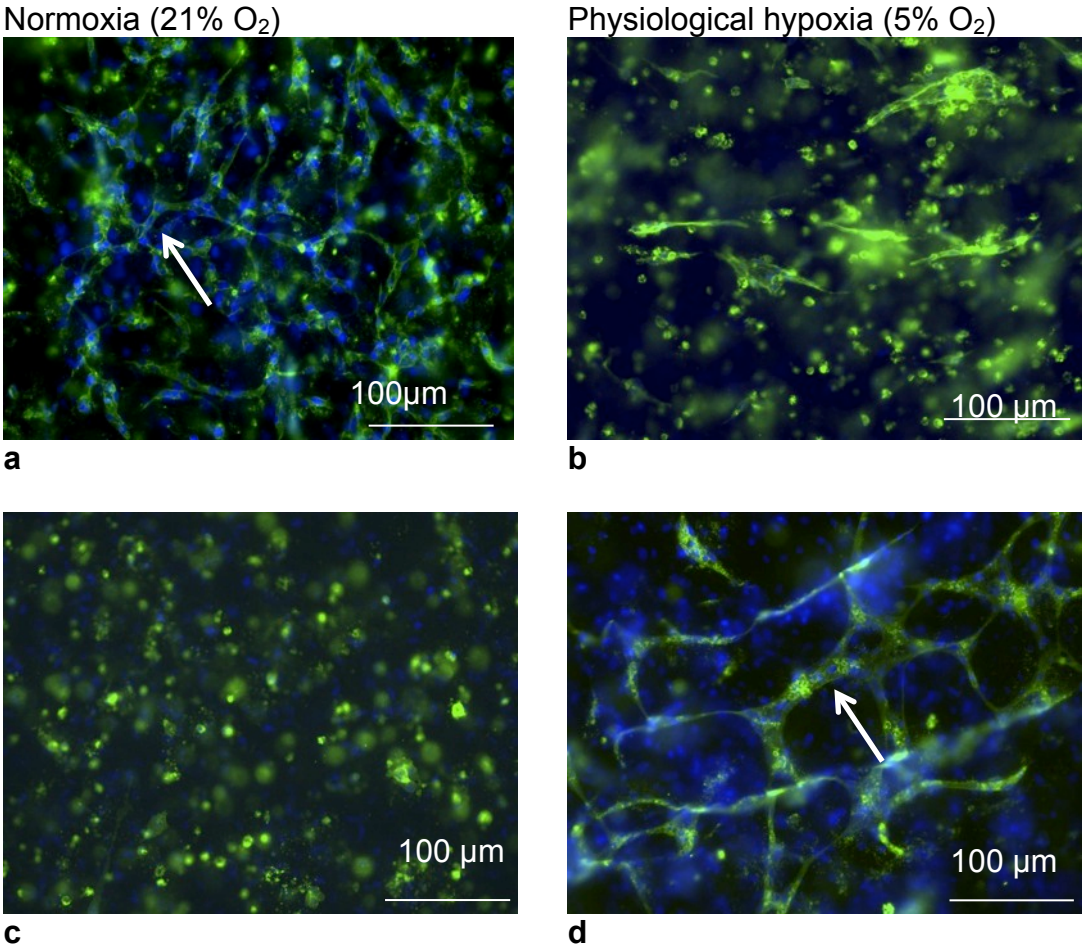

Figure 3.25. HUVEC aggregation in co-cultures with HBMSCs and HDFs in normoxia and hypoxia. Scale bar=100 µm. Upper panels (a,b) are the HBMSC co-cultures and lower panels (c,d) are HDF co-cultures. Arrows show network aggregation in HBMSC co-cultures in normoxia and HDF co-cultures in physiological hypoxia.

To test the hypothesis that differences in HUVEC aggregation in the two oxygen conditions were correlated to greater angiogenic growth factor release by the

support cells PDGF, VEGF, Angiopoietin-1 and TGFβ_1 were tested using ELISA. Protein levels were then correlated to HUVEC aggregation.

3.19 PDGF protein levels

PDGF was selected as it was previously tested in other experimental setups and was found to be produced by HUVECs. PDGF levels were analysed using ELISA in normoxia and hypoxia cultures. It was hypothesised that PDGF would only be present in HUVEC only cultures and that higher levels would be present in physiological hypoxia than normoxia.

HUVEC only cultures, HBMSC only, HDF only and co-cultures with HBMSC-HUVEC and HDF-HUVEC were all tested. ELISA results supported previous findings and showed that PDGF was only present when HUVECs were cultured alone (Figure 3.26). HUVECs produced nearly double the amount of PDGF in normoxia (~430pg/ml) compared to hypoxia (230pg/ml) ($p<0.001$). HBMSCs and HDFs did not produce any PDGF in either normoxia or hypoxia when cultured alone. PDGF was also absent in co-cultures with both supplementary cells in both oxygen conditions. These results were in agreement with initial findings in collagen hydrogels with HBMSCs where PDGF was also absent in co-cultures.

Overall, PDGF protein levels showed that oxygen levels affected PDGF release, with more efficient release by HUVECs in normoxia compared to physiological hypoxia. This disproved the hypothesis that cells would be releasing more PDGF in physiological hypoxia. However, the absence of any protein in co-cultures or HBMSC/HDF cultures proved the hypothesis that HUVECs were the

only PDGF releasing cells. This suggests either uptake of the protein by HBMSCs and HDFs or the presence of a feedback mechanism that slows PDGF release. *PDGF findings at this stage do not provide a correlation between PDGF levels and HUVEC morphology and aggregation.*

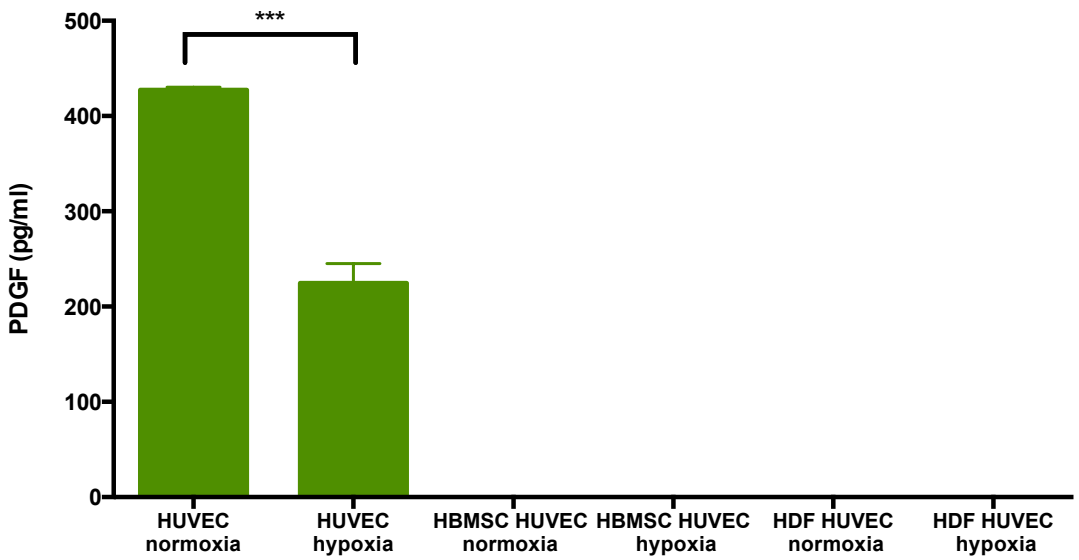

Figure 3.26. PDGF protein levels in cultures in normoxia and hypoxia. PDGF was only produced in HUVEC cultures and was absent in any of the co-cultures. PDGF was not detected in any of the HBMSC only or HDF only cultures.

*** $p<0.001$

3.20 VEGF protein levels

VEGF protein levels were also quantified, as both VEGF release and uptake was shown to be important for HUVEC response and aggregation (collagen vs collagen-laminin experiments). The hypothesis under test here was that HBMSCs and HDFs would be releasing more VEGF under physiological

hypoxia than normoxia. Based on previous findings it was hypothesised that HUVECs would not be producing any VEGF.

VEGF levels were tested in HUVEC only cultures, HBMSC only cultures, HDF cultures and in co-cultures of HUVECs with HBMSCs and HDFs in normoxia and hypoxia. HUVECs did not produce any VEGF, either in normoxia or hypoxia, in agreement with the hypothesis and initial findings.

HBMSCs produced the same amount of VEGF in both oxygen conditions (Figure 3.27). In co-cultures, there was significantly ($p<0.01$) less VEGF present in normoxia (880pg/ml) compared to hypoxia (~1700pg/ml). There was also a significant drop ($p<0.001$) in the levels of VEGF in normoxia co-cultures (880pg/ml) compared to the amount produced by HBMSCs when cultured alone (2000pg/ml) (Figure 3.27). In hypoxia co-cultures (~1700pg/ml) there was no difference in VEGF levels compared to the HBMSC only cultures (~2000pg/ml). These findings showed that VEGF levels were in fact lower when HUVECs aggregated into networks in normoxia. The significant drop in VEGF compared to HBMSC monocultures, suggested greater uptake of the protein by HUVECs. In order to test this hypothesis VEGF receptor levels were quantified.

HDFs produced fourfold less VEGF than HBMSCs in both normoxia and hypoxia cultures (Figure 3.27). As with HBMSC monocultures, there was no difference in the amount of VEGF produced when HDFs were cultured alone in the two oxygen conditions. There was however a significant difference ($p<0.01$) in VEGF levels in co-cultures, with more VEGF present in hypoxia (~400pg/ml) co-cultures than normoxia cultures (~30pg/ml). In this case, higher VEGF levels correlated with the greatest network aggregation of the cells. However, the

overall VEGF levels in HDF cultures were much lower than HBMSC cultures. This suggested that the mechanisms involved in promoting end-to-end network aggregation were different depending on the support cells present. Other soluble growth factors could be more significant in HDF co-cultures such as angiopoietin-1 and TGFβ, which were tested and the results shown in the next sections. In addition, other factors, such as extracellular matrix proteins, which were not tested in these cultures, could also be involved in the process.

To test the role of VEGF release and its uptake by HUVECs in these conditions, VEGF receptor types and levels were quantified in both normoxia and hypoxia cultures.

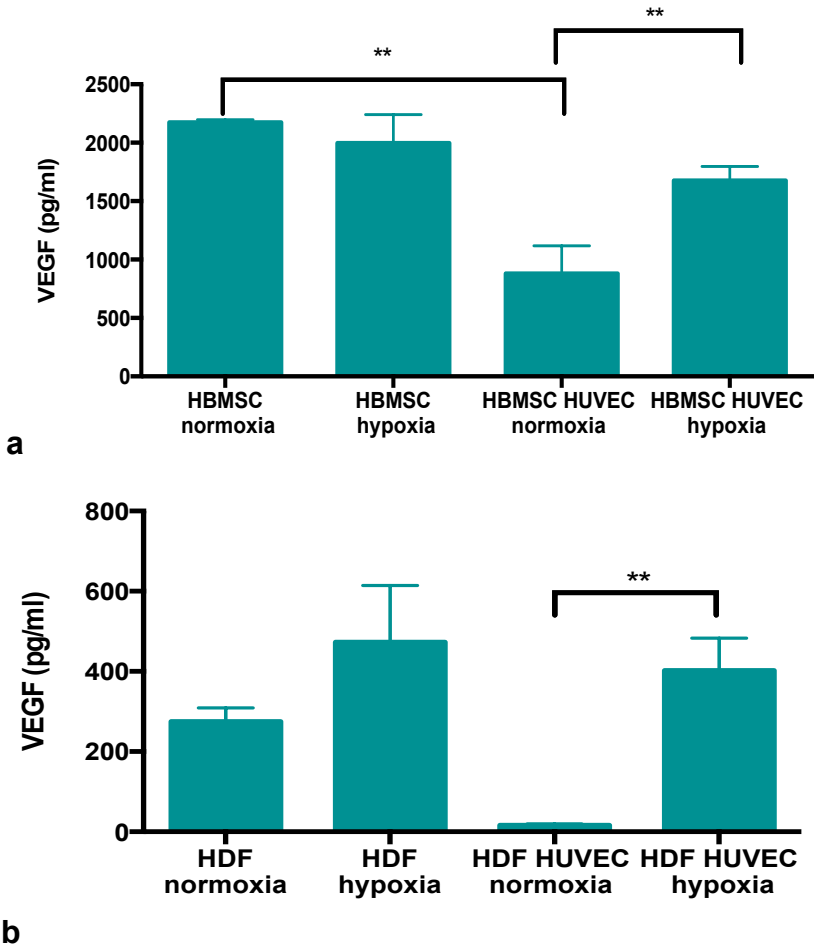

Figure 3.27. VEGF levels quantified by ELISA. a) VEGF levels in the medium of HBMSC only and HBMSC-HUVEC cultures in normoxia and physiological hypoxia, b) VEGF levels in HDF only and HDF-HUVEC cultures in normoxia and physiological hypoxia . Error bars are SD ** $p<0.01$

3.21 VEGF receptors

VEGF receptors are important mediators of VEGF action to the cells. As shown in experiments with and without laminin, the number and type of VEGF receptors significantly influences VEGF uptake and consequently HUVEC aggregation. VEGFR1 acts as a decoy receptor, while VEGFR2 acts as a pro-angiogenic receptor.

VEGF protein levels were significantly lower in HBMSC co-cultures in normoxia compared to i) HBMSC only in normoxia and ii) HBMSC-HUVEC in physiological hypoxia. This led to the hypothesis that VEGF uptake was greatest in normoxia, where the greatest HUVEC end-to-end network aggregation was also found. Since the pro-angiogenic VEGFR2 receptors were associated with HUVEC end-to-end network aggregation in collagen-laminin experiments, it was specifically hypothesised that VEGFR2 positive HUVECs would be higher in normoxia than hypoxia.

In HDF co-cultures the greatest HUVEC end-to-end network aggregation was in hypoxia, while there were no networks in normoxia. However, VEGF levels were higher in hypoxia than normoxia. This was in direct contrast to HBSMC co-culture results. It was therefore hypothesised that VEGF uptake was not increased in HDF co-cultures in physiological hypoxia and therefore receptor levels did not increase.

The levels of the two main receptors VEGFR1 and VEGFR2 were quantified using flow cytometry in co-culture conditions in both normoxia and physiological

hypoxia. The percentage of VEGFR1 and VEGFR2 positive HUVECs were quantified and the number of receptors per HUVEC was also calculated.

HUVEC monocultures were tested first for VEGFR1 and VEGFR2 levels in both normoxia and physiological hypoxia. This was done in order to obtain baseline levels of receptor levels in the absence of any support cells. When HUVECs were cultured alone, there were significantly more VEGFR2 positive HUVECs in both normoxia and hypoxia (~15% and 12%) compared to VEGFR1 (~2% and ~5%) ($p<0.001$ and $p<0.05$ respectively). There was no difference however in the number of positive cells for either VEGFR1 or VEGFR2 between the two oxygen conditions, when comparing the same receptor type (Figure 3.28). This suggests that oxygen levels did not affect the percentage of positive cells for each receptor type.

The number of receptors per HUVEC was also calculated by using the calibrated beads. In HUVEC only cultures, there was no difference in the number of receptors per HUVEC in normoxia, (~30000 receptors/cell vs 33000 receptors/cell) while in hypoxia there were significantly more VEGFR1 (~30000 receptors/HUVEC) receptors than VEGFR2 per cell (~26000 receptors/cell) ($p<0.05$) (Figure 3.28). In addition, when comparing the two oxygen conditions, VEGFR2 levels were significantly higher in normoxia (~33000 receptors/cell) compared to hypoxia (26 000 receptors/cell) ($p<0.01$).

The levels of the receptors were then quantified in both HBMSC and HDF co-cultures.

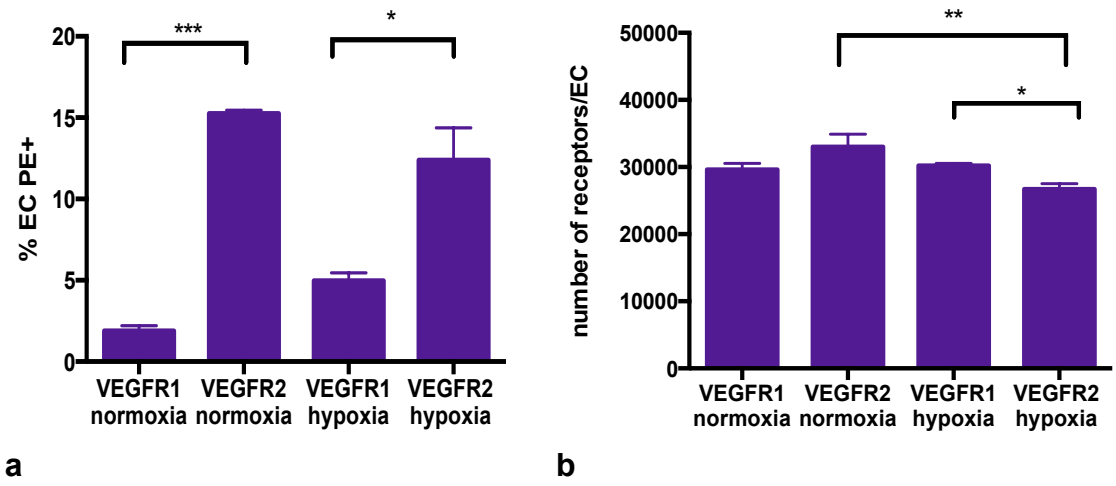

Figure 3.28. VEGF receptor flow cytometry results in HUVEC only cultures in normoxia and hypoxia. Receptors were quantified using flow cytometry with PE conjugated VEGFR1 and VEGFR2 receptors. a) The percentage of positive HUVECs for each receptor type was quantified in both normoxia and hypoxia, b) the number of receptors per HUVEC was calculated using quantibrite beads. triplicate samples were analysed, and error bars represent SD. *p<0.05, **p<0.01, ***p<0.001

In HBMSC co-cultures in normoxia there were significantly (p<0.05) more VEGFR2 positive cells (~11%) compared to VEGFR1 (~6%). In addition, there were significantly (p<0.05) more VEGFR2 (~11%) positive HUVECs in normoxia compared to hypoxia (~5%) (Figure 3.29). Higher percentages of VEGFR2 positive cells allow for greater pro-angiogenic response by HUVECs. This is as a result of the role of VEGFR2 as a positive angiogenesis inducer. This was evidenced by the greater network aggregation in normoxia co-cultures compared to hypoxia. In contrast, in hypoxia cultures there was no difference in the percentage of cells expressing each type of receptors.

Receptor numbers per cell were also calculated, with significantly higher numbers found for both receptor types in physiological hypoxia conditions. Specifically, there were 30 000 VEGFR1 receptors in normoxia and 40 000 receptors in hypoxia ($p<0.01$). There were also significantly more ($p<0.05$) VEGFR2 receptors in hypoxia (~40 000 receptors/cell) compared to normoxia (~30 000 receptors/cell).

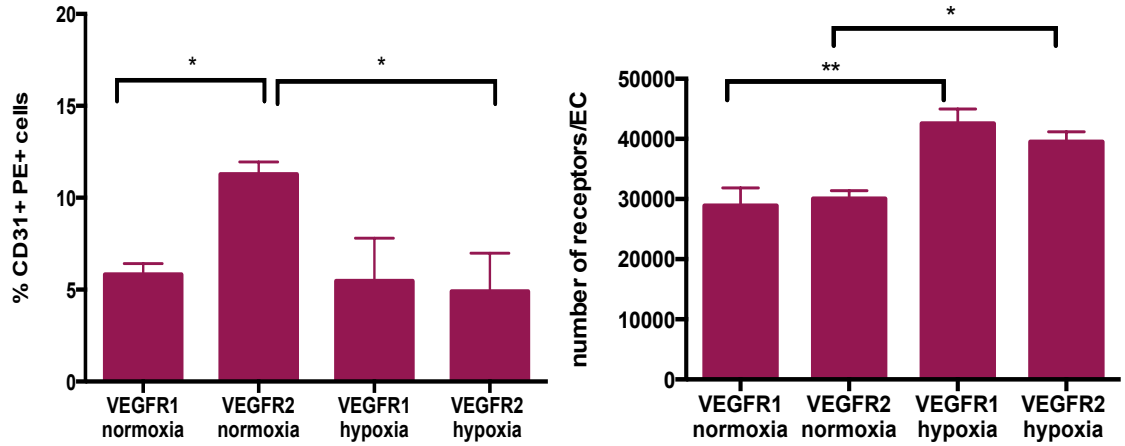

Figure 3.29. VEGF receptors in HBMSC HUVEC cultures in normoxia and physiological hypoxia. Receptors were quantified using flow cytometry with PE conjugated VEGFR1 and VEGFR2 receptors. CD31 (FITC conjugated) antibody was used to select the HUVECs. a) The percentage of positive HUVECs for each receptor type was quantified in both normoxia and hypoxia, b) the number of receptors per HUVEC was calculated using quantibrite beads. * $p<0.05$, **$p<0.01$, triplicate samples were analysed, and error bars represent SD.

The lower VEGF protein levels found in normoxia co-cultures (with HBMSCs) in conjunction with the receptor findings, suggest greater protein uptake by HUVECs. More importantly the significance of VEGFR2 differences, further support the greater angiogenic response by HUVECs in normoxia where cells

aggregated into more end-to-end networks as shown with CD31 immunofluorescence.

In HDF co-cultures, there was no difference in the number of HUVECs positive for VEGFR1 (~ 15%) or VEGFR2 (~17%) between the two oxygen conditions (5% vs 21%). There was also no difference in the type of receptors present (R1vs R2) within the same oxygen condition (figure 3.30). This would suggest that VEGF receptors and as a result VEGF was not as important in promoting network aggregation in HDF co-cultures.

The number of receptors per HUVEC was then calculated. There were no differences between VEGFR1 and VEGFR2 within the same oxygen condition. In normoxia levels averaged around 36000 receptors per cell and in hypoxia 25000 receptors per cell. Thus, there was a significant ($p<0.01$) decrease in the numbers of receptors in hypoxia compared to normoxia. The low levels, as with HBMSC co-cultures, coincided with the greatest network aggregation of HUVECs. This again could suggest greater receptor internalisation and HUVEC response in these conditions.

These results strongly suggest that in HBMSC co-cultures, VEGF and its receptors have a significant role in HUVEC aggregation. Especially, the higher number of VEGFR2 positive cells in normoxia, compared to hypoxia suggest both greater uptake of VEGF by the cells and a greater pro-angiogenic response. This resulted in greater network aggregation of HUVECs. The similarity in the percentage of HUVECs positive for the two types of receptors in HDF co-cultures in the two oxygen conditions and the lower levels of VEGF

(~800pg/ml vs 400pg/ml) present compared to HBMSC cultures, suggest a smaller role for VEGF and its receptors in the angiogenic response of HUVECs. However, the presence of significantly fewer ($p<0.01$) receptors per HUVEC in hypoxia compared to normoxia, indicate greater receptor internalisation and VEGF uptake compared to normoxia. In the absence of a supplementary cell type, HUVECs show some differences between normoxia and hypoxia, however these differ in co-cultures. Thus, the presence of supplementary cells influences receptor expression as well as internalisation.

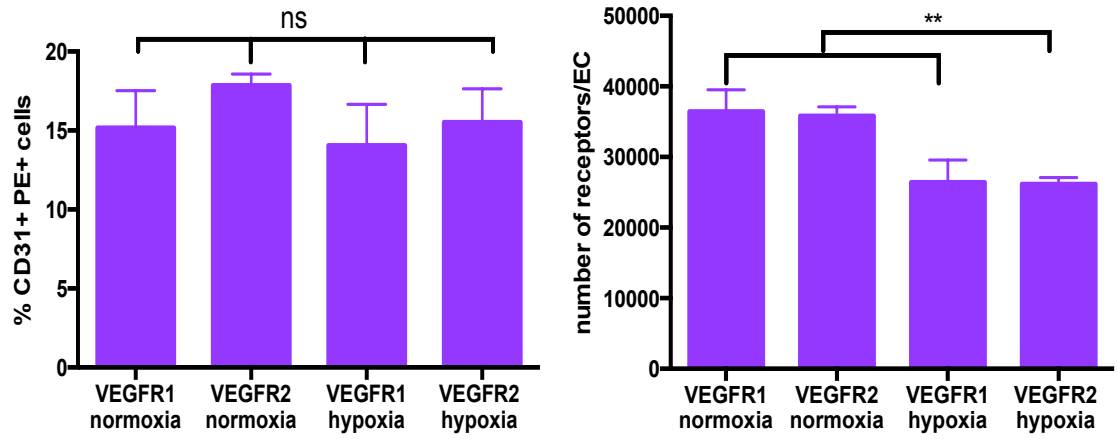

Figure 3.30. VEGF receptors in HDF HUVEC cultures in normoxia and hypoxia. Receptors were quantified using flow cytometry with PE conjugated VEGFR1 and VEGFR2 receptors. CD31 (FITC conjugated) antibody was used to select the HUVECs. a) The percentage of positive HUVECs for each receptor type was quantified in both normoxia and hypoxia, b) the number of receptors per HUVEC was calculated using quantibrite beads. * $p<0.05$, ** $p<0.01$, triplicate samples were analysed, and error bars represent SD.

To further elucidate the effect of angiogenic growth factors and oxygen culture conditions on HUVEC response other protein levels were quantified. Specifically, the role of angiogenic proteins such as Angiopoietin-1 and TGFβ_1 was tested.

	Normoxia (21% O_2)		Physiological hypoxia (5% O_2)	
	HBMSC	**HDF**	**HBMSC**	**HDF**
Ang-1	0pg/ml	133.25±22.98	0pg/ml	not quantified
TGFβ_1	0pg/ml	121pg/ml± 2.12pg/ml	0pg/ml	0pg/ml
PDGF	0pg/ml	0pg/ml	0pg/ml	0pg/ml

Table 3.2. Angiopoetin-1, TGFβ_1 and PDGF levels in HBMSC and HDF only cultures in normoxia and physiological hypoxia.

3.22 Angiopoietin-1 protein levels

Angiopoietin-1 is usually released by surrounding cells during angiogenesis and has been found to promote EC migration and sprouting and prevent apoptosis in *in vitro* experiments (Metheny-Barlow and Li, 2003). The hypothesis under test was that angiopoietin-1 levels would be higher in co-culture conditions where HUVECs aggregated into greater end-to-end network aggregates; i.e. HBMSC-HUVEC co-cultures in normoxia and in HDF-HUVEC co-cultures in hypoxia.

Angiopoietin-1 levels were quantified using ELISA from the medium of HBMSC only cultures, HDF only cultures HUVEC only cultures and co-cultures of HMBSC-HUVECs and HDF-HUVECs in both normoxia and physiological hypoxia.

Angiopoietin-1 was not produced in any of the HUVEC only cultures (figure 3.31) or the HBMSC only (table 3.2) cultures. However, high levels of angiopoietin-1 were found in HBMSC co-cultures in normoxia (1000pg/ml/) and lower levels in hypoxia co-cultures (400pg/ml) (Figure 3.31). The hypothesis is that HUVECs stimulated HBMSCs to produce angiopoetin-1. Although this was not directly tested here, HUVECs are known to produce angiopoeietin-2 rather than angiopoietin-1 (Fagiani and Christofori, 2013). Therefore, HUVECs were unlikely to be the source of angiopoietin-1 release in these conditions. In HDF co-cultures there were higher levels of angiopoietin-1 in hypoxia co-cultures (190pg/ml) compared to normoxia (33pg/ml).

Although these results were not statistically different, higher levels of angiopoietin-1 in both HBMSC and HDF co-cultures correlated with the greatest network aggregation. This proved the hypothesis that angiopoietin-1, in addition to other factors, promoted HUVEC network aggregation. These results also show that ECs stimulate the production of angiopoietin-1 by HBMSCs.

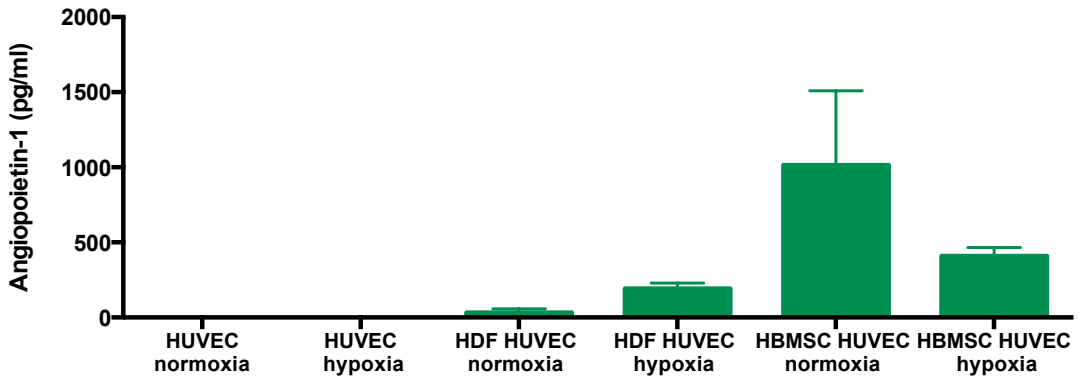

Figure 3.31. Angiopoietin-1 levels quantified by ELISA. Angiopoietin-1 was absent in HUVEC only cultures in both oxygen conditions. The highest levels were present in HBMSC co-cultures in normoxia. Error bars= SEM., p=ns

3.23 TGFβ$_1$ protein levels

TGFβ$_1$ levels in these cultures were tested, as TGFβ$_1$ is an angiogenic growth factor often added to culture media to promote tubulogenesis. TGFβ$_1$ levels were quantified in the medium of HUVEC only cultures, HDF only, HBMSC only and HBSMC-HUVEC, HDF-HUVEC cultures in normoxia and hypoxia using ELISA.

In our experiments we found that both HUVECs and HDFs produced TGFβ$_1$ (Figure 3.32). HBMSCs did not produce any TGFβ$_1$ when cultured alone (table 3.2). HUVECs produced ~800pg/ml in normoxia and ~500pg/ml, not significantly different in the two oxygen conditions. In HBMSC co-cultures the levels quantified in normoxia and hypoxia were the same as the levels found in HUVEC only cultures (800 and 500pg/ml respectively, not statistically significant). These results suggested that HUVECs were the TGFβ$_1$ producing cells (figure 3.32). In HDF co-cultures there was no significant difference between the levels found in normoxia (~300pg/ml) and hypoxia (~450pg/ml); however TGFβ$_1$ in this case could have been produced by either of the two cell types. In both HBMSC and HDF co-cultures the highest levels of TGFβ$_1$ corresponded to the greatest EC network aggregation seen, suggesting a link between its presence and EC end-to-end network aggregation. However, these differences were not statistically significant, thus definite conclusions about TGFβ$_1$ levels and HUVEC aggregation cannot be drawn.

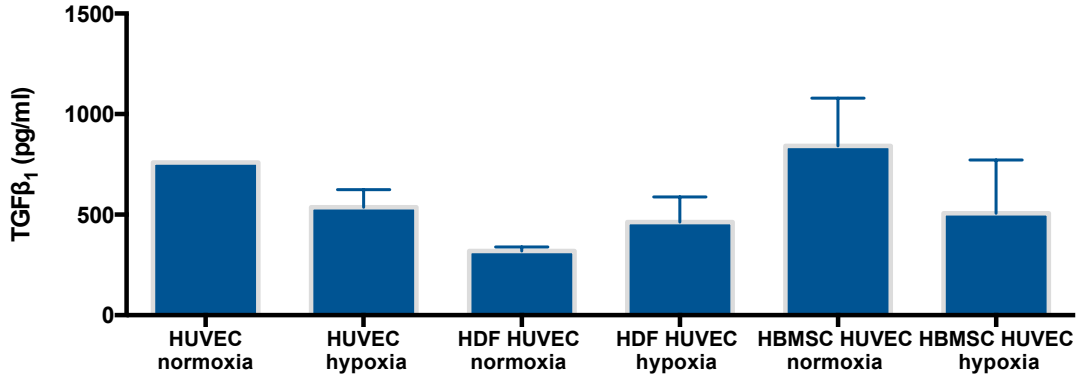

Figure 3.32. TGFβ$_1$ protein levels quantified by ELISA. There were no significant differences between the levels of TGFβ$_1$ in the different culture conditions tested. Error bars are SD, triplicate samples in each condition, p=not significant

4 Discussion

4.1 Endothelial cell culture in 3D scaffolds

One of the major limitations of 3D scaffolds is maintaining cell viability, especially within the core of constructs, where there is limited oxygen and nutrients (Kaully et al., 2009). A key aim of engineering complex and functional 3D structures is to successfully integrate capillary networks. This will increase long-term success of future implants (Duffy et al. 2011, Kaully et al 2009). In the current study cells were incorporated into the 3D collagen scaffold in order to ensure that network aggregates formed throughout the constructs. For tissue engineering purposes this is superior to many studies that seed cells on the surface of scaffolds and either rely on exogenous factors (growth factors, PMA) to promote cell invasion within the constructs (Bayless et al., 2009; Davis et al., 2000; Joung et al., 2006; Montesano and Orci, 1987; Montesano et al., 1983) or study EC organisation into networks in 2D on the scaffold surface (Ingber and Folkman, 1989; Kubota et al., 1988; Vailhé et al., 2001, 1997; Vernon et al., 1995).

In addition to tissue engineering applications, these 3D constructs can be used as models for testing different aspects of angiogenesis and vasculogenesis. Using *in vitro* models where possible, limits the use of *ex vivo* and *in vivo* models, such as the aortic ring outgrowth assay (Nicosia, 2009; Nicosia et al., 2011), the chick chorioallantoic membrane assay (CAM) (Hudlicka et al., 1989; Primo et al., 2010; Slevin et al., 2007; West et al., 1985), the corneal assay (Ali et al., 2013; Staton et al., 2009) zebrafish models and others using mice and rabbits (Staton et al., 2009). These models have contributed substantially to

understanding angiogenesis, for example by highlighting the importance of a6 integrins in the aortic ring and CAM assays (Primo et al., 2010), the role of basement membrane proteins in the aortic ring assay (Nicosia, 2009; Nicosia et al., 1994) and the role of hyaluronan and its receptors in angiogenesis using the CAM assay (Slevin et al., 2007; West et al., 1985). However, it is becoming increasingly necessary to work towards reducing the number of animals required for medical research ("reduce, refine, replace" principle).

By mixing ECs within the collagen hydrogel in this study, the assay was a closer mimic of vasculogenesis (Davis and Camarillo, 1996; Morin and Tranquillo, 2013). While important, especially in development, *in vitro* studies are more rare due to the 3D nature of the assays. Cells are interspersed throughout the scaffold, which make practical quantification and assessment more challenging (Staton et al., 2004). Thus, in addition to the benefit for tissue engineering applications, the current 3D *in vitro* study tested vasculogenesis, a less researched process.

There are numerous scaffolds available, used in different types of assays and experimental designs. These include fibrin and collagen I (Bayless and Davis, 2003; Bayless et al., 2009; Montesano and Orci, 1987; Rao et al., 2012), matrigel (Kubota et al., 1988), starch-polycaprolactone (Ghanaati et al., 2011) and silk fibroin (Unger et al., 2004). Collagen I hydrogels are not commonly selected as scaffolds in vasculogenesis. Davis and colleagues in the USA have done the majority of work using collagen hydrogels both for angiogenesis and vasculogenesis. Their vasculogenesis study design involves embedding ECs in a 3D collagen hydrogel, overlaid with Phorbol Myristate Acetate (PMA) and

growth factor supplemented media. PMA is a tumour promoter agent, which drives EC invasion within the scaffold and promotes EC tubulogenesis very quickly (Bayless and Davis, 2003; Bayless et al., 2000; Bell et al., 2001; Davis and Camarillo, 1996; Salazar et al., 1999).

PMA was added in some of the cultures in the present study as a control to test and compare the PMA effect to the other parameters tested. My results showed HUVEC network formation in 3D collagen hydrogels, within 48 hours in the presence of PMA without any additional growth factors. There was no evidence of flattened or cobblestone cells in any stage of the cultures. Network lengths at this early time point with PMA were (almost) equal to network lengths found in day 7 mixed co-cultures with laminin. However, the results also showed that networks in PMA cultures peaked by day 7 and appeared to plateau or disintegrate after that (Figure 3.5). Therefore the stability of these structures beyond that point is unclear. This quick network aggregation and network disintegration shows similarities to tumour angiogenesis, where blood vessels form quickly but are abnormal in both structure and function showing blood vessel leakiness, branching and lumen abnormalities (Carmeliet and Jain, 2011). While PMA may not directly affect cellular DNA (Powerski et al., 2011) its use raises concerns about safety and relevance to healthy EC response. Therefore, PMA experiments were only used as controls as this method is traditionally used to induce EC network aggregation. The use of supplementary cells and matrix proteins used maximises the translation of findings to the physiological cell response.

4.2 The effect of co-cultures

Co-cultures of ECs with supplementary cells are based on various cell sources in literature (Morin and Tranquillo, 2013). These range from MSCs (Au et al., 2008; Duffy et al., 2011; Kaigler et al., 2003; Kang et al., 2013; Kolbe et al., 2011; Rao et al., 2012), HDFs (Alekseeva et al., 2014; Kunz-Schughart et al., 2006; Newman et al., 2011) and osteoblasts (Fuchs et al., 2009; Herzog et al., 2014; Hofmann et al., 2008; Pirraco et al., 2014; Unger et al., 2007) to smooth muscle cells and pericytes (Sacharidou et al., 2012; Stratman et al., 2011, 2010, 2009). The most common sources are MSCs or HDFs, which were both used in this study (Duffy et al., 2011; Ghajar et al., 2010; Grainger et al., 2013; Morin and Tranquillo, 2013; Rao et al., 2012). Despite the extensive use of supplementary cells in studies using various scaffolds (eg. fibrin) (Morin and Tranquillo, 2013; Rao et al., 2012) the majority of collagen hydrogel work relies on growth factor addition and PMA (Bayless and Davis, 2003; Bayless et al., 2009; Bell et al., 2001; Salazar et al., 1999). There is limited published work using native collagen scaffolds and mixed co-cultures of HUVECs with supplementary cells. The current work addressed this by testing co-cultures of ECs with the two most commonly used supplementary cells, HBMSCs and HDFs in 3D collagen scaffolds.

MSCs are mainly selected due to both MSC multi-potentiality and the release of pro-angiogenic growth factors (Au et al., 2008; Bronckaers et al., 2014; Duffy et al., 2011; Kaigler et al., 2003; Kolbe et al., 2011; Rao et al., 2012). Incorporating multi-potential HBMSCs within the collagen hydrogels increases future applications, mainly for vascularised bone tissue engineering. A 1:1 media composition was selected to allow favourable culture conditions for both

cell types. Some published studies use EC medium only in co-cultures, to ensure the viability of ECs, which have greater culture medium demands and are more sensitive *in vitro* (Bulnheim et al., 2014; Kirkpatrick et al., 2011; Kolbe et al., 2011). From the cultures tested in the current study there was no evidence that using a mixture of EC medium with MSC medium compromised cell response and ECs successfully formed end-to-end networks. Interestingly, in literature, an increase in MSC osteogenic markers in co-cultures of MSCs and HDMECs compared to MSC monocultures, in the absence of osteogenic supplements has been shown (Bulnheim et al., 2014). Osteogenic markers were not tested in any of the cultures here but this is an important area for future work. On the other hand, some studies add osteogenic supplements to cultures to induce osteogenesis with varying degrees of success (Bulnheim et al., 2014; Kolbe et al., 2011). Therefore, further work focusing on MSC differentiation in MSC- HUVEC co-cultures can be useful for engineering vascularised bone tissues and fine-tuning media composition will be an important factor in this (Bulnheim et al., 2014; Kolbe et al., 2011; Vater et al., 2011).

One of the difficulties of co-culturing two or more different cell types is optimising the ratios used without compromising cell response (Kirkpatrick et al., 2011). In literature, cell ratios used vary and are dependent on the cells, scaffolds and overall experimental design used. Despite the use of different cell ratios, a lower proportion of the more robust, proliferative cells, is usually chosen (Bulnheim et al., 2014; Duffy et al., 2011; Kirkpatrick et al., 2011; Rao et al., 2012). At the same time, adequate growth factor release by supplementary cells has to be ensured as emphasised by findings by Rao et al (2012) where

MSC factors were insufficient due to the low number of cells used. Therefore, the optimum cell ratios that would agree with these principles had to be determined for the conditions and experimental design used in the current study. The 1:2 MSC:EC ratio used (200000:400000/ml) showed the balance between growth factor release by supplementary cells and EC aggregation. It is worth noting that Bulnheim et al (2012) also chose a 1:2 ratio in their study, as this was the best for long term EC viability. Despite this ratio not being the optimum for MSC osteogenic differentiation there was still an up-regulation of several osteogenic markers (Bulnheim et al., 2014). This emphasises the potential future use of the cultures described in this thesis, for the purpose of vascularised bone tissues.

The other popular source of supplementary cells used in literature is HDFs (Berthod, 2013; Newman et al., 2011; Sorrell et al., 2007). HDF- HUVEC co-cultures were also tested using similar conditions to HBMSC cultures and found HUVEC network aggregation in physiological hypoxia. The effect of physiological hypoxia will be discussed further in section 4.8. While the data showed a significant role for VEGF release and uptake in HBMSC co-cultures when ECs formed networks (as discussed in 4.5), in HDF co-cultures there was no such evidence. VEGF released by HDFs was very low and VEGF receptors showed no up-regulation, suggesting no direct VEGF effect on HUVEC aggregation. This was in agreement with some studies showing that VEGF is not necessary for EC network formation (Newman et al 2011) but disagreed with others showing VEGF mediated network aggregation (Levenberg et al 2005). Newman et al also showed that in a 3D fibrin bead assay, the combination of angiopoietin-1, angiogenin, hepatocyte growth factor, TGFα and

TNFα were necessary for EC network aggregation. Angiopoeitin-1 was quantified here, however levels were low in HDF co-cultures. When HDFs are used most studies emphasise the deposition of matrix protein by HDFs as the main mechanism by which fibroblasts affect EC response (Berthod, 2013; Kunz-Schughart et al., 2006; Newman et al., 2011; Sorrell et al., 2007). Matrix protein deposition by HDFs was not tested in the current study, however a potential link between matrix and hypoxia will be discussed in section 4.8.

As mentioned, HBMSC co-cultures have the potential to be useful for bone tissue engineering applications. Studies using EC co-cultures with fibroblasts have focused on tissues such as muscle and skin, more closely related to fibroblasts. For example, Levenberg et al (2005) used a PLLA/PLGA scaffold seeded with myoblasts, endothelial cells and fibroblasts. Myoblasts differentiated and organised into multinucleated myotubes while at the same time endothelial cells organised into capillary networks throughout the scaffolds (Levenberg et al., 2005). Fibroblasts were found to increase and stabilise the capillary structures, mainly through the release of VEGF (Levenberg et al., 2005). A similar study using fibrin and fibrin-PLLA-PLGA by Lesman et al (2011) showed successful integration of capillary structures with myotubes. Other attempts in literature include skin vascularisation using keratinocytes, fibroblasts and endothelial cells on 3D porous chitosan/collagen (Black et al., 1998; Kaully et al., 2009). Thus, by showing data that EC end-to-end networks can form within 3D collagen scaffolds using either HBMSCs or HDFs, tissue-engineering applications in the future can expand into different areas.

The data presented in co-cultures focused on the effect of the supplementary cells on ECs. However, ELISAs show PDGF protein release by HUVECs in monocultures (table 3.1), which is absent in co-cultures (with both HBMSCs and HDFs). This suggests PDGF protein uptake by HBMSCs and HDFs, a finding supported by different published studies (Au et al., 2008; Berthod, 2013; Duttenhoefer et al., 2013; Loibl et al., 2014; McFadden et al., 2013). PDGF is one of the main factors attracting pericytes to newly formed capillaries *in vivo* (Andrae et al., 2008; Berthod, 2013; Carmeliet and Jain, 2011). Others have shown evidence that HBMSCs and HDFs acquire a pericyte-like phenotype in co-cultures with ECs through a PDGF effect (Au et al., 2008; Berthod, 2013; Duttenhoefer et al., 2013; Loibl et al., 2014). Interestingly, McFadden et al (2013) recently suggested that the delayed addition of MSCs to EC cultures in collagen-proteoglycan scaffolds further enhances the perivascular role of MSCs. Their findings suggested PDGF release by ECs prior to MSC addition, which was utilised by MSCs after addition to EC cultures, quickly promoting a supportive role for EC networks that had formed.

In addition, different PDGF isoforms have been shown to affect collagen gel contraction by HDFs and crucially HDF migration in scratch wound assays (Donovan et al., 2013). Thus, in the current study PDGF uptake could result in HBMSC/HDF migration towards EC networks, promoting network stability and maturation. PDGF uptake by supplementary cells needs to be confirmed in future studies. In addition, supplementary cells should be tested for pericyte markers such as CD146, NG2 and αSMA (Berthod, 2013; Duttenhoefer et al., 2013; Loibl et al., 2014). If proven, the acquisition of a perivascular role by

HBMSCs and HDFs will be important for the long-term maintenance and maturity of engineered capillary structures.

4.3 The effect of matrix composition

When pure collagen I was used in my cultures, ECs migrated to the top surface and aggregated into the cobblestone morphology. This was an important finding as HUVEC migration to the surface of 3D scaffolds over time has not been described elsewhere. Others have described EC aggregation in cobblestone in 2D on the surface of scaffolds but not in 3D (Kubota et al., 1988; Kumar et al., 1987). As will be discussed in more detail in 4.4, this cell behaviour can have significant implications both for testing developmental pathways and tissue engineering applications.

Despite HBMSC addition to collagen I cultures and the presence of VEGF, HUVECs aggregated into cobblestone. This suggested that collagen I prevented HUVEC end-to-end network aggregation. Kroon et al (Kroon et al., 2002) also showed that collagen I inhibited EC (using human foreskin microvascular ECs) tube formation on fibrin constructs. More recently, Rao et al (Rao et al., 2012) used EC-MSC co-cultures and tested the effect of collagen I addition to a fibrin matrix. Their study also showed that EC tubules became increasingly longer when fibrin was added and the percentage of collagen I was decreased. These findings suggested that collagen I prevents or slows down end-to-end network formation. However, results in the current study prove that by fine-tuning matrix composition different HUVEC aggregation patterns can be achieved. Collagen I remains an ideal scaffold for tissue engineering, as it is abundant, biomimetic and can be used for several tissue engineering

applications (Brown et al., 2005; O'Brien, 2011). These include on-going studies testing collagen I for muscle (Brady et al., 2008; Cheema et al., 2003; Smith et al., 2012), nerve (Georgiou et al., 2013; Phillips et al., 2005) and cornea (Levis et al., 2010) applications.

Laminin was added to collagen I in the current study, to create an environment conducive to both EC proliferation and "differentiation" (Kubota et al., 1988) so that ECs formed end-to-end networks. The end-to-end network aggregation of HUVECs when laminin was present emphasised the importance of matrix composition as also show in the aortic ring outgrowth assay (Nicosia, 2009; Nicosia et al., 1994) and 2D angiogenesis assays (Kubota et al., 1988). Kubota et al (1988) first showed that laminin was essential for network formation when ECs were cultured on top of a collagen I scaffold without any supplements. However, Kubota et al (1988) relied on the organisation of cells in 2D, on the surface of the scaffold. In contrast, the findings here are of great importance with EC network organisation throughout the collagen constructs, in 3D. While other studies using collagen I have shown EC tubulogenesis in 3D, this has mainly been in the presence of PMA, S1P (Bayless and Davis, 2003; Davis et al., 2000) or growth factors (Davis et al., 2000). In contrast, I relied on EC organisation in the absence of any supplements by fine-tuning cell-cell and cell-matrix interactions. Relying on the effect of these physiological parameters was a major advantage to the use of exogenous factors.

The importance of laminin in tube morphogenesis has also previously been shown by blocking it in matrigel experiments (Davis and Camarillo, 1995; Grant et al., 1989). Laminin is a main component of matrigel, which is widely used in

EC studies (Arnaoutova and Kleinman, 2010; Arnaoutova et al., 2009; Kubota et al., 1988). However, matrigel has an incompletely defined, predetermined composition (Bayless et al., 2009), which limits its long-term applicability for EC biology testing and tissue engineering. In addition, matrigel has been shown to induce cell fusion and tubulogenesis in fibroblasts (Bayless et al., 2009; Bikfalvi et al., 1991; Donovan et al., 2001; Emonard et al., 1987), which suggests that its effect is not unique to ECs. In contrast all network aggregates in co-cultures here were CD31 positive, while CD31 negative cell nuclei were single cells. Since HBMSCs and HDFs are primarily CD31 negative, this suggests an EC specific aggregation. This is important to ensure that the collagen-laminin scaffold is a controlled 3D environment that promotes a specific and reproducible response by ECs.

HUVEC end-to-end networks were visible for a week in culture. Two-week cultures were hindered by extensive contraction of the collagen by both HBMSCs and HDFs and therefore could not be analysed. This has also been noted in some fibrin cultures in literature with shrinkage by 7 days (Lesman et al., 2011). This is due to the weak mechanical strength of the scaffold (Brown et al., 2005; Cross et al., 2010), which allows cells such as HBMSCs and HDFs to freely contract the matrix (Brown et al., 1998; Eastwood et al., 1998; Karamichos et al., 2007). This is a limitation of using collagen hydrogels, which can be overcome by using plastically compressed collagen scaffolds (Brown et al., 2005) while crosslinking of collagen fibrils can further increase its mechanical strength (Cheema et al., 2012; Wong et al., 2013). In fact, recent work by Alekseeva and colleagues (2014) has begun testing the behaviour and response of microvascular ECs in compressed collagen constructs, in

monocultures and in co-cultures with fibroblasts. Further modifications of the collagen scaffolds will be tested in the future to promote longer culture times and improve mechanical strength. Nevertheless, the findings in the current study show promising results for engineering stable network aggregates. Most importantly this is an improvement to some matrigel studies where despite the quick response and tube formation by ECs (Arnaoutova et al., 2009) tubular structures disintegrate after 2-3 days in culture (Sorrell et al., 2009).

4.4 Cell polarity and tubulogenesis

ECs *in vivo* are polarised cells, with an apical side facing the blood vessel lumen and a basal side attached to the basement membrane (Chung and Andrew, 2008). In addition, cell-cell junctions on the lateral surfaces allow cell-cell communication. Differences on each cell surface establish cell polarity, which is controlled by proteins including Par3, Par6 and PKC isoforms (Iruela-Arispe and Davis, 2009; Sacharidou et al., 2012) and allows for different functions and cell permeability (Chung and Andrew, 2008).

The two main aggregation patterns described in this study, the cobblestone and end-to-end network aggregation, mimic developmental mechanisms for tubulogenesis. As cell polarity is an important part of both tubulogenesis and the endothelium anatomy and function, these aggregation patterns are also linked to cell polarity. Developmentally tubular organs form as a result of five main processes: wrapping, budding, cavitation, cord hollowing and cell hollowing (Lubarsky and Krasnow, 2003). Chung and Andrew (2008) describe wrapping and budding as two processes that lead to tubulogenesis from an existing polarised epithelium. In contrast, de novo acquisition of cell polarity

alongside lumen formation occurs in cavitation, cord hollowing and cell hollowing (Chung and Andrew, 2008).

Indeed cobblestone aggregation of HUVECs described in this study, especially in single cultures where a cobblestone cell sheet forms on the ventral surface of the constructs, appears to mimic “wrapping”. Cell migration to the ventral surface of the constructs is especially important as HUVECs establish apical-basal polarity. Wrapping, found in processes such as neurulation, involves changes in the organisation and shape of the cells, which have formed a polarised epithelium (Chung and Andrew, 2008). The cells from a columnar shape become more pyramidal and cell contraction results in bending of the cell sheet (Chung and Andrew, 2008). This continues until the edges meet and form a tubular structure that is parallel to the initial sheet (Lubarsky and Krasnow, 2003). While *in vivo* this is not commonly found in capillary formation, it is a process used by other epithelial cell types (Iruela-Arispe and Davis, 2009; Lubarsky and Krasnow, 2003). Both the time-dependent changes in cell shape from multipolar, to flattened to cobblestone and the migration to the surface as described here, could resemble the initial stages of wrapping.

On the contrary, end-to-end networks found in HBMSC-HUVEC co-cultures with laminin in normoxia and HDF-HUVEC co-cultures in physiological hypoxia could be mimicking cell or cord hollowing. In both cord hollowing and cell hollowing, vesicles or vacuoles are involved in creating a lumen (Lubarsky and Krasnow, 2003). In cell hollowing these vacuoles are found intracellularly within single cells, while in cord hollowing vacuoles are found extracellularly between cells of a solid structure (Iruela-Arispe and Davis, 2009; Lubarsky and Krasnow, 2003).

The vacuoles eventually coalesce to form a complete lumen. These processes are more commonly described in capillary formation and have been studied both *in vitro* and *in vivo* (Davis et al., 2007; Iruela-Arispe and Davis, 2009; Lubarsky and Krasnow, 2003).

Ultimately, these morphological changes and aggregation patterns in this study could aim to create a tubular structure- with a hollow lumen- and establish apical-basal cell polarity (Chung and Andrew, 2008). Further work is needed to establish the presence of hollow lumens and cell polarity in both the cobblestone and end-to-end network aggregation. Real-time lapse microscopy can be used to test the process of end-to-end network aggregation, similar to the work done by others (Davis et al., 2007; Koh et al., 2008; Sacharidou et al., 2012). This in conjunction with further histological tests can determine lumen presence. Monitoring real time cell aggregation will also test vacuole formation. If vacuoles are found intracellularly, network formation would mimic cell hollowing, while if vacuoles are extracellular the process is a better mimic of cord hollowing (Lubarsky and Krasnow, 2003; Sacharidou et al., 2012).

As mentioned, establishing apical-basal cell polarity is an important part of lumen formation. Studies in literature have shown that blocking proteins Par3 and Par6b, which control cell polarity, prevent lumen formation *in vitro* (Davis et al., 2007; Koh et al., 2008; Sacharidou et al., 2012). However, EC polarity is not as defined as in epithelial cells and there are no specific membrane markers that would distinguish the two EC surfaces (such as annexin 2 or podocalyxin found on the apical surface in epithelial cells) (Iruela-Arispe and Davis, 2009; Sacharidou et al., 2012). Co-localisation on the basal EC surface of support

cells such as pericytes and basement membrane proteins are currently the best indicators for cell polarity (Sacharidou et al., 2012). Future testing of the interaction between HUVECs and HBMSCs, as well as basement membrane localisation can determine EC polarity.

4.5 Integrins, matrix composition and VEGF receptors

Integrins provide cell attachment to the surrounding matrix and orchestrate intracellular cell signalling, affecting cell behaviour (Brooks, 1996; Davis and Camarillo, 1995; Hynes, 2009; Primo et al., 2010; Ross, 2004). My results showed that α6 integrin, was important for network aggregation of HUVECs. This was shown when α6 integrin was blocked, resulting in EC morphology in cultures with collagen-laminin reverting back to the morphologies found in collagen I only cultures. My work has shown for the first time the importance of α6 integrin in a 3D collagen-laminin vasculogenesis assay. Others have shown similar results where the addition of α6 antibodies inhibit or reduce capillary networks (Lee et al., 2006; Primo et al., 2010). However, these were done in matrigel or laminin coated plates in 2D with VEGF supplemented media (Davis and Camarillo, 1995; Lee et al., 2006; Primo et al., 2010). By using collagen I in this study the effect of individual matrix parameters and integrins were tested in a controlled environment. This is an advantage to using matrigel, where the mixture of different matrix components and growth factors could compromise the effect of integrins or matrix components.

There is a complex relationship between matrix, integrins and growth factors (Brooks, 1996; Hynes, 2009; Primo et al., 2010), including an increase in integrin expression following growth factor addition to cultures (Lee et al., 2006;

Primo et al., 2010). The complex relationship between matrix and growth factors also involves growth factor binding to certain ECM proteins. There is evidence that VEGF binds to heparin (Hynes, 2009; Wu et al., 2011), but there are no studies describing VEGF binding to laminin. Indeed the current study showed that despite significantly lower VEGF levels in collagen-laminin co-cultures compared to collagen only co-cultures, HBMSCs alone released the same amount of VEGF in both matrices. Thus, laminin does not affect HBMSC signalling and the addition of laminin to collagen hydrogels does not trap extra VEGF. This is the first study to show this in an *in vitro* controlled setting. The difference in VEGF levels in co-cultures, suggested higher VEGF uptake by ECs in the presence of laminin. VEGF receptors were quantified using flow cytometry, further deducing the link between laminin, VEGF receptor levels and protein uptake (Stamati et al., 2014).

While the current work was done in 3D culture, published studies quantifying receptor levels mainly use cells grown on tissue culture plastic. By using the methods described by Imoukhuede and colleagues for cells cultured in 2D or cells extracted from tissues, (Imoukhuede and Popel, 2012, 2011; Imoukhuede et al., 2013) the number of receptors per cell was quantified. Receptor surface levels per EC were much higher than previously published work using similar quantitation methods (Imoukhuede and Popel, 2012, 2011). Imoukhuede and Popel (2012) showed significant differences in receptor levels quantified in *ex vivo* cells (from mouse tissues) and cultured cells in 2D. These differences mainly related to the balance between VEGFR1 and VEGFR2, i.e. whether VEGFR1 levels were higher than VEGFR2 (Imoukhuede and Popel, 2012).These differences between *ex vivo* and *in vitro* results emphasise the

important relationship between matrix and integrins on receptor expression. A systematic approach to unravel more details of these interactions will be necessary in the future and using such an *in vitro* controlled environment is ideal.

Higher VE-cadherin levels have been correlated to higher VEGFR2 expression (Calera et al., 2004; Lampugnani et al., 2006; Nakayama et al., 2013; Scott and Mellor, 2009). VEGFR2 surface expression is stabilised as a result of the interaction with cadherins, decreasing receptor internalisation (Calera et al., 2004; Lampugnani et al., 2006; Nakayama et al., 2013; Scott and Mellor, 2009). In effect, this stabilisation works to "negatively" regulate VEGFR2 function, preventing internalisation and VEGF signalling (Chen et al., 2010). Immunofluorescence staining for VE-cadherin showed more intense surface staining in collagen-laminin co-cultures, where ECs formed end-to-end networks, compared to collagen only co-cultures, where cobblestone formed, on day 7 Figure 3.14). At the same time, on day 7, a higher number of VEGFR2 receptors per HUVEC was also measured in collagen-laminin co-cultures (~40000 receptors) compared to collagen only (~30000 receptors). Therefore, VE-cadherin surface localisation on day 7 stabilises VEGFR2 and stops internalisation. At this stage ECs have already established cell-cell contact and formed networks, as shown by CD31 immunofluorescence (Figure 3.11), which suggests that VEGFR2 signalling is no longer required.

It should be noted that differences in the role of VE-cadherin in EC aggregation were also highlighted by Bach et al (1998) who found that a VE cadherin antibody disrupted capillary tubes (by preventing new capillary structure

formation and disrupting pre-existing capillaries) but did not disrupt EC monolayers *in vitro*. This supports initial findings here that significant differences in VE-cadherin expression exist depending on EC aggregation. Staining provided qualitative evidence suggesting a link between VE cadherin and VEGFR2 surface levels in these co-cultures. Further tests quantifying these VE cadherin (eg. Western blots) differences can prove the relationship between VE cadherin and VEGFR2 in 3D collagen-laminin constructs.

Collectively, these findings suggest that VEGF binds to VEGF receptors on ECs, resulting in "outside-inside" signalling as described by Ross (Ross, 2004). VEGF binding to (mainly) VEGFR2 results in receptor internalisation and subsequent α6 integrin expression (Davis and Camarillo, 1995; Primo et al., 2010), which increases EC attachment to laminin. As a result, intracellular signalling orchestrated by α6 leads to EC reorganisation and changes in EC morphology and aggregation (Ross, 2004). Most importantly, the reorganisation of the cells into end-to-end networks has been shown here to be integrin and matrix dependant, i.e. will only occur when α6 and laminin are present. This complex signalling loop between integrins and growth factors has also been described in other cells including fibroblasts, skeletal myoblasts and oligodendrocytes (Ross, 2004). These initial findings have shown that this *in vitro* model is a relatively easy and reproducible way to test the exact mechanisms that orchestrate specific EC responses.

Future work will test the addition of fluorescently labelled VEGF in culture medium, which can be tracked and quantified within cells, similar to work by (Nakayama and Berger, 2013). VEGF receptor levels combined with the rate of

VEGF uptake can definitively prove the link between matrix composition and growth factor uptake.

4.6 HDMEC cultures

HUVECs were selected due to their widespread use in studies using ECs (Morin and Tranquillo, 2013). They are relatively easy to obtain (purchase or extract), although extracting them can result in a low cell yield (Unger et al., 2002). With the correct media composition they can be maintained in 2D culture for a limited doubling time (Unger et al., 2002). The second most popular type of ECs are HDMECs (Morin and Tranquillo, 2013; Unger et al., 2007). Both HUVEC and HDMECs are primary cells with a degree of variability between samples (Bouïs et al., 2001) and most importantly, differences between EC sources (Aird, 2007b; Bouïs et al., 2001; Kumar et al., 1987; Morin and Tranquillo, 2013). Thus, results using one type of EC may not be representative of other sources of cells. Some researchers use EC lines, however not all cell lines have the same characteristics and respond in the same way as these primary cell sources (Unger et al., 2002).

In this study there were significant morphological differences when HDMECs were cultured in the same conditions as HUVECs. HUVECs showed extensive migration (Figure 3.3) (in HUVEC only cultures) with time, to the top of the collagen scaffold and aggregated from single cells to form a cobblestone cell sheet. In contrast, when HDMECs were cultured alone in collagen hydrogels cells did not form a cobblestone cell sheet and showed mainly a multipolar morphology (Figure 3.19). Differences in cell morphology have also been described in literature in 2D, with large vessel ECs showing cobblestone

morphology, while microvascular ECs have a more elongated morphology (Kumar et al., 1987). HUVECs and HDMECs have also been found to proliferate and respond to growth factors differently in 2D culture (Lang et al., 2003, 2001).

HUVECs are extracted from the umbilical artery, a large vessel of fetal origin, while HDMECs are extracted from adult skin. A study by Lang et al (2003) addressed whether organ origin and "maturity" (fetal vs adult) was more relevant to EC differences than vessel size and function (macrovascular vs microvascular). Lang et al (2003) extracted microvascular ECs from human placenta (PLEC), an organ of fetal origin, and compared them to HUVECs and HDMECs. Their findings showed that PLECs had a more elongated morphology, more akin to HDMECs. In addition, cell proliferation and response to cytokines was more similar to HDMECs, rather than HUVECs (Lang et al., 2003). This supports the theory that differences between the two cell types exist due to the differences in vessel size and function rather than organ maturity. Testing additional EC sources in 3D cultures can prove or disprove this in the future.

In addition, HDMECs did not form any end-to-end network aggregates in HBMSC co-cultures in collagen-laminin hydrogels. Future work can also focus on co-cultures of HDMECs with pericytes or HDFs, rather than HBMSCs, which more closely mimic *in vivo* cell interactions (Armulik et al., 2005).

These results therefore emphasise the morphological differences between ECs depending on the cell source (Bouïs et al., 2001; Kumar et al., 1987; Morin and

Tranquillo, 2013). While only the morphological differences were tested here other differences in growth factor release, receptors and cell markers have been identified elsewhere (Aird, 2007a, 2007b; Kumar et al., 1987; Lang et al., 2003). EC heterogeneity, including other EC sources such as outgrowth endothelial cells (Fuchs et al., 2010; Ghanaati et al., 2011) can be extensively studied using these 3D cultures as described, where cell-cell and cell-matrix interactions can be easily controlled.

4.7 Segregated co-cultures

Several published studies have tested the presence of gradients of angiogenic factors in 3D *in vitro* to guide EC migration and mimic angiogenesis. The majority of these studies use immobilised growth factor addition, most commonly VEGF (Gerhardt et al., 2003; Odedra et al., 2011; Shen et al., 2008). Despite the fact that VEGF is known to be an important regulator of angiogenesis and critical for EC migration, it is one of many factors involved in the process. While some studies have paired VEGF with other factors, such as angiopoietin-1 (Odedra et al., 2011; Shin et al., 2011), exogenous growth factor addition is not as physiological as a cascade of growth factors released by supplementary cells.

Segregated co-cultures in the current study tested the effect of HBMSC-HUVEC cultures in the absence of direct cell contact. The aim here was to use a physiological approach, by relying on HBMSC released growth factors and using the unique features of compressed collagen constructs (Brown et al., 2005; Cheema et al., 2010; Hadjipanayi et al., 2012, 2011). Previous work in this group adopted a similar approach where HDF seeded collagen spirals were

used in segregated cultures with HUVECs (Hadjipanayi et al., 2011, 2010). While both *in vitro* and *in vivo* work in these previous studies had shown promising results for HUVEC network aggregation, this was not found in the current study. There were however, significant differences in the experimental setup and the choice of cells between these studies.

4.8 Normoxia vs physiological hypoxia cultures

Cell culture in lower oxygen conditions than the commonly used atmospheric oxygen conditions (21% O_2, 5% CO_2 and 37C) is physiologically relevant, since most cells in the body are normally exposed to much lower oxygen levels than 21% (Stamati et al., 2011).

Physiological hypoxia levels of 5%O_2 were chosen based on experimental observations in this group and others, which resulted in HBMSC growth factor up-regulation (Cheema et al., 2010; Das et al., 2010; Kinnaird, T, Stabile, E Burnett, M S Lee et al., 2004; Tsai et al., 2012). For example, Kinnaird et al (2004) found that MSC culture at 5% O_2 results in a twofold increase in VEGF levels compared to 21% O_2. Previous work from this group showed that cell density dependent oxygen consumption gradients formed in compressed spiralled collagen constructs. Real time oxygen monitoring readings averaged between 5%O_2 in the core and 17%O_2 in the periphery (Cheema et al., 2010, 2008; Streeter and Cheema, 2011). These oxygen levels correlated with significant differences in angiogenic growth factor levels (at the gene level), with higher levels in the core, where oxygen levels were lower (Cheema et al., 2010, 2008; Hadjipanayi et al., 2010). In addition, it was important to select an oxygen concentration within the physiological range because while physiological

hypoxia is an angiogenic stimulus, extreme hypoxia (eg. 0.2% O_2) can lead to EC apoptosis (Li et al., 2003).

In the current study there was no difference in VEGF protein levels released by HBMSCs when cultured alone. However, VEGF levels in HBMSC co-cultures in physiological hypoxia were higher than normoxia but this did not correlate to greater end-to-end network aggregation. In fact, as described in the results (Figure 3.25, Figure 3.27, Figure 3.29) VEGF levels, VEGF receptor levels and EC network aggregation suggest that protein uptake was greater in normoxia than physiological hypoxia.

Overall, comparisons of protein findings with published literature are made with caution. Differences in experimental design, oxygen levels used to culture cells and the presence or absence of a 3D matrix significantly affect cell signalling and protein release. For example, Gawlitta and colleagues (Gawlitta et al., 2012) used a “pellet” vasculogenesis assay and cultured endothelial colony forming cells and MSCs in osteogenic medium and found that hypoxia inhibited network aggregation of ECs in MSC co-cultures. While the effect on EC morphology was similar to the current study, protein levels showed contrasting stories. VEGF levels were lower in co-cultures in hypoxia (3-5% O_2) than normoxia but were higher in MSC only cultures in hypoxia. Both the different source of ECs used and the lower oxygen levels could have contributed to the difference in protein levels. Another study by Ben-Yosef (2005) used very low levels of 0.3% O_2 and found that lower oxygen levels inhibited HUVEC tubulogenesis on matrigel. These low oxygen levels are within the pathological hypoxia range and therefore the effect on EC viability could significantly influence network formation.

In addition, some researchers have found that exposing ECs to hypoxic conditions induces VEGF production by the cells (Namiki et al., 1995; Nilsson et al., 2004). VEGF protein was not detected in normoxia or physiological hypoxia when HUVECs were cultured alone in the cultures here. However, HUVECs cultured in physiological hypoxia showed significantly higher levels of VEGFR1 compared to VEGFR2 in physiological hypoxia (Figure 3.28). Cells also had significantly lower VEGFR2 levels compared to normoxia. These findings were in agreement with studies by (Nilsson et al., 2004; Ulyatt et al., 2011), where ECs were cultured in hypoxia. However, it is worth noting that these studies used much lower oxygen levels (1% and 0.5% O_2) compared to the 5%O_2 used here.

In HDF cultures there were significantly higher VEGF levels in hypoxia co-cultures, where there was greater network aggregation. However, there was no difference between VEGF levels in HDF only cultures and co-cultures in physiological hypoxia. In addition, VEGF levels were 4-5 times lower than HBMSC cultures, suggesting a limited VEGF effect, similar to findings by others (Han et al., 2006; Newman et al., 2011).

There were also no significant differences in TGFβ_1 levels in the two oxygen conditions. TGFβ_1 signalling has been shown to promote EC proliferation, migration and vessel maturation *in vivo* (Dallas et al., 2008; Warrington et al., 2005), such as in the CAM assay (Li and Keller, 2000; Yang and Moses, 1990). However, *in vitro* TGFβ_1 has been shown to both promote and inhibit tube formation. Its *in vitro* effect is dependent on the concentration used, time added

and the experimental conditions used (Dallas et al., 2008). Some studies suggest that concentrations of up to 10ng/ml promote EC migration and tube formation (Dallas et al., 2008; Warrington et al., 2005) while others have shown inhibition and regression of tubular structures (in the collagen sandwich assay) at lower concentrations (0.1ng/ml) (Li and Keller, 2000). The $TGF\beta_1$ amount detected in all co-cultures in the current study was significantly lower than 10ng/ml (Figure 3.32) and therefore could have a pro-angiogenic effect. Most importantly, $TGF\beta_1$ was not exogenously added but was released by the cells within the cultures. Cell-cell interactions could significantly influence the uptake and effect of $TGF\beta_1$ as well as its interaction with other growth factors released by both cell types (Warrington et al., 2005). Therefore, further work is needed to determine the effect of $TGF\beta_1$ in end-to-end network aggregation within these co-culture conditions.

In addition, there is a body of work testing the effect of CD105, which is part of the TGFβ receptor complex. CD105 can also be found independently and does not exert all its functions through TGFβ. CD105 is up- regulated in angiogenic ECs in hypoxia *in vivo* (Duff et al., 2003; Li and Keller, 2000; Warrington et al., 2005) and has been linked to a decrease in EC apoptosis in extreme hypoxia (0.2% O_2) in the presence of TGFβ. The effect and role of CD105 is complex and would be interesting to test its effect in these co-cultures and to compare any differences based on the oxygen conditions used.

Overall, co-culture results suggested that different mechanisms exist depending on the supplementary cells present. The absence of specific growth factor up-

regulation and uptake in HDF co-cultures further highlighted the importance of non soluble growth factors and cell-cell interactions (Velazquez et al., 2002). Fibroblasts are primarily responsible for the deposition of collagen and other ECM proteins *in vivo* (Newman et al., 2011; Shi-wen et al., 2001; Steinbrech et al., 1999). Soluble growth factors therefore may not be as important as ECM proteins (and collagens) when ECs are co-cultured with HDFs (Newman et al., 2011; Sorrell et al., 2007). Collagen deposition by HDFs relies on ascorbic acid addition in culture medium (Berthod, 2013; Horino et al., 2002). Ascorbic acid is a co-factor in the hydroxylation of proline into hydroxyproline, which results in the stabilisation of the collagen triple helix (Berthod, 2013). However, some researchers suggest that culturing fibroblasts in hypoxic conditions is sufficient for stable ECM deposition, both *in vivo* and *in vitro* without the need for ascorbic acid (Horino et al., 2002; Tajima et al., 2001; Takahashi, 2000). While ECM deposition was not tested in any of the cultures, this is an area that requires further testing. This is an area that could unravel the mechanisms that preferentially drive HUVEC network aggregation in physiological hypoxia but not in normoxia in HDF co-cultures.

5 Conclusion

The research presented in this PhD thesis details the effect of introducing biomimetic parameters into 3D cultures of ECs to study how they influence EC morphology and aggregation. The research presented shows data for the first time in 3D collagen hydrogels that VEGFR2 is up- regulated on ECs when the end-to-end EC aggregation pattern occurs, increasing VEGF uptake. This was shown to be integrin and matrix dependent and only occurs in the presence of HBMSCs. These findings show this as a mechanism that drives end-to-end aggregation in 3D cultures.

Furthermore, my results clearly show HUVEC migration to the ventral aspect of the 3D scaffold and cell aggregation into a cobblestone sheet. This HUVEC response has not been shown previously. Cobblestone aggregation mimics the wrapping process in development whilst end-to-end networks mimic cell or cord hollowing. These aggregation patterns can be used for testing these developmental pathways in 3D in vitro. In addition, while the majority of research focuses on engineering and integrating small capillaries into scaffolds through end-to-end network aggregates, the cobblestone aggregation can be useful for mimicking the structure of larger vessels. The first step towards that will be incorporating smooth muscle cells into cobblestone aggregates.

Finally, I have shown that HDFs can promote EC end-to-end network aggregation but in a VEGF independent manner and only in physiological hypoxia. Although matrix deposition by HDFs was not tested here, data in literature and here suggest that this is the main mechanism driving EC network aggregation.

In summary, I proved the hypotheses that support cells such as HBMSCs and HDFs and basement membrane proteins are necessary to promote end-to-end network aggregation of ECs. I have also proved the hypothesis that physiological hypoxia significantly promotes end-to-end network aggregation of ECs (in the presence of HDFs), but disproved the hypothesis that this was through the up-regulation of angiogenic growth factors (at least the angiogenic growth factors tested here).

6 Bibliography

Aird, W.C., 2007a. Phenotypic heterogeneity of the endothelium: I. Structure, function, and mechanisms. Circ. Res. 100, 158–73.

Aird, W.C., 2007b. Phenotypic heterogeneity of the endothelium: II. Representative vascular beds. Circ. Res. 100, 174–90.

Aird, W.C., 2012. Endothelial cell heterogeneity. Cold Spring Harb. Perspect. Med. 2, a006429.

Alekseeva, T., Unger, R.E., Brochhausen, C., Brown, R. a, Kirkpatrick, J.C., 2014. Engineering a Microvascular Capillary Bed in a Tissue-Like Collagen Construct. Tissue Eng. Part A 20, 2656–65.

Ali, S., Saik, J.E., Gould, D.J., Dickinson, M.E., West, J.L., 2013. Immobilization of Cell-Adhesive Laminin Peptides in Degradable PEGDA Hydrogels Influences Endothelial Cell Tubulogenesis. Biores. Open Access 2, 241–9.

Andrae, J., Gallini, R., Betsholtz, C., 2008. Role of platelet-derived growth factors in physiology and medicine. Genes Dev. 22, 1276–312.

Armulik, A., Abramsson, A., Betsholtz, C., 2005. Endothelial/pericyte interactions. Circ. Res. 97, 512–23.

Arnaoutova, I., George, J., Kleinman, H.K., Benton, G., 2009. The endothelial cell tube formation assay on basement membrane turns 20: state of the science and the art. Angiogenesis 12, 267–74.

Arnaoutova, I., Kleinman, H.K., 2010. In vitro angiogenesis: endothelial cell tube formation on gelled basement membrane extract. Nat. Protoc. 5, 628–35.

Au, P., Tam, J., Fukumura, D., Jain, R.K., 2008. Bone marrow-derived mesenchymal stem cells facilitate engineering of long-lasting functional vasculature. Blood 111, 4551–8.

Aurrand-Lions, M., Johnson-Léger, C., Imhof, B. a., 2002. Role of interendothelial adhesion molecules in the control of vascular functions. Vascul. Pharmacol. 39, 239–246.

Bach, T.L., Barsigian, C., Chalupowicz, D.G., Busler, D., Yaen, C.H., Grant, D.S., Martinez, J., 1998. VE-Cadherin mediates endothelial cell capillary tube formation in fibrin and collagen gels. Exp. Cell Res. 238, 324–34.

Bayless, K.J., Davis, G.E., 2003. Sphingosine-1-phosphate markedly induces matrix metalloproteinase and integrin-dependent human endothelial cell invasion and lumen formation in three-dimensional collagen and fibrin matrices. Biochem. Biophys. Res. Commun. 312, 903–913.

Bayless, K.J., Kwak, H.-I., Su, S.-C., 2009. Investigating endothelial invasion and sprouting behavior in three-dimensional collagen matrices. Nat. Protoc. 4, 1888–98.

Bayless, K.J., Salazar, R., Davis, G.E., 2000. RGD-Dependent Vacuolation and Lumen Formation Observed during Endothelial Cell Morphogenesis in Three-Dimensional Fibrin Matrices Involves the αvβ3 and α5β1 Integrins. Am. J. Pathol. 156, 1673–1683.

Bazzoni, G., Dejana, E., 2004. Endothelial cell-to-cell junctions: molecular organization and role in vascular homeostasis. Physiol. Rev. 84, 869–901.

Bell, S.E., Mavila, a, Salazar, R., Bayless, K.J., Kanagala, S., Maxwell, S. a, Davis, G.E., 2001. Differential gene expression during capillary morphogenesis in 3D collagen matrices: regulated expression of genes involved in basement membrane matrix assembly, cell cycle progression, cellular differentiation and G-protein signaling. J. Cell Sci. 114, 2755–73.

Ben-Yosef, Y., Miller, A., Shapiro, S., Lahat, N., 2005. Hypoxia of endothelial cells leads to MMP-2-dependent survival and death. Am. J. Physiol. Cell Physiol. 289, C1321–31.

Berthod, F., 2013. Fibroblasts and Endothelial Cells : The Basic Angiogenic Unit In Vitro Models to Study the Angiogenic Process. In: Gaetano, S. (Ed.), Angiogenesis. Nova Science Publishers, pp. 145–157.

Bikfalvi, a, Cramer, E.M., Tenza, D., Tobelem, G., 1991. Phenotypic modulations of human umbilical vein endothelial cells and human dermal fibroblasts using two angiogenic assays. Biol. Cell 72, 275–8.

Black, A.F., Berthod, F., L'heureux, N., Germain, L., Auger, F.A., 1998. In vitro reconstruction of a human capillary-like network in a tissue-engineered skin equivalent. FASEB J. 12, 1331–40.

Bouïs, D., Hospers, G. a, Meijer, C., Molema, G., Mulder, N.H., 2001. Endothelium in vitro: a review of human vascular endothelial cell lines for blood vessel-related research. Angiogenesis 4, 91–102.

Brady, M.A., Lewis, M.P., Mudera, V., 2008. Synergy between myogenic and non-myogenic cells in a 3D tissue-engineered craniofacial skeletal muscle construct. J. Tissue Eng. Regen. Med. 2, 408–417.

Bronckaers, A., Hilkens, P., Martens, W., Gervois, P., Ratajczak, J., Struys, T., Lambrichts, I., 2014. Mesenchymal stem/stromal cells as a pharmacological and therapeutic approach to accelerate angiogenesis. Pharmacol. Ther. 143, 181–96.

Brooks, P.C., 1996. Role of integrins in angiogenesis. Eur. J. Cancer 32A, 2423–9.

Brown, M., Wittwer, C., 2000. Flow cytometry: principles and clinical applications in hematology. Clin. Chem. 46, 1221–9.

Brown, R. a, Prajapati, R., McGrouther, D. a, Yannas, I. V, Eastwood, M., 1998. Tensional homeostasis in dermal fibroblasts: mechanical responses to

mechanical loading in three-dimensional substrates. J. Cell. Physiol. 175, 323–32.

Brown, R., Wiseman, M., Chuo, C.-B., Cheema, U., Nazhat, S.N., 2005. Ultrarapid Engineering of Biomimetic Materials and Tissues: Fabrication of Nano- and Microstructures by Plastic Compression. Adv. Funct. Mater. 15, 1762–1770.

Bulnheim, U., Müller, P., Neumann, H., Peters, K., Unger, R.E., Kirkpatrick, C.J., Rychly, J., 2014. Endothelial cells stimulate osteogenic differentiation of mesenchymal stem cells on calcium phosphate scaffolds. J. Tissue Eng. Regen. Med. 8, 831–840.

Calera, M.R., Venkatakrishnan, A., Kazlauskas, A., 2004. VE-cadherin increases the half-life of VEGF receptor 2. Exp. Cell Res. 300, 248–256.

Carmeliet, P., 2000. Mechanisms of angiogenesis and arteriogenesis. Nat. Med. 6, 389–95.

Carmeliet, P., Jain, R.K., 2011. Molecular mechanisms and clinical applications of angiogenesis. Nature 473, 298–307.

Cébe-Suarez, S., Zehnder-Fjällman, a, Ballmer-Hofer, K., 2006. The role of VEGF receptors in angiogenesis; complex partnerships. Cell. Mol. Life Sci. 63, 601–15.

Cheema, U., Alekseeva, T., Abou-Neel, E. a, Brown, R., 2010. Switching off angiogenic signalling: creating channelled constructs for adequate oxygen delivery in tissue engineered constructs. Eur. Cell. Mater. 20, 274–80; discussion 280–1.

Cheema, U., Brown, R. a, Alp, B., MacRobert, a J., 2008. Spatially defined oxygen gradients and vascular endothelial growth factor expression in an engineered 3D cell model. Cell. Mol. Life Sci. 65, 177–86.

Cheema, U., Rong, Z., Kirresh, O., Macrobert, A.J., Vadgama, P., Brown, R., 2012. Oxygen diffusion through collagen scaffolds at defined densities : implications for cell survival in tissue models. J. Tissue Eng. Regen. Med. 6, 77–84.

Cheema, U., Yang, S.-Y., Mudera, V., Goldspink, G.G., Brown, R., 2003. 3-D in vitro model of early skeletal muscle development. Cell Motil. Cytoskeleton 54, 226–36.

Chen, T.T., Luque, A., Lee, S., Anderson, S.M., Segura, T., Iruela-Arispe, M.L., 2010. Anchorage of VEGF to the extracellular matrix conveys differential signaling responses to endothelial cells. J. Cell Biol. 188, 595–609.

Chung, S., Andrew, D.J., 2008. The formation of epithelial tubes. J. Cell Sci. 121, 3501–4.

Connolly, J.O., Simpson, N., Hewlett, L., Hall, A., 2002. Rac Regulates Endothelial Morphogenesis and Capillary Assembly. Mol. Biol. Cell 13, 2474–8.

Contois, L., Akalu, A., Brooks, P.C., 2009. Integrins as “functional hubs” in the regulation of pathological angiogenesis. Semin. Cancer Biol. 19, 318–28.

Cross, V.L., Zheng, Y., Won Choi, N., Verbridge, S.S., Sutermaster, B. a, Bonassar, L.J., Fischbach, C., Stroock, A.D., 2010. Dense type I collagen matrices that support cellular remodeling and microfabrication for studies of tumor angiogenesis and vasculogenesis in vitro. Biomaterials 31, 8596–607.

Dallas, N. a, Samuel, S., Xia, L., Fan, F., Gray, M.J., Lim, S.J., Ellis, L.M., 2008. Endoglin (CD105): a marker of tumor vasculature and potential target for therapy. Clin. Cancer Res. 14, 1931–7.

Das, R., Jahr, H., van Osch, G., Farrell, E., 2010. The Role of Hypoxia in Bone Marrow – Derived Mesenchymal Stem Cells : Considerations. Tissue Eng. Part B. Rev. 16, 159–168.

Davis, G.E., Black, S.M., Bayless, K.J., 2000. Capillary morphogenesis during human endothelial cell invasion of three-dimensional collagen matrices. In Vitro Cell. Dev. Biol. Anim. 36, 513–9.

Davis, G.E., Camarillo, C.W., 1995. Regulation of endothelial cell morphogenesis by integrins, mechanical forces, and matrix guidance pathways. Exp. Cell Res. 216, 113–23.

Davis, G.E., Camarillo, C.W., 1996. An alpha 2 beta 1 integrin-dependent pinocytic mechanism involving intracellular vacuole formation and coalescence regulates capillary lumen and tube formation in three-dimensional collagen matrix. Exp. Cell Res. 224, 39–51.

Davis, G.E., Koh, W., Stratman, A.N., 2007. Mechanisms controlling human endothelial lumen formation and tube assembly in three-dimensional extracellular matrices. Birth Defects Res. C. Embryo Today 81, 270–85.

Davis, G.E., Senger, D.R., 2005. Endothelial extracellular matrix: biosynthesis, remodeling, and functions during vascular morphogenesis and neovessel stabilization. Circ. Res. 97, 1093–107.

Dietrich, F., Lelkes, P.I., 2006. Fine-tuning of a three-dimensional microcarrier-based angiogenesis assay for the analysis of endothelial-mesenchymal cell co-cultures in fibrin and collagen gels. Angiogenesis 9, 111–25.

Donovan, D., Brown, N.J., Bishop, E.T., Lewis, C.E., 2001. Comparison of three in vitro human “angiogenesis” assays with capillaries formed in vivo. Angiogenesis 4, 113–21.

Donovan, J., Shiwen, X., Norman, J., Abraham, D., 2013. Platelet-derived growth factor alpha and beta receptors have overlapping functional activities towards fibroblasts. Fibrogenesis Tissue Repair 6, 10.

Drake, C.J., 2003. Embryonic and adult vasculogenesis. Birth Defects Res. C. Embryo Today 69, 73–82.

Duff, S.E., Li, C., Garland, J.M., Kumar, S., 2003. CD105 is important for angiogenesis : evidence and potential applications. FASEB J. 17, 984–992.

Duffy, G.P., McFadden, T.M., Byrne, E.M., Gill, S.-L., Farrell, E., O'Brien, F.J., 2011. Towards in vitro vascularisation of collagen-GAG scaffolds. Eur. Cell. Mater. 21, 15–30.

Duttenhoefer, F., Lara de Freitas, R., Meury, T., Loibl, M., Benneker, L.M., Richards, R.G., Alini, M., Verrier, S., 2013. 3D scaffolds co-seeded with human endothelial progenitor and mesenchymal stem cells: evidence of prevascularisation within 7 days. Eur. Cell. Mater. 26, 49–64; discussion 64–5.

Eastwood, M., Mudera, V., McGrouther, D. a, Brown, R., 1998. Effect of precise mechanical loading on fibroblast populated collagen lattices: morphological changes. Cell Motil. Cytoskeleton 40, 13–21.

Eichmann, A., Simons, M., 2012. VEGF signaling inside vascular endothelial cells and beyond. Curr. Opin. Cell Biol. 24, 188–93.

Emonard, H., Calle, A., Grimaud, J. a, Peyrol, S., Castronovo, V., Noel, A., Lapière, C.M., Kleinman, H.K., Foidart, J.M., 1987. Interactions between fibroblasts and a reconstituted basement membrane matrix. J. Invest. Dermatol. 89, 156–63.

Fagiani, E., Christofori, G., 2013. Angiopoietins in angiogenesis. Cancer Lett. 328, 18–26.

Fischer, C., Schneider, M., Carmeliet, P., 2006. Principles and therapeutic implications of angiogenesis, vasculogenesis and arteriogenesis. Handb. Exp. Pharmacol. 176, 157–212.

Francis, M.E., Uriel, S., Brey, E.M., 2008. Endothelial cell-matrix interactions in neovascularization. Tissue Eng. Part B. Rev. 14, 19–32.

Fuchs, S., Dohle, E., Kolbe, M., Kirkpatrick, C.J., 2010. Outgrowth Endothelial Cells : Sources , Characteristics and Potential Applications in Tissue Engineering and Regenerative Medicine. Adv. Biochem. Eng. Biotechnol. 123, 201–217.

Fuchs, S., Jiang, X., Schmidt, H., Dohle, E., Ghanaati, S., Orth, C., Hofmann, A., Motta, A., Migliaresi, C., Kirkpatrick, C.J., 2009. Dynamic processes involved in the pre-vascularization of silk fibroin constructs for bone regeneration using outgrowth endothelial cells. Biomaterials 30, 1329–38.

Gagnon, E., Cattaruzzi, P., Griffith, M., Muzakare, L., LeFlao, K., Faure, R., Béliveau, R., Hussain, S.N., Koutsilieris, M., Doillon, C.J., 2002. Human vascular endothelial cells with extended life spans: in vitro cell response, protein expression, and angiogenesis. Angiogenesis 5, 21–33.

Gawlitta, D., Ph, D., Fledderus, J.O., Rijen, M.H.P. Van, Sc, B., Dokter, I., Alblas, J., Verhaar, M.C., Dhert, W.J.A., 2012. Hypoxia Impedes Vasculogenesis of In Vitro Engineered Bone 18, 208–218.

Georgiou, M., Bunting, S.C.J., Davies, H. a, Loughlin, A.J., Golding, J.P., Phillips, J.B., 2013. Engineered neural tissue for peripheral nerve repair. Biomaterials 34, 7335–43.

Gerhardt, H., Golding, M., Fruttiger, M., Ruhrberg, C., Lundkvist, A., Abramsson, A., Jeltsch, M., Mitchell, C., Alitalo, K., Shima, D., Betsholtz, C., 2003. VEGF guides angiogenic sprouting utilizing endothelial tip cell filopodia. J. Cell Biol. 161, 1163–77.

Ghajar, C.M., Blevins, K.S., Hughes, C.C.W., Ph, D., George, S.C., Putnam, A.J., 2006. Mesenchymal Stem Cells Enhance Angiogenesis Early Matrix Metalloproteinase Upregulation. Tissue Eng. 12, 2875–88.

Ghajar, C.M., Kachgal, S., Kniazeva, E., Mori, H., Costes, S. V, George, S.C., Putnam, A.J., 2010. Mesenchymal cells stimulate capillary morphogenesis via distinct proteolytic mechanisms. Exp. Cell Res. 316, 813–25.

Ghanaati, S., Fuchs, S., Webber, M.J., Orth, C., Barbeck, M., Gomes, M.E., Reis, R.L., Kirkpatrick, C.J., 2011. Rapid vascularization of starch – poly (caprolactone) in vivo by outgrowth endothelial cells in co-culture with primary osteoblasts. J. Tissue Eng. Regen. Med. 5, 136–143.

Glowacki, J., Mizuno, S., 2007. Collagen scaffolds for tissue engineering. Biopolymers 89, 338–44.

Grainger, S.J., Carrion, B., Ceccarelli, J., Putnam, A.J., 2013. Stromal Cell Identity Influences the In Vivo Functionality of Engineered Capillary Networks Formed by Co-delivery. Tissue Eng. Part A 19, 1209–1222.

Grant, D.S., Kleinman, H.K., Martin, G.R., 1990. The role of basement membranes in vascular development. Ann. N. Y. Acad. Sci. 588, 61–72.

Grant, D.S., Lelkes, P.I., Fukuda, K., Kleinman, H.K., Al, G.E.T., 1991. Intracellular mechanisms involved in basement membrane induced blood vessel differentiation in vitro. Vitr. Cell. Dev. Biol. 27A, 327–336.

Grant, D.S., Tashiro, K., Segui-Real, B., Yamada, Y., Martin, G.R., Kleinman, H.K., 1989. Two different laminin domains mediate the differentiation of human endothelial cells into capillary-like structures in vitro. Cell 58, 933–43.

Hadjipanayi, E., Brown, R., Mudera, V., Deng, D., Liu, W., Cheema, U., 2010. Controlling physiological angiogenesis by hypoxia-induced signaling. J. Control. Release 146, 309–17.

Hadjipanayi, E., Cheema, U., Hopfner, U., Bauer, a, Machens, H.G., Schilling, a F., 2012. Injectable system for spatio-temporally controlled delivery of hypoxia-induced angiogenic signalling. J. Control. Release 161, 852–60.

Hadjipanayi, E., Cheema, U., Mudera, V., Deng, D., Liu, W., Brown, R., 2011. First implantable device for hypoxia-mediated angiogenic induction. J. Control. Release 153, 217–224.

Han, S.-K., Chun, K.-W., Gye, M.-S., Kim, W.-K., 2006. The effect of human bone marrow stromal cells and dermal fibroblasts on angiogenesis. Plast. Reconstr. Surg. 117, 829–35.

Herzog, D.P.E., Dohle, E., Bischoff, I., Kirkpatrick, C.J., 2014. Cell communication in a coculture system consisting of outgrowth endothelial cells and primary osteoblasts. Biomed Res. Int. 2014, 1–15.

Ho, T.K., Rajkumar, V., Ponticos, M., Leoni, P., Black, D.C.M., Abraham, D.J., Baker, D.M., 2006. Increased endogenous angiogenic response and hypoxia-inducible factor-1alpha in human critical limb ischemia. J. Vasc. Surg. 43, 125–33.

Hofmann, A., Ritz, U., Verrier, S., Eglin, D., Alini, M., Fuchs, S., Kirkpatrick, C.J., Rommens, P.M., 2008. The effect of human osteoblasts on proliferation and neo-vessel formation of human umbilical vein endothelial cells in a long-term 3D co-culture on polyurethane scaffolds. Biomaterials 29, 4217–26.

Horino, Y., Takahashi, S., Miura, T., Takahashi, Y., 2002. Prolonged hypoxia accelerates the posttranscriptional process of collagen synthesis in cultured fibroblasts. Life Sci. 71, 3031–45.

Huang, N.F., Okogbaa, J., Lee, J.C., Jha, A., Zaitseva, T.S., Paukshto, M. V, Sun, J.S., Punjya, N., Fuller, G.G., Cooke, J.P., 2013. The modulation of endothelial cell morphology, function, and survival using anisotropic nanofibrillar collagen scaffolds. Biomaterials 34, 4038–47.

Hudlicka, O., West, D., Kumar, S., Khelly, F. El, Wright, A.J.A., 1989. Can growth of capillaries in the heart and skeletal muscle be explained by the presence of an angiogenic factor? Br. J. Exp. Pathol. 70, 237–246.

Hynes, R.O., 2007. Cell-matrix adhesion in vascular development. J. Thromb. Haemost. 5 Suppl 1, 32–40.

Hynes, R.O., 2009. The extracellular matrix: not just pretty fibrils. Science 326, 1216–9.

Igarashi, A., Segoshi, K., Sakai, Y., Pan, H., Kanawa, M., Higashi, Y., Sugiyama, M., Nakamura, K., Kurihara, H., Yamaguchi, S., Tsuji, K.,

Kawamoto, T., Kato, Y., 2007. Selection of common markers for bone marrow stromal cells from various bones using real-time RT-PCR: effects of passage number and donor age. Tissue Eng. 13, 2405–17.

Iivanainen, E., Kähäri, V.-M., Heino, J., Elenius, K., 2003. Endothelial cell-matrix interactions. Microsc. Res. Tech. 60, 13–22.

Imoukhuede, P.I., Dokun, A.O., Annex, B.H., Popel, A.S., 2013. Endothelial cell-by-cell profiling reveals the temporal dynamics of VEGFR1 and VEGFR2 membrane localization after murine hindlimb ischemia. Am. J. Physiol. Heart Circ. Physiol. 304, H1085–93.

Imoukhuede, P.I., Popel, A.S., 2011. Quantification and cell-to-cell variation of vascular endothelial growth factor receptors. Exp. Cell Res. 317, 955–65.

Imoukhuede, P.I., Popel, A.S., 2012. Expression of VEGF receptors on endothelial cells in mouse skeletal muscle. PLoS One 7, e44791.

Ingber, D.E., Folkman, J., 1989. How does extracellular matrix control capillary morphogenesis? Cell 58, 803–5.

Iruela-Arispe, M.L., Davis, G.E., 2009. Cellular and molecular mechanisms of vascular lumen formation. Dev. Cell 16, 222–31.

Joung, I.S., Iwamoto, M.N., Shiu, Y.-T., Quam, C.T., 2006. Cyclic strain modulates tubulogenesis of endothelial cells in a 3D tissue culture model. Microvasc. Res. 71, 1–11.

Kachgal, S., Putnam, A.J., 2011. Mesenchymal stem cells from adipose and bone marrow promote angiogenesis via distinct cytokine and protease expression mechanisms. Angiogenesis 14, 47–59.

Kaigler, D., Krebsbach, P.H., Polverini, P.J., Mooney, D.J., 2003. Role of vascular endothelial growth factor in bone marrow stromal cell modulation of endothelial cells. Tissue Eng. 9, 95–103.

Kang, Y., Kim, S., Fahrenholtz, M., Khademhosseini, A., Yang, Y., 2013. Osteogenic and angiogenic potentials of monocultured and co-cultured human-bone-marrow-derived mesenchymal stem cells and human-umbilical-vein endothelial cells on three-dimensional porous beta-tricalcium phosphate scaffold. Acta Biomater. 9, 4906–15.

Karamichos, D., Brown, R., Mudera, V., 2007. Collagen stiffness regulates cellular contraction and matrix remodeling gene expression. J. Biomed. Mater. Res. A 83A, 887–894.

Kaully, T., Kaufman-Francis, K., Lesman, A., Levenberg, S., 2009. Vascularization--the conduit to viable engineered tissues. Tissue Eng. Part B. Rev. 15, 159–69.

Kinnaird, T, Stabile, E Burnett, M S Lee, C.W., Barr, S., Fuchs, S., Epstein, S.E., 2004. Marrow-derived stromal cells express genes encoding a broad

spectrum of arteriogenic cytokines and promote in vitro and in vivo arteriogenesis through paracrine mechanisms. Circ. Res. 94, 678–85.

Kirkpatrick, C.J., Fuchs, S., Unger, R.E., 2011. Co-culture systems for vascularization--learning from nature. Adv. Drug Deliv. Rev. 63, 291–9.

Koch, S., Tugues, S., Li, X., Gualandi, L., Claesson-Welsh, L., 2011. Signal transduction by vascular endothelial growth factor receptors. Biochem. J. 437, 169–83.

Koh, W., Mahan, R.D., Davis, G.E., 2008. Cdc42- and Rac1-mediated endothelial lumen formation requires Pak2, Pak4 and Par3, and PKC-dependent signaling. J. Cell Sci. 121, 989–1001.

Kolbe, M., Xiang, Z., Dohle, E., Tonak, M., Kirkpatrick, C.J., Fuchs, S., 2011. Paracrine Effects Influenced by Cell Culture Medium and Consequences on Microvessel-Like Structures in Cocultures of Mesenchymal Stem Cells. Tissue Eng. Part A 17, 2199–212.

Kroon, M.E., van Schie, M.L.J., van der Vecht, B., van Hinsbergh, V.W.M., Koolwijk, P., 2002. Collagen type 1 retards tube formation by human microvascular endothelial cells in a fibrin matrix. Angiogenesis 5, 257–65.

Kubota, Y., Kleinman, H.K., Martin, G.R., Lawley, T.J., 1988. Role of laminin and basement membrane in the morphological differentiation of human endothelial cells into capillary-like structures. J. Cell Biol. 107, 1589–98.

Kumar, S., West, D.C., Ager, A., 1987. Heterogeneity in endothelial cells from large vessels and microvessels. Differentiation 36, 57–70.

Kunz-Schughart, L. a, Schroeder, J. a, Wondrak, M., van Rey, F., Lehle, K., Hofstaedter, F., Wheatley, D.N., 2006. Potential of fibroblasts to regulate the formation of three-dimensional vessel-like structures from endothelial cells in vitro. Am. J. Physiol. Cell Physiol. 290, C1385–98.

Lampugnani, M.G., Orsenigo, F., Gagliani, M.C., Tacchetti, C., Dejana, E., 2006. Vascular endothelial cadherin controls VEGFR-2 internalization and signaling from intracellular compartments. J. Cell Biol. 174, 593–604.

Lang, I., Hoffmann, C., Olip, H., Pabst, M. a, Hahn, T., Dohr, G., Desoye, G., 2001. Differential mitogenic responses of human macrovascular and microvascular endothelial cells to cytokines underline their phenotypic heterogeneity. Cell Prolif. 34, 143–55.

Lang, I., Pabst, M. a, Hiden, U., Blaschitz, A., Dohr, G., Hahn, T., Desoye, G., 2003. Heterogeneity of microvascular endothelial cells isolated from human term placenta and macrovascular umbilical vein endothelial cells. Eur. J. Cell Biol. 82, 163–73.

Lawley, T., Kubota, Y., 1989. Induction of morphologic differentiation of endothelial cells in culture. Soc. Investig. Dermatology 93, 9–11.

Lee, K., Silva, E.A., Mooney, D.J., 2011. Growth factor delivery-based tissue engineering : general approaches and a review of recent developments. J. R. Soc. Interface 8, 153–170.

Lee, T.-H., Seng, S., Li, H., Kennel, S.J., Avraham, H.K., Avraham, S., 2006. Integrin regulation by vascular endothelial growth factor in human brain microvascular endothelial cells: role of alpha6beta1 integrin in angiogenesis. J. Biol. Chem. 281, 40450–60.

Lesman, A., Koffler, J., Atlas, R., Blinder, Y.J., Kam, Z., Levenberg, S., 2011. Engineering vessel-like networks within multicellular fibrin-based constructs. Biomaterials 32, 7856–69.

Levenberg, S., Rouwkema, J., Macdonald, M., Garfein, E.S., Kohane, D.S., Darland, D.C., Marini, R., van Blitterswijk, C. a, Mulligan, R.C., D'Amore, P. a, Langer, R., 2005. Engineering vascularized skeletal muscle tissue. Nat. Biotechnol. 23, 879–84.

Levis, H.J., Brown, R., Daniels, J.T., 2010. Plastic compressed collagen as a biomimetic substrate for human limbal epithelial cell culture. Biomaterials 31, 7726–37.

Li, C., Issa, R., Kumar, P., Hampson, I.N., Lopez-Novoa, J.M., Bernabeu, C., Kumar, S., 2003. CD105 prevents apoptosis in hypoxic endothelial cells. J. Cell Sci. 116, 2677–85.

Li, W., Keller, G., 2000. VEGF nuclear accumulation correlates with phenotypical changes in endothelial cells. J. Cell Sci. 113, 1525–34.

Liu, H., Slamovich, E.B., Webster, T.J., 2006. Less harmful acidic degradation of poly(lactic-co-glycolic acid) bone tissue engineering scaffolds through titania nanoparticle addition. Int. J. Nanomedicine 1, 541–545.

Loibl, M., Binder, A., Herrmann, M., Duttenhoefer, F., Richards, R.G., Nerlich, M., Alini, M., Verrier, S., 2014. Direct cell-cell contact between mesenchymal stem cells and endothelial progenitor cells induces a pericyte-like phenotype in vitro. Biomed Res. Int. 2014, 395781.

Lubarsky, B., Krasnow, M.A., 2003. Tube Morphogenesis : Making and Shaping Biological Tubes. Cell 112, 19–28.

Matsumoto, T., Yung, Y.C., Fischbach, C., Kong, H.J., Nakaoka, R., Mooney, D.J., 2007. Mechanical strain regulates endothelial cell patterning in vitro. Tissue Eng. 13, 207–17.

McFadden, T.M., Duffy, G.P., Allen, a B., Stevens, H.Y., Schwarzmaier, S.M., Plesnila, N., Murphy, J.M., Barry, F.P., Guldberg, R.E., O'Brien, F.J., 2013. The delayed addition of human mesenchymal stem cells to pre-formed endothelial cell networks results in functional vascularization of a collagen-glycosaminoglycan scaffold in vivo. Acta Biomater. 9, 9303–16.

Metheny-Barlow, L.J., Li, L.Y., 2003. The enigmatic role of angiopoietin-1 in tumor angiogenesis. Cell Res. 13, 309–17.

Montesano, R., Orci, L., 1987. Phorbol esters induce angiogenesis in vitro from large-vessel endothelial cells. J. Cell. Physiol. 130, 284–91.

Montesano, R., Orci, L., Vassalli, P., 1983. In vitro rapid organization of endothelial cells into capillary-like networks is promoted by collagen matrices. J. Cell Biol. 97, 1648–52.

Morin, K.T., Tranquillo, R.T., 2013. In vitro models of angiogenesis and vasculogenesis in fibrin gel. Exp. Cell Res. 319, 2409–17.

Nakatsu, M.N., Sainson, R.C. a., Aoto, J.N., Taylor, K.L., Aitkenhead, M., Pérez-del-Pulgar, S., Carpenter, P.M., Hughes, C.C.W., 2003. Angiogenic sprouting and capillary lumen formation modeled by human umbilical vein endothelial cells (HUVEC) in fibrin gels: the role of fibroblasts and Angiopoietin-1. Microvasc. Res. 66, 102–112.

Nakayama, M., Berger, P., 2013. Coordination of VEGF receptor trafficking and signaling by coreceptors. Exp. Cell Res. 319, 1340–7.

Nakayama, M., Nakayama, A., van Lessen, M., Yamamoto, H., Hoffmann, S., Drexler, H.C. a, Itoh, N., Hirose, T., Breier, G., Vestweber, D., Cooper, J. a, Ohno, S., Kaibuchi, K., Adams, R.H., 2013. Spatial regulation of VEGF receptor endocytosis in angiogenesis. Nat. Cell Biol. 15, 249–60.

Namiki, A., Brogi, E., Kim, E.A., Wu, T., Couffinhal, T., Varticovski, L., Isner, J.M., Kearney, M., 1995. Cell Biology and Metabolism : Hypoxia Induces Vascular Endothelial Growth Factor in Cultured Human Endothelial Cells. J. Biol. Chem. 270, 31189–31195.

Nehls, V., Detlev, D., 1995. A Novel, Microcarrier-Based in vitro assay for rapid and reliable quantification of three-dimensional cell migration and angiogenesis. Microvasc. Res. 50, 311–322.

Newman, A.C., Nakatsu, M.N., Chou, W., Gershon, P.D., Hughes, C.C.W., 2011. The requirement for fibroblasts in angiogenesis: fibroblast-derived matrix proteins are essential for endothelial cell lumen formation. Mol. Biol. Cell 22, 3791–800.

Nicosia, R.F., 2009. The aortic ring model of angiogenesis: a quarter century of search and discovery. J. Cell. Mol. Med. 13, 4113–36.

Nicosia, R.F., Bonanno, E., Smith, M., Yurchenco, P., 1994. Modulation of angiogenesis in vitro by laminin-entactin complex. Dev. Biol. 164, 197–206.

Nicosia, R.F., Zorzi, P., Ligresti, G., Morishita, A., Aplin, A.C., 2011. Paracrine regulation of angiogenesis by different cell types in the aorta ring model. Int. J. Dev. Biol. 55, 447–53.

Nilsson, I., Shibuya, M., Wennström, S., 2004. Differential activation of vascular genes by hypoxia in primary endothelial cells. Exp. Cell Res. 299, 476–85.

O'Brien, F.J., 2011. Biomaterials & scaffolds for tissue engineering. Mater. Today 14, 88–95.

Odedra, D., Chiu, L.L.Y., Shoichet, M., Radisic, M., 2011. Endothelial cells guided by immobilized gradients of vascular endothelial growth factor on porous collagen scaffolds. Acta Biomater. 7, 3027–35.

Phelps, E. a, Garcia, A.J., 2009. Update on therapeutic vascularization strategies. Regen. Med. 4, 65–80.

Phillips, J.B., Bunting, S.C.J., Hall, S.M., Brown, R., 2005. Neural tissue engineering: a self-organizing collagen guidance conduit. Tissue Eng. 11, 1611–7.

Pirraco, R.P., Iwata, T., Yoshida, T., Marques, A.P., Yamato, M., Reis, R.L., Okano, T., 2014. Endothelial cells enhance the in vivo bone-forming ability of osteogenic cell sheets. Lab. Invest. 94, 663–73.

Powerski, M., Henrich, D., Sander, A., Teiler, A., Marzi, I., 2011. In vitro manipulation of endothelial progenitor cell adhesion to vascular endothelium and extracellular matrix by the phorbol ester PMA. Artif. Cells. Blood Substit. Immobil. Biotechnol. 39, 214–22.

Primo, L., Seano, G., Roca, C., Maione, F., Gagliardi, P.A., Sessa, R., Martinelli, M., Giraudo, E., di Blasio, L., Bussolino, F., 2010. Increased expression of alpha6 integrin in endothelial cells unveils a proangiogenic role for basement membrane. Cancer Res. 70, 5759–69.

Rao, R.R., Peterson, A.W., Ceccarelli, J., Putnam, A.J., Stegemann, J.P., 2012. Matrix composition regulates three-dimensional network formation by endothelial cells and mesenchymal stem cells in collagen/fibrin materials. Angiogenesis 15, 253–64.

Ross, R.S., 2004. Molecular and mechanical synergy: cross-talk between integrins and growth factor receptors. Cardiovasc. Res. 63, 381–90.

Sacharidou, A., Stratman, A.N., Davis, G.E., 2012. Molecular mechanisms controlling vascular lumen formation in three-dimensional extracellular matrices. Cells. Tissues. Organs 195, 122–43.

Salazar, R., Bell, S.E., Davis, G.E., 1999. Coordinate induction of the actin cytoskeletal regulatory proteins gelsolin, vasodilator-stimulated phosphoprotein, and profilin during capillary morphogenesis in vitro. Exp. Cell Res. 249, 22–32.

Scott, A., Mellor, H., 2009. VEGF receptor trafficking in angiogenesis. Biochem. Soc. Trans. 37, 1184–8.

Serini, G., Valdembri, D., Bussolino, F., 2006. Integrins and angiogenesis: a sticky business. Exp. Cell Res. 312, 651–8.

Shen, Y.H., Shoichet, M.S., Radisic, M., 2008. Vascular endothelial growth factor immobilized in collagen scaffold promotes penetration and proliferation of endothelial cells. Acta Biomater. 4, 477–89.

Shi-wen, X., Denton, C.P., Dashwood, M.R., Holmes, A.M., Bou-gharios, G., Pearson, J.D., Black, C.M., Abraham, D., 2001. Fibroblast matrix gene expression and connective tissue remodeling: role of endothelin-1. Soc. Investig. Dermatology 116, 417–425.

Shin, Y., Jeon, J.S., Han, S., Jung, G.-S., Shin, S., Lee, S.-H., Sudo, R., Kamm, R.D., Chung, S., 2011. In vitro 3D collective sprouting angiogenesis under orchestrated ANG-1 and VEGF gradients. Lab Chip 11, 2175–81.

Slevin, M., Krupinski, J., Gaffney, J., Matou, S., West, D., Delisser, H., Savani, R.C., Kumar, S., 2007. Hyaluronan-mediated angiogenesis in vascular disease: uncovering RHAMM and CD44 receptor signaling pathways. Matrix Biol. 26, 58–68.

Smith, A., Passey, S., Greensmith, L., Mudera, V., Lewis, M.P., 2012. Characterization and optimization of a simple, repeatable system for the long term in vitro culture of aligned myotubes in 3D. J. Cell. Biochem. 113, 1044–53.

Sorrell, J.M., Baber, M. a, Caplan, A.I., 2007. A self-assembled fibroblast-endothelial cell co-culture system that supports in vitro vasculogenesis by both human umbilical vein endothelial cells and human dermal microvascular endothelial cells. Cells. Tissues. Organs 186, 157–68.

Sorrell, J.M., Baber, M. a, Caplan, A.I., 2009. Influence of adult mesenchymal stem cells on in vitro vascular formation. Tissue Eng. Part A 15, 1751–61.

Stamati, K., Mudera, V., Cheema, U., 2011. Evolution of oxygen utilization in multicellular organisms and implications for cell signalling in tissue engineering. J. Tissue Eng. 2, 1–12.

Stamati, K., Priestley, J. V, Mudera, V., Cheema, U., 2014. Laminin promotes vascular network formation in 3D in vitro collagen scaffolds by regulating VEGF uptake. Exp. Cell Res. 327, 68–77.

Staton, C. a, Reed, M.W.R., Brown, N.J., 2009. A critical analysis of current in vitro and in vivo angiogenesis assays. Int. J. Exp. Pathol. 90, 195–221.

Staton, C.A., Stribbling, S.M., Tazzyman, S., Hughes, R., Brown, N.J., Lewis, C.E., 2004. Current methods for assaying angiogenesis in vitro and in vivo. Int. J. Exp. Pathol. 85, 233–248.

Steinbrech, D.S., Longaker, M.T., Mehrara, B.J., Saadeh, P.B., Chin, G.S., Gerrets, R.P., Chau, D.C., Rowe, N.M., Gittes, G.K., 1999. Fibroblast

response to hypoxia: the relationship between angiogenesis and matrix regulation. J. Surg. Res. 84, 127–33.

Stratman, A.N., Davis, M.J., Davis, G.E., 2011. VEGF and FGF prime vascular tube morphogenesis and sprouting directed by hematopoietic stem cell cytokines. Blood 117, 3709–19.

Stratman, A.N., Saunders, W.B., Sacharidou, A., Koh, W., Fisher, K.E., Zawieja, D.C., Davis, M.J., Davis, G.E., 2009. Endothelial cell lumen and vascular guidance tunnel formation requires MT1-MMP-dependent proteolysis in 3-dimensional collagen matrices. Blood 114, 237–47.

Stratman, A.N., Schwindt, A.E., Malotte, K.M., Davis, G.E., 2010. Endothelial-derived PDGF-BB and HB-EGF coordinately regulate pericyte recruitment during vasculogenic tube assembly and stabilization 116, 4720–4730.

Streeter, I., Cheema, U., 2011. Oxygen consumption rate of cells in 3D culture: the use of experiment and simulation to measure kinetic parameters and optimise culture conditions. Analyst 136, 4013–9.

Tajima, R., Kawaguchi, N., Horino, Y., Takahashi, Y., Toriyama, K., Inou, K., Torii, S., Kitagawa, Y., 2001. Hypoxic enhancement of type IV collagen secretion accelerates adipose conversion of 3T3-L1 fibroblasts. Biochim. Biophys. Acta 1540, 179–87.

Takahashi, Y., 2000. Hypoxic Induction of Prolyl 4-Hydroxylase alpha (I) in Cultured Cells. J. Biol. Chem. 275, 14139–14146.

Tsai, C.-C., Yew, T.-L., Yang, D.-C., Huang, W.-H., Hung, S.-C., 2012. Benefits of hypoxic culture on bone marrow multipotent stromal cells. Am. J. Blood Res. 2, 148–59.

Ulyatt, C., Walker, J., Ponnambalam, S., 2011. Hypoxia differentially regulates VEGFR1 and VEGFR2 levels and alters intracellular signaling and cell migration in endothelial cells. Biochem. Biophys. Res. Commun. 404, 774–9.

Unger, R.E., Krump-Konvalinkova, V., Peters, K., Kirkpatrick, C.J., 2002. In Vitro Expression of the Endothelial Phenotype: Comparative Study of Primary Isolated Cells and Cell Lines, Including the Novel Cell Line HPMEC-ST1.6R. Microvasc. Res. 64, 384–397.

Unger, R.E., Peters, K., Wolf, M., Motta, a, Migliaresi, C., Kirkpatrick, C.J., 2004. Endothelialization of a non-woven silk fibroin net for use in tissue engineering: growth and gene regulation of human endothelial cells. Biomaterials 25, 5137–46.

Unger, R.E., Sartoris, A., Peters, K., Motta, A., Migliaresi, C., Kunkel, M., Bulnheim, U., Rychly, J., Kirkpatrick, C.J., 2007. Tissue-like self-assembly in cocultures of endothelial cells and osteoblasts and the formation of microcapillary-like structures on three-dimensional porous biomaterials. Biomaterials 28, 3965–76.

Vailhé, B., Ronot, X., Tracqui, P., Usson, Y., Tranqui, L., 1997. In vitro angiogenesis is modulated by the mechanical properties of fibrin gels and is related to alpha(v)beta3 integrin localization. In Vitro Cell. Dev. Biol. Anim. 33, 763–73.

Vailhé, B., Vittet, D., Feige, J., 2001. In Vitro Models of Vasculogenesis and Angiogenesis 81, 439–452.

Vater, C., Kasten, P., Stiehler, M., 2011. Culture media for the differentiation of mesenchymal stromal cells. Acta Biomater. 7, 463–77.

Velazquez, O., Snyder, R., Liu, Z.-J., Fairman, R.M., Herlyn, M., 2002. Fibroblast-dependent differentiation of human microvascular endothelial cells into capillary-like 3-dimensional networks 1 1316–1318.

Vernon, R.B., Lara, S.L., Drake, C.J., Iruela-Arispe, M.L., Angello, J.C., Little, C.D., Wight, T.N., Sage, E.H., 1995. Organized type I collagen influences endothelial patterns during “spontaneous angiogenesis in vitro”: planar cultures as models of vascular development. In Vitro Cell. Dev. Biol. Anim. 31, 120–31.

Vernon, R.B., Sage, E.H., 1999. A novel, quantitative model for study of endothelial cell migration and sprout formation within three-dimensional collagen matrices. Microvasc. Res. 57, 118–33.

Vestweber, D., Winderlich, M., Cagna, G., Nottebaum, A.F., 2009. Cell adhesion dynamics at endothelial junctions: VE-cadherin as a major player. Trends Cell Biol. 19, 8–15.

Wallez, Y., Vilgrain, I., Huber, P., 2006. Angiogenesis: the VE-cadherin switch. Trends Cardiovasc. Med. 16, 55–9.

Warrington, K., Hillarby, M.C., Li, C., Letarte, M., Kumar, S., 2005. Functional Role of CD105 in TGFβ1 Signalling in Murine and Human Endothelial Cells. Anticancer Res. 25, 1851–1864.

West, D.C., Sattar, A., Kumar, S., 1985. A Simplified in Situ Solubilization Procedure for the Determination of DNA and Cell Number in Tissue Cultured Mammalian Cells. Anal. Biochem. 147, 289–295.

Wong, J.P.F., MacRobert, A.J., Cheema, U., Brown, R. a, 2013. Mechanical anisotropy in compressed collagen produced by localised photodynamic cross-linking. J. Mech. Behav. Biomed. Mater. 18, 132–9.

Wu, J., Sheibani, N., 2003. Modulation of VE-cadherin and PECAM-1 mediated cell-cell adhesions by mitogen-activated protein kinases. J. Cell. Biochem. 90, 121–37.

Wu, J.M., Xu, Y.Y., Li, Z.H., Yuan, X.Y., Wang, P.F., Zhang, X.Z., Liu, Y.Q., Guan, J., Guo, Y., Li, R.X., Zhang, H., 2011. Heparin-functionalized collagen matrices with controlled release of basic fibroblast growth factor. J. Mater. Sci. Mater. Med. 22, 107–14.

Yang, E.Y., Moses, H.L., 1990. Transforming growth factor beta 1-induced changes in cell migration, proliferation, and angiogenesis in the chicken chorioallantoic membrane. J. Cell Biol. 111, 731–41.